Published in final edited form as:
Chem Rev. 2013 March 13; 113(3): . doi:10.1021/cr200358s.

X-Ray Computed Tomography Contrast Agents

Hrvoje Lusic and **Mark W. Grinstaff***
Boston University, Departments of Biomedical Engineering and Chemistry, Metcalf Center for Science and Engineering, 590 Commonwealth Ave., Boston, MA 02215. Fax: 617-358-3186; Tel: 617-353-3871

1.0 Introduction

X-ray computed tomography (CT) is a well-established tissue imaging technique employed in a variety of research and clinical settings.[1] Specifically, CT is a non-invasive clinical diagnostic tool that allows for 3D visual reconstruction and segmentation of tissues of interest. High resolution CT systems can be used to perform non-destructive 3D imaging of a variety of tissue types and organ systems, such as: the gastrointestinal tract, cardiovascular system, renal tract, liver, lungs, bone, cartilage, tumorous tissue, etc. CT is one of the most prevalent diagnostic tools in terms of frequency-of-use and hospital availability.[2] The use of CT is on the rise and the number of clinical CT scanners in operation worldwide is estimated at over 45,000.[1b] Today, over 70 million clinical CT scans are performed yearly in the U.S. alone. For a recent detailed analysis of the use of clinical CT imaging and data regarding the number of regular and contrast-enhanced CT scans performed annually in the U.S. we refer the reader to the "Nationwide Evaluation of X-ray Trends" survey published by the Conference for Radiation Control Program Directors (CRCPD).[3]

The idea of using tomography (Greek: *tomos* = slice, *graphein* = draw) as a diagnostic tool in medicine was adopted soon after the discovery of X-rays by W. C. Roentgen in 1895. However, several more decades passed before the technology advanced sufficiently to bring those ideas to fruition. The first successful CT imaging device was built in 1972 by G. N. Hounsfield, at Electric and Musical Industries Ltd. In 1979, G. N. Hounsfield and South African physicist A. M. Cormack shared a Nobel Prize in medicine for their contributions to the field of X-ray CT imaging and diagnostics.[4]

X-rays are a form of electromagnetic radiation with wavelengths roughly between 0.01 nm and 10 nm. Traditionally, X-rays are generated by a vacuum tube using high voltage to accelerate electrons from a cathode to a (usually) tungsten-alloy anode. In the process, the accelerated electrons release electromagnetic radiation in the form of X-rays and the maximum energy of the radiation is limited by the energy of the incident electron. Operating voltages of modern clinical CT scanners differ among instrument models and manufacturers, but generally fall between 80 kVp to 150 kVp.

As a rule, materials possessing higher density (ρ) or high atomic number (Z) tend to better absorb X-rays. The relationship is best expressed in the formula for X-ray absorption coefficient (μ):

Corresponding author: mgrin@bu.edu.

Competing Interests Statement
The authors have no conflict of interest.

$$\mu \approx \frac{\rho Z^4}{AE^3} \quad (1)$$

where “A” is the atomic mass and “E” is the X-ray energy. The strong relationship between absorption and atomic number is of significant importance in clinical applications. The Z^4 factor allows for contrast levels of several orders of magnitude between different tissues and types of contrast agents.

When an incident X-ray has energy equal or slightly greater than the binding energy of the K-shell electron of the atom, a large sudden increase in absorption coefficient is observed. This energy value is known as absorption edge (*k*), and the *k* value increases with atomic number of the element. Consequently, X-ray attenuating contrast media containing atoms of high atomic number (most commonly iodine or barium), are frequently used in clinical settings to obtain images of soft tissues. To generate images with the highest contrast to the surrounding tissue, the energy of the X-ray source can be adjusted to closely match the absorption edge value (*k*) of the relevant imaging-agent atoms (i.e., iodine, barium, gold, etc.). Thus, it is also possible to do selective X-ray imaging and to differentiate between attenuating materials by fine tuning the energy source to the appropriate absorption edge value.

A CT image is obtained by rotating an X-ray source around an object, with a detector positioned directly opposite the radiation source. Alternatively, in many preclinical CT scanners the object sometimes is rotated around its own axis. Such preclinical scanners are often being used for small animal *in vivo* imaging. Generally, X-ray scans are taken at small angular increments during rotation around the object over 360°. A series of attenuation profiles or projections is thus obtained. The projections are then processed mathematically to create a 3D rendition of the scanned object. An in depth description of the engineering principles underlying modern CT imaging instruments is beyond the scope of this manuscript, and the reader is referred to other published works.[1c,5]

A diagnostic imaging method related to CT is X-ray fluoroscopy. Fluoroscopy allows for the acquisition of real-time, continuous images of the internal organs. Like in CT, imaging agents are often used in fluoroscopy for better contrast resolution. Small iodinated agents are commonly injected into blood vessels for use in fluoroscopic angiography, allowing for the evaluation of blood flow and visualization of the vasculature system, while barium contrast media are introduced orally or with an enema to investigate the anatomy (and pathology) of the gastrointestinal tract.

The introduction of magnetic resonance imaging (MRI) resulted in a loss of interest and reduction in CT contrast agent development throughout the 1980s. However, advances in computer technology, and the introduction and widespread adoption of spiral-CT in the mid-1990s have sparked a revival of interest in CT imaging and CT contrast media. Current clinical CT scanners are capable of acquiring high resolution 3D isotropic images of the body within several minutes. CT imaging today is less time consuming, less expensive, and more readily available than other medical imaging technologies such as MRI and positron emission tomography (PET). In the last several years, the emergence of novel technologies such as dual-source CT, and multi-detector CT has advanced the field of CT imaging even further. As a comparison to X-ray imaging diagnostic methods, PET imaging employs gamma-ray emitting radioactive nuclei “tracers” as contrast agents while MRI takes advantage of nuclear magnetic resonance principles by applying high magnetic fields to align magnetization of certain atomic nuclei. In contrast to CT and PET imaging, MRI uses no ionizing radiation and it is therefore often deemed safer than the other two.

2.0 Contrast agents

Many bodily tissues are easily visualized by CT imaging. The ability of matter to attenuate X-rays is measured in Hounsfield units (HU). By definition, water is assigned a "density value" of 0 HU and air a value of −1000 HU. Attenuation values for most soft tissues fall within 30–100 HU. Notable exceptions are lung tissue with attenuation values approaching −1000 HU (due to high air content) and mineralized tissues such as bone, with attenuation values of approximately 1000 HU. Most CT scanners are calibrated with a reference to water. For a material with a linear X-ray attenuation coefficient "μ" the corresponding HU value is calculated by:

$$HU = \frac{(\mu - \mu_{water})}{(\mu_{water})} \times 1000 \quad (2)$$

where μ_{water} is the linear X-ray attenuation coefficient of water.

While different types of bodily tissues can exhibit contrast, it can be challenging to image and identify the interface between two adjacent tissues (e.g., liver/tumor) or to image soft tissues (e.g., clot) in contact with blood or other physiological fluids. A difference of 50–100 HU can be used to differentiate between some tissue types of interest. But greater differences in CT attenuation will facilitate the process and improve the quality of the images (i.e., greater signal to noise and contrast to noise ratios). Hence, contrast imaging agents are often used and required for better visualization of the tissue of interest by X-ray CT.[6] Consequently, contrast agents that can: 1) increase CT sensitivity and enhance differentiation among different tissues; 2) provide specific biochemical information of a tissue; or 3) enable evaluation of tissue/organ function or performance, are of significant interest and are highly sought after.

Today, an effective diagnostic dose of a contrast agent for CT imaging is in the molar concentration range. For example, an adult patient (weighing approximately 75 kg) undergoing a selective coronary arteriography with left ventriculography will be injected intravenously with ~45 mL of Hexabrix™ (Mallinckrodt Imaging), a common clinically approved iodinated CT imaging agent solution, in a single dose, containing 24 g of ioxaglate (an equivalent to 14.4 g iodine). The total administered amount of Hexabrix™ solution over the course of the procedure may reach up to ~150 mL, totaling 80 g of ioxaglate (an equivalent of 48 g of iodine). The dosage information was obtained from the insert and product label. The high contrast media concentrations required for CT place it at a disadvantage as compared to other imaging techniques such as MRI (mmol conc. range), nuclear imaging (μmol conc. range), and optical imaging (nmol conc. range). As a consequence, the search for an optimal CT contrast agent with maximum imaging capabilities, minimal dose requirements, and reduced toxicity is an ongoing task. We have identified several general requirements that need to be satisfied in the design of a CT contrast agent for clinical applications:

- The contrast agent should improve the visualization of the target tissue by increasing the absolute CT attenuation difference between the target tissue and surrounding tissue and fluids by a factor of ≈ 2×;
- The imaging media should contain a high mol% of the X-ray attenuating atom per agent (molecule, macromolecule, or particle) in order to reduce the volume used and concentrations needed for imaging;
- The tissue retention-time of the contrast agent should be sufficiently long for completion of a CT scan and scheduling the instrument time in the hospital (2 – 4 h);

- The contrast agent should localize or target the tissue of interest and possess favorable biodistribution and pharmacokinetic profiles;
- The contrast agent should be readily soluble or form stable suspensions at aqueous physiological conditions (appropriate pH and osmolality) with low viscosity;
- The contrast agent and its metabolites should be non-toxic; and
- The contrast agent should (for most applications) be cleared from the body in a reasonably short amount of time, usually within several hours (< 24 h).

To fulfill the above stated requirements, various materials and contrast agent designs are currently being proposed and assessed in both clinical and laboratory settings. In this review we summarize the literature and developments in the field of contrast agent research over the past ten years. Specifically, we focus on advances in the fields of iodine- and metal-based imaging agents, including those presented in nanoparticulate format.

3.0 Iodine-based CT contrast agents

In order to achieve higher levels of X-ray attenuation than observed for biological tissue, elements of higher atomic number (Z) are incorporated into the contrast agent molecule. Iodine (Z = 53) has historically been the atom of choice for CT imaging applications. Sodium and lithium iodide were among the first water-soluble imaging agents. However, due to the associated toxicity at the iodine concentrations necessary for imaging they are not suitable for most clinical applications. Consequently, covalently bound iodine provides a better option in contrast media design, as described in the literature.

3.1 Small-molecule iodinated contrast agents

Small-molecule iodinated contrast agents can be separated into two general categories: the “ionic,” and the “non-ionic” molecules. Most ionic iodinated contrast agents studied to date are negatively charged species. Although widely used in the clinic, these ionic iodinated imaging agents possess several inherent disadvantages, compared to non-ionic contrast media.[7] Ionic compounds have a higher tendency to interact with biological structures such as peptides, cell membranes, etc. The aqueous formulations of ionic contrast agent species possess high intrinsic osmolality, potentially leading to renal toxicity and other physiological problems such as vasodilatation, bradycardia, and pulmonary hypertension. Increased pain and sensation of heat at the site of the injection is often reported, as compared to injection of low-osmolality contrast agent formulations.[8] Moreover, use of high-osmolality contrast media *in vivo* results in lower radio-density due to osmotic dilution.

To circumvent the problems associated with high-osmolality, non-ionic iodinated imaging media are used.[7,9] These non-ionic contrast agents possess lower osmolality and exhibit a lower incidence of adverse health-effects.[10] In order to achieve sufficient water solubility at physiological conditions hydrogen bonding hydroxyl and amide functionalities are often introduced into the molecular structure.

In addition to osmolality of the imaging media formulations, attention also needs to be paid to the viscosity of the prepared solutions. High viscosity of the contrast media preparations may make it difficult to deliver the required large volumes in a speedy and facile manner. Moreover, the use of higher-viscosity contrast media has been linked to prolonged retention of the contrast agent in the kidneys with associated renal damage.[11]

Most common small-molecule iodinated contrast agents are low molecular weight (< 2000 Da) iodinated aromatics. Such compounds exhibit higher stability and lower toxicity than iodinated aliphatic molecules. Often two iodinated aromatic rings are covalently joined

together via a linker, thus increasing the iodine atom count per molecule. The two-ring structures generally result in reduced osmolality of the imaging media formulation, at effective X-ray CT imaging media concentrations. However, the formulations of contrast media containing two-ring structures tend to exhibit higher viscosity, compared to formulations of mono-ring contrast agents, at equivalent iodine concentrations. Overall, potential adverse health-effects of ionic vs. non-ionic, high- vs. low-osmolal, high- vs. low-viscosity, and mono- vs. two-ring contrast media designs have been extensively studied over the last 20 years.[10b,11c,d,12]

Over the past few decades, small-molecule iodinated imaging agent design has been highly optimized. This is achieved by exploiting the functional groups present on the aromatic ring (commonly carboxylic acids, or imines) which allow for facile structural modifications. As such the contrast agents' physical, chemical, and pharmacological properties can be manipulated and modified to fit the desired application and its design specifications.

Contrast media today exhibit high water solubility, low binding to biological receptors, low toxicity and high bio-tolerability. A number of such contrast agents (both ionic and non-ionic, and mono- and two-ring structures) are approved for medical use and are administered clinically world-wide (Figure 1, Table 1). To name a few: iohexol (Omnipaque™, GE Healthcare); iopromide (Ultravist™, Bayer Healthcare); iodixanol (Visipaque™, GE Healthcare); ioxaglate (Hexabrix™, Mallinckrodt Imaging); iothalamate (Cysto-Conray II™, Mallinckrodt Imaging); and iopamidol (Isovue™, Bracco Imaging). These contrast agents are produced on a commodity scale of tons per year. The total estimate for worldwide iodinated X-ray contrast agent production was ~3,500 tons in 2000.[13] The synthesis and purification of these contrast agents is optimized to afford high yields in large-scale production. The synthesis of iopamidol from a recent patent is shown in Scheme 1,[14] to serve as an example of the scaled-up chemical reactions that are performed routinely to meet the daily commercial needs.

Regardless of the already well-established contrast agent industry, efforts to improve on the current state of the art with the aim to increase water solubility, to reduce osmolality and viscosity, to introduce tissue targeting, or to enable diagnostic measurements while being mindful of potential health risks such as contrast-induced nephropathy, adverse cardiac events, and renal toxicity are ongoing.[9,15]

With regards to low-viscosity, low-osmolality contrast media, a couple of novel structures are reported with experimental results showing improved physical and pharmacological properties, compared to the currently clinically approved contrast agents (Figure 2).[16] Both iosimenol, and GE-145 improve on the structure of iodixanol and iotrolan (Isovist™, Bayer Healthcare), two currently clinically approved low-osmolality, non-ionic, two-ring, iodinated contrast agents. Iosimenol shows significantly lower viscosity than iodixanol (Table 2), while the viscosity of GE-145 is comparable to the two clinically approved contrast agents. Of note are the osmolality values. Iosimenol, GE-145, and iodixanol all exhibit osmolality results lower than expected. It is believed that this effect may be due to formation of small, temporary, multi-molecular clusters of transient nature in solution.[16e] The lower than predicted osmolality allows for additional electrolytes to be added to the clinical formulation (e.g., sodium and calcium ions), providing a solution more physiological in nature. Thus far both iosimenol and GE-145 show minimal toxicity and encouraging bio-tolerability data, and both are being evaluated in clinical trials.

Of interest to this discussion are two additional classes of iodinated contrast agents – the proposed application of 1,3,5-trialkyl-2,4,6-triodobenzenes as gastrointestinal imaging media, and phosphonate/peptide conjugated iodobenzene derivatives as potential targeted

imaging agents (Figure 3).[17] While barium sulfate is the most prevalent contrast media for imaging of gastrointestinal tract, alternative contrast agents have been sought. Within a library of thirteen synthesized and tested derivatives of 1,3,5-trialkyl-2,4,6-triodobenzene, 1,3,5-tri-*n*-hexyl-2,4,6-triodobenzene was shown to be the optimal structural candidate.[17a] The latter derivative exhibited the lowest observed toxicity *in vivo*, in rodents, by both oral and intraperitoneal mode of delivery. The substance is an oil at 25 °C and is intended for oral administration as an oil-in-water emulsion. No metabolism of 1,3,5-tri-*n*-hexyl-2,4,6-triodobenzene was detected in rat, hamster, dog, and monkey, indicating poor absorption. The ingested emulsion demonstrated excellent mucosal coating and improved radiodensity, compared to barium sulfate.

A small library of contrast agents with potential specific-tissue targeting capability are reported, using di- and tri-iodinated aromatics that are conjugated with short peptide chains and phosphonate groups.[17b] The peptide chain can be modified to selectively target a tissue or small biological structures. However, no follow-up studies using the prepared imaging media *in vivo* have been published thus far.

To provide qualitative and quantitative information on the biochemical state of a tissue, the extent of disease, or structural damage, research groups are investigating ionic contrast agent as functional CT imaging media. For example, several novel anionic CT contrast agents with Ca^{2+} ion chelating capability are reported as targeted imaging media for identification of microdamage in bone tissue. The structure of one such agent is shown in Figure 4a.[18] Preliminary studies on bovine cortical bone specimens *ex vivo* show good contrast enhancement when using the contrast agent in a powdered form. However, differentiation between bone and contrast agent proves difficult when the contrast agent is used as an aqueous solution, possibly due to beam hardening effect of bone tissue. There exists a possibility that differentiation could be improved using dual-energy-CT. Further optimization of the imaging media for use in solution phase is ongoing.

With regards to characterizing tissue composition and function, several recent reports describe the evaluation of cartilage tissue.[19] Articular cartilage contains negatively charged glycosaminoglycan (GAG) polysaccharide chains (typically 5–10 wt. %) and it is known that a reduction in this GAG concentration is an early indicator of osteoarthritis. Consequently, methods to detect and quantify the GAG content are desired. High correlation (typically $R^2 > 0.75$) between the GAGs found in *ex vivo* cartilage tissue samples and the CT attenuation can be obtained using commercially available anionic CT agents such as ioxaglate, iothalamate with concentrations typically greater than 80 mg of iodine per milliliter (mg I/mL).[20] This approach relies on the diffusion of the anionic contrast agent into the cartilage in inverse proportion to the negatively charged GAGs. In addition to characterizing the biochemical composition of cartilage, evaluating the biomechanical properties is also of interest. A study using iothalamate on mated osteochondral plugs, excised from bovine patella-femoral joints describes the variation in X-ray attenuation. Measured by peripheral quantitative computed tomography (pQCT), the variation in CT attenuation accounts for 93% of the variation in the equilibrium compressive modulus.[21]

To exploit the potential of intermolecular coulombic interactions, and to increase sensitivity and tissue differentiation capability, new cationic iodinated imaging agents are described and an example of one such agent is shown in Figure 4b.[21–22] Due to the favorable electrostatic interactions between the cationic contrast agent and the GAG chains, the contrast agent is retained in the cartilage, allowing for improved CT imaging results as compared to commercially available imaging media possessing an overall negative molecular charge, which are repelled from cartilage tissue. As shown in Figure 5, the cationic contrast agent CA4+ achieves higher equilibrium concentrations in the tissue,

allowing for facile differentiation between bone and cartilage, as well as mapping the heterogeneous state of GAG within the cartilage. Specifically, the CA4+ affords 2.9-times higher mean attenuation values for cartilage compared to ioxaglate. Additional studies using *ex vivo* bovine osteochondral plugs with varying amounts of GAG content show a high correlation between GAG content and CT attenuation as shown in Figure 6.[23] Cationic CT imaging media for cartilage imaging may thus allow for better clinical diagnostics in joint damage and joint disease, such as osteoarthritis.

The inherent high intrinsic osmolality of ionic contrast agents has often been associated with adverse health effects in patients. While this is of concern, the several-fold lower required effective concentration of cationic agent CA4+ “per dose” (as compared to ioxaglate) may potentially reduce adverse side-effects of this imaging media, as the solution can be made iso-osmolal with respect to synovial fluid. Moreover, as the CA4+ is delivered by intra-articular injection into the synovial cavity, significantly less contrast agent is required for imaging (36 mg I). Preliminary studies after intraarticular injection of CA4+ show no adverse reaction, and the H&E stained histological sections of cartilage tissue samples reveal no negative outcomes with results comparable to ioxaglate.[24]

Outlook—While current clinically approved small-molecule iodinated CT contrast agents (see Table 1) offer safety and imaging efficacy, they do suffer from several drawbacks, which prevent them from being used for all applications:

- they exhibit non-specific biodistribution;
- due to their relatively small size they tend to undergo rapid renal clearance from the body;
- the often high osmolality and/or high viscosity of the contrast media formulations can lead to renal toxicity[12c,25] and adverse physiological effects;[11c,d,26]
- high “per dose” concentrations are required; and
- high rates of extravasation and equilibration between intravascular and extravascular compartments at the capillary level often make it difficult to obtain meaningful and clear CT images.[6a,6d,27]

While development will continue on improving the physical and toxicological characteristics of small-molecule iodinated contrast agents, future developments should focus on designing, synthesizing and evaluating tissue/organ-specific small molecule contrast agents. New imaging media should also offer information on the biochemical composition, mechanical properties, and overall tissue health in addition to morphological assessment. Such CT agents may lead to more effective imaging modalities for the evaluation of new drug and surgical treatments through *ex vivo* and *in vivo* pre-clinical studies, as well as advances in patient clinical care.

3.2 Nanoparticulate iodine-containing contrast agents

Contrast media exhibiting long blood circulation times are called “blood-pool” agents. Nanosized contrast agents are proposed as one possible solution to increase the blood residence time, and to reduce the rate of renal clearance, and “leakage” across the capillary vessels.[6a,6d] Various approaches and compositions are being explored in the development of nanoparticulate contrast agents, including: nanosuspensions, nanoemulsions, microspheres,[6h] liposomes, micelles, polymeric particles, nanospheres, and nanocapsules. Early in the research activities, it was observed that nanoparticles of larger sizes (greater than 400 nm) are preferentially taken up by macrophage cells. This is due to the process of nanoparticle opsonization. Consequently, high concentrations of nanoparticulate imaging

agents (and corresponding CT image enhancement) are observed in liver, spleen, and lymphatic tissues, which possess high concentrations of phagocytic cells. While phagocyte uptake can in certain cases be desirable, it also can lead to causation of flu- and allergy-like symptoms in animals and in humans.[6d,28] Recently, an immune response to certain nanoparticulate drug (or contrast media) formulations, called "complement activation-related pseudoallergy" (CARPA), has come to increased attention.[29] CARPA represents a subcategory of acute (type I) hypersensitivity reactions. In most patients the symptoms are mild, transient, and preventable by applying appropriate precautions. However, in some patients CARPA can manifest in a severe or even a lethal way. Since the main manifestation of CARPA is cardio-pulmonary distress, it is of particular concern in patients that already suffer from cardiac problems. CARPA is thought to be triggered by nanoparticles (e.g., liposomes, lipid-complexes, nanocapsules, nano-micelles, nano-emulsions, etc.) mimicking the size and shape of pathogenic microbes, and subcellular organelles. Because of the many potential side-effects, use of nanoparticulate iodinated contrast media in clinical applications presents significant challenges. However, it is reported that by carefully controlling nanoparticle composition, charge, and size it is possible to reduce the chances of an unwanted physiological response, while at the same time optimizing the radiopacity properties of the nanoparticulate contrast media.[30]

3.2.1 Liposomal contrast agents—Liposomes, spherical nanoparticles composed of a lipid bilayer and an aqueous inner core, have long been of interest in CT contrast media research.[31] Generally, liposomes serve as a vehicle for small-molecule, water-soluble iodinated contrast agents. Initial attempts at formulating an effective liposomal contrast agent suffered from side-effects associated with the rapid uptake of the liposomes by the phagocytes of reticulo-endothelial system (RES), and by leakage of the encapsulated iodinated material from the liposomes, causing potential renal issues.[28b,32] More recently, the use of the so called "stealth liposomes" (PEG-containing liposomes)[30a,33] and careful control of liposome size is achieving longer blood circulation times of the nanoparticles, as well as a slower rate of uptake by the RES cells.

Stealth liposomes containing iohexol,[30a,34] or iodixanol[32a] are described as effective blood-pool contrast media. Liposomes measuring ~100 nm in size exhibit prolonged blood circulation times in rodents and a slow uptake by phagocytes. Good visualization of vasculature and cardiac structure is obtained when using the media, especially when compared to imaging with "free" non-liposomal iodixanol, which is rapidly cleared from the body within minutes. Moreover, these liposomes are shown to be of use in detecting pulmonary embolisms,[34] and in monitoring subsequent embolism resolution in real time, following injection of tissue plasminogen activator in a rabbit model. The liposomes are eventually cleared from the blood via RES rather than through renal filtration. This can lower the risk of nephrotoxicity, especially when multiple repeat imaging sessions are required, making liposomal contrast media a viable alternative for CT imaging in at risk patients who are contraindicated for administration of regular small-molecule imaging media.

"Nanoparticles preferentially accumulate in solid tumors by means of passive convective transport through leaky endothelium (extravasation) that is caused by pores varying from approximately 100 to 800 nm in size. The phenomenon is termed the 'enhanced permeation and retention effect.'"[35] As such, PEGylated liposomes, of 100 nm in size, carrying iodinated contrast agents such as iopamidol, or iodixanol can be used as blood-pool imaging agents for visualization of breast tumor lesions (Figure 7).[35–36] Utility of these liposomal contrast agents for imaging of tumor angiogenesis is successfully demonstrated in rodents. Enhancement of tumor microvasculature is observed and the X-ray data obtained can be used to predict the proper therapeutic dosage and the effectiveness of chemotherapeutic

treatment by liposomal drug delivery vehicles (carrying the chemotherapeutic drug doxorubicin).[35,36d]

Intercellular adhesion molecule 1 (ICAM-1) is expressed preferentially on the surface of inflamed endothelial cells during the early stages of atherosclerosis. It has been shown that ICAM-1 expression can be used to predict cardiovascular risk (myocardial infarction). Iohexol-carrying stealth liposomes covalently labeled with ICAM-1 monoclonal antibodies can be used to image atherosclerotic plaques *in vitro*. These so called "immunoliposomes" exhibit an average size of 140 nm. Preliminary *in vitro* results with human coronary artery endothelial cells (HCAEC) show 4-fold higher binding levels of the labeled liposomes to the activated HCAEC vs. the non-activated HCAEC, and a 10-fold increase in binding specificity for labeled liposomes as compared to non-labeled liposomes, to activated HCAEC cells.[37]

Liposomes with iodine covalently incorporated into the lipid bilayer structure are described as an alternative contrast media design, and an example is shown in Figure 8.[38] The liposomes are prepared with a modified phosphatidylcholine lipid commonly used in liposome formulations, (*E*)-10,11-diiodoundec-10-enoic acid. Initial characterization studies on the particles *in vitro* reveal formation of structures between 50 to 150 nm in diameter. Since this particular class of iodinated liposomes contains an empty inner cavity, these nanoparticles may show potential for encapsulation of additional pharmaceutical agents, acting simultaneously both as drug delivery vehicles and as CT imaging media. A 5 mg/mL suspension of these liposomes contains ~1.4 mg I/mL. The maximum stable concentration achieved for these iodo-liposomes is estimated at 120 mg/mL, resulting in iodine concentration of ~34 mg I/mL. The relatively low iodine content, however, can be augmented by co-encapsulation of a conventional small-molecule contrast agent such as iohexol. The authors estimate the encapsulation efficiency of iohexol to be ~20%, thus the resulting contrast media possess sufficient radiopacity for CT imaging applications. However, further studies showing successful application of this class of contrast media and performance *in vivo* are necessary.

Liposomes co-loaded with water-soluble iopamidol and water-insoluble iodinated poppy-seed oil (with trade names lipiodol or Ethiodol™, Guerbet) can be utilized as RES targeted contrast media.[39] The co-loaded nanoparticles measure 280 nm in diameter. They contain high iodine concentrations due to the iodinated oil being incorporated into the liposomal membrane, in addition to the encapsulated iopamidol in the liposome core cavity. The contrast agent exhibits high uptake by the spleen and liver RES in rats. The RES uptake of the lipiodol/iopamidol co-loaded particles is higher than that observed for liposomes containing only iopamidol. High mol% of iodine per liposome and enhanced phagocyte uptake suggest that these co-loaded liposomes are a good choice for imaging of RES-rich organs.

Another example of advantageous RES uptake can be found in imaging of hepatic metastases.[40] Most hepatic metastatic lesions do not contain any phagocytic Kupffer cells. By using macrophage activating nanoparticulate contrast agents, it is possible to obtain an enhanced CT image of the liver, showing the location, size, and number of metastatic lesions, which are identified due to lack of imaging agent uptake.[6a] Iomeprol (trade name Imeron™, Bracco Imaging) loaded liposomes of ~400 nm are reported to allow for prolonged blood residence time of the contrast agent, as well as an enhanced RES uptake at the liver and spleen in mice, resulting in a good CT contrast differentiation between healthy and metastatic liver tissue.

Liposomes combining multiple imaging modalities are also being explored. Stealth liposomes carrying both an iodine-based CT contrast agent iohexol and a gadolinium-based MRI contrast agent gadoteridol (trade name ProHance™, Bracco Imaging) are reported as dual-modality nanoparticulate imaging media.[41] The liposomes measure 70–85 nm in size and exhibit a blood-pool half-life of several days in rabbits. This contrast media is used to obtain enhanced CT and MRI images of vasculature in small animal models. As tumor vasculature generally exhibits enhanced leakage and extravasation rates, the prolonged blood circulation time of this imaging agent enables detection and observation of tumors in rabbits, by following the localized increase (due to enhanced capillary leakage) of the contrast media concentration.

3.2.2 Nanosuspensions, nanoemulsions and nanocapsules—Nanosuspensions are colloidal dispersions of pure (water-insoluble) drug particles stabilized by surfactants.[42] An example of such, 6-ethoxy-6-oxohexyl 3,5-diacetamido-2,4,6-triiodobenzoate (trade name N1177, Nanoscan Imaging) is a water-insoluble surfactant-stabilized crystalline substance designed as a macrophage-targeting CT contrast agent (Figure 9).[43] An N1177 nanosuspension with a mean particle size of 259 nm is successfully used to identify atherosclerotic plaques in a rabbit cardiovascular system. An atherosclerotic plaque with high macrophage density is at higher risk of rupture and arterial thrombosis. Hence, CT contrast enhancement of potential at risk plaques makes N1177 nanosuspensions an attractive diagnostic tool for detection and prevention of arterial thrombosis and other cardiovascular problems.[43–44] An alternative use of N1177 is demonstrated in a study where N1177 is delivered in a form of a NanoCluster aerosol (by way of insufflation and inhalation) to the lungs of rats.[45] The aerosol particles measuring 1–5 μm in diameter show significant contrast enhancement of lung tissue. While use of micron-sized particles *in vivo* may present challenges due to potential adverse health effects, the rats in the study did not exhibit any observable acute toxicity.

Nanoemulsions[46] are stable nanostructures of one liquid material within an immiscible second liquid (e.g., oil in water). Nanoemulsions of lipid-soluble iodinated CT contrast agents are a promising approach to nanoparticulate imaging media. The ethiodized oil nanoemulsion, trade name lipiodol, is one of the earliest successful nanoparticulate contrast agents. Lipiodol (also known under trade names EOE-13; and Ethiodol™, Guerbet) is a low-viscosity, aliphatic iodinated contrast media manufactured from poppy-seed oil (mostly mono-, di-, and tri-iodinated ethyl esters of linoleic, oleic, palmitic, and stearic acids).[47] Lipiodol is approved for clinical use and is indicated for use as a radio-opaque medium for hysterosalpingography and lymphography, and in certain cases for imaging of liver lesions. Administration of lipiodol via general i.v., i.a., or i.p. mode is not advised. The contrast agent is generally administered in a localized manner to the imaged tissue.

Lipiodol is also indicated for use in interventional radiology procedures, namely in chemoembolization of hepatocellular carcinoma (HC). Primary HC is one of the most common liver malignancies in the world. Chronic infection with hepatitis B or C is the most important risk factor for HC. Patients with HC have a five-year survival rate of less than 5%. For many patients, transplantation or surgical resection is not an option. For these patients, Lipiodol + chemotherapeutic agent (e.g., cisplatin, doxorubicin) formulations are one promising approach that remains.[48] Recent studies show that injection of radioactively labeled ^{131}I-lipiodol or ^{188}Re labeled lipiodol through hepatic artery allows for target- and site-specific delivery of the radio-therapeutic (RT) agent to HC lesions. The therapy shows good tolerance in patients with an increased 5-year survival rate of up to 25%.[49]

Additionally, lipiodol can be used as a CT imaging agent for the liver and spleen in animal models.[28c] A lipiodol nanoemulsion formulation with average particle size of less than 150

nm exhibits prolonged blood circulation times with subsequent uptake by the phagocytic cells in liver and spleen, and it can be used for hepatic tumor imaging. Due to the differences in phagocyte content of healthy and metastatic liver tissue, the contrast enhancement of hepatoma is clearly observable.

For some time, 1,3-disubstituted polyiodinated triglycerides (ITG) have been reported to be efficient nanoemulsion type contrast media.[28a,50] Unlike most other nanoparticulate contrast agents, ITG contrast agents do not trigger the phagocytosis mechanism. This biological response is due to the ITG mimicking the chylomicron remnant particles, which are a part of the body's lipid metabolism. ITG are hepatocyte selective contrast agents and are metabolized by lipolytic liver enzymes and eliminated through bile. Several studies document using ITG nanoemulsions as hepatocyte targeting contrast media in rat,[51] dog,[50a] rabbit,[52] and mouse models.[53] In these studies the particle size is generally kept below 200 nm in order to reduce the chances of macrophage activation. By altering the length of the chain containing the iodinated aromatic structure of the ITG, it is possible to affect the half-life of the contrast agent in the liver.[50b] The shorter chain-length derivatives exhibit slower metabolism and clearance from the liver than longer-chain derivatives, with half-lives ranging from ~48 h for the shortest-chain ($n_{\text{-}CH2\text{-}}$ = 1) analog to ~3 h for the longest-chain ($n_{\text{-}CH2\text{-}}$ = 6) analog. Imaging of vasculature and cardiac structure is possible when ITG nanoemulsions are formulated to provide for extended blood circulation times, by using stealth PEG-formulations of the contrast agent.[52,53b,54] Moreover, successful imaging of lymph nodes in dogs is described following subcutaneous injection of a stealth ITG nanoemulsion with particles of ~90 nm in size.[55]

Two ITG formulations are commercially available under the trade names Fenestra LC™ and Fenestra VC™ (ART Inc.).[6d] Fenestra LC™ is a non-stealth nanoemulsion formulation with a shorter blood circulation time and faster hepatocyte uptake, indicated for hepatobiliary system and liver function imaging. Fenestra VC™ is a stealth blood-pool nanoemulsion formulation of the identical contrast agent, generally used for imaging of vasculature and for applications requiring prolonged blood-circulation times of the imaging media.

The use of poly(butadiene)-*b*-poly (ethylene oxide) (PBD-PEO) block-copolymer stabilized nanoemulsion of 3,7-dimethyloctyl-2,3,5-triiodobenzoate oil is reported as a novel CT blood-pool contrast agent formulation (Figure 10).[30b] Particles of ≤ 100 nm in size are prepared using the iodinated oil and PBD-PEO. The resulting nanoemulsion contrast medium shows no appreciable cytotoxicity (A431 cell line) and has good *in vivo* stability in mice, similar to the commercially available imaging agent Fenestra VC™. Prolonged blood circulation time, followed by eventual uptake of the nanoparticles by spleen and liver tissues is observed.

Nanocapsules are stable nanoparticles consisting of a crosslinked polymeric membrane enveloping a payload-material that is often insoluble/immiscible with the surrounding solvent. The polymeric shell provides favorable interactions (enhanced solubility) with the surrounding solvent, allowing for the immiscible nanocapsule-payload to be used in aqueous solution. Nanocapsules can be formed by crosslinking Pluronic™ F127 polymer (serving as a nanocapsule membrane) around lipiodol oil nanodroplets.[56] The encapsulation is achieved by means of emulsification-sonication in a biphasic (water:DCM) system, with dropwise addition of the activated-Pluronic™ polymer and lipiodol oil to the water phase, containing amine-PEG, at pH > 9. In cytotoxicity studies (A549 cell line) the nanomaterial exhibits cell viability comparable to that of the clinically approved contrast agent iopromide. Use of the nanocapsule contrast agent (average particle size of 160 nm) provides good image enhancement of the cardiovascular system in a mouse. Eventually, the nanocapsules are taken up by phagocytic cells in liver and lymph nodes.

3.2.3 Polymeric nanoparticles—An alternative approach to the preparation of iodine-containing nanoparticles is the synthesis of iodinated polymers. Macromolecular synthetic approaches to CT imaging agents possess intrinsic advantages. Covalent incorporation of iodine containing moieties into a macromolecular structure prevents leakage and loss of contrast agent from the nanoparticle. Synthetic macromolecules also permit formation of stable particles of a controlled size. Moreover, the range of available polymer structural types allows for design of a variety of imaging media with favorable properties.

Using an emulsion co-polymerization technique, 2-methacryloyloxyethyl-2,3,5-triiodobenzoate (MAOETIB) – glycidyl methacrylate (GMA), based nanoparticles are described as potential macrophage-targeting CT contrast agents. The nanoparticles are between 30 and 50 nm in average size, and appear stable to agglomeration at physiological conditions. Following an i.v. administration the nanoparticles exhibit prolonged blood-pool residence time, and subsequently show significant uptake by macrophages and allow for enhanced liver, spleen, and lymph node imaging in rat and mice models (Scheme 2).[57]

Poly(vinyl alcohol) microparticles with iopamidol physically encapsulated in the structure are also reported as potential X-ray imaging flow-tracers.[58] A set of particulate contrast agents ranging in size from 1–5 μm and containing 50% wt. or 90% wt. iopamidol is reported. The imaging agents show good stability in water, have no appreciable cytotoxicity (A549 human lung carcinoma cell line), and exhibit CT attenuation comparable to pure iopamidol at equivalent iodine concentrations. The microparticles may serve as a platform for future studies on CT imaging flow-tracers in various biomedical applications; however, the *in vivo* use of these micron-sized particles may be complicated by capillary occlusion.

Amphiphilic polymers tend to spontaneously form relatively stable nanomicelles[6c,59] in aqueous media. Aliphatic 2,3,5-triiodobenzoyl substituted poly-*L*-lysine/MPEG copolymer is reported as an excellent stealth blood-pool CT agent (Figure 11).[60] The nanomicellar particles sufficiently large in diameter (10–80 nm) to avoid renal clearance from the blood, but small enough not to activate the rapid macrophage uptake, show prolonged blood circulation times in rabbits and rats. They are eventually taken up and metabolized by the liver.

In contrast to conventional polymers, dendrimers offer highly ordered structure, stability, and low polydispersity values. Depending on the molecular composition they can be tailored to exhibit high water solubility and good biocompatibility. Evaluation of a set of symmetrical iodinated bowtie polymers, as CT contrast media, is described in a recent report (Figure 12).[61] Macromolecules containing a PEG-core and a poly-*L*-lysine dendron at each end are functionalized with iobitridol (trade name Xenetix™, Guerbet) moieties. A generation-4 dendrimer with a PEG-12,000 Da core shows favorable physical properties, low toxicity and prolonged blood circulation times (as compared to iohexol contrast agent), and can be applied to observe tumor angiogenesis in rats.[62] High quality CT angiographic images can be obtained for a prolonged time (upwards of 30 min) and serial quantitative changes in vascular leakiness at tumor sites can be observed following the administration of an angiogenesis inhibition drug over a 9-day-treatment regimen.

Another example of the dendrimer approach comes from a report of a 4th generation starburst PAMAM dendrimer labeled with a water-soluble, triiodobenzene amino acid derivative (Figure 12). This dendrimer design is envisioned as a potential blood-pool contrast agent.[63] However, follow-up studies evaluating the imaging agent toxicity, and performance *in vivo* or *ex vivo* are not yet published.

As an alternative to conventional polymers and dendrimers, a new metal-based coordination-polymer is described as a potential CT contrast media. A pair of iodinated coordination-polymers is prepared from 2,3,5,6-tetraiodo-1,4-benzenedicarboxylic acid and Zn^{2+}, or Cu^{2+}, as bridging ions.[64] The compounds form "one-dimensional" crystalline polymeric metal-organic structures with sizes between 200 to 600 nm. The material exhibits X-ray attenuation properties *in vitro*, comparable to those of the iodixanol CT contrast agent. Toxicity, biodistribution, and potential applications of such imaging media *in vivo*, however, are not yet been reported.

Outlook: Diverse approaches to nanoparticulate iodinated CT contrast media design allow us to tailor the unique properties of nanoparticulate contrast agents to suit the intended applications. In general, the nanoparticulate iodinated contrast agents demonstrate significantly prolonged blood circulation times, as compared to small-molecule iodinated contrast agents, and are used to enhance CT imaging of vasculature and the cardiac system. Of particular importance is the observation that nanoparticles of larger sizes are preferentially taken up by macrophage cells. This latter property can be successfully exploited (and the undesired side-effects curtailed) to selectively target and image phagocyte rich organs and tissues (e.g., as spleen and liver). It can also allow us to avoid or reduce nephrotoxicity that is associated with the use of small-molecule CT imaging agents, thus making it possible to attain CT images in patients who are at risk for renal complications. The nanosize imaging agents also show potential for improved CT detection and imaging of tumors. Moreover, some studies have shown the utility of such agents in real-time monitoring of disease development and the progress of the relevant treatment regimen.

All of the CT imaging agents discussed in the preceding text utilize iodine as the attenuating atom, however. The relatively moderate atomic number of iodine, the absorption spectrum, and the suboptimal absorption edge value (k = 33 keV) for the 120–130 kVp employed by many current CT scanners (along with current detectors) leave iodine-based CT imaging agents at a disadvantage compared to other potential contrast agent media (discussed in the subsequent sections in this manuscript) in terms of X-ray attenuation capabilities and overall performance.

4.0 Lanthanide-based contrast agents

Lanthanide-based contrast agents are commonly used in MRI imaging, but their use as CT contrast agents is also being explored given their high atomic numbers. Free lanthanide ions are extremely toxic. For example, the toxicity of Gd^{3+} partly stems from the fact that its ionic radius is 0.99 Å, very close to ionic radius of Ca^{2+} (1.00 Å). Consequently, Gd^{3+} can compete with Ca^{2+} in biological systems and alter the biological processes. However, many lanthanides form highly stable (and non-toxic) polyaminocarboxylic acid chelate complexes. Gadolinium (Z = 64), dysprosium (Z = 66), and ytterbium (Z = 70) form some of the most stable of such complexes ($\log_{10} k$ = 22 or higher).[65] Lanthanide ions commonly form complexes with oxidation state of +3, and several lanthanide ion complexes, such as with Gd^{3+} and Dy^{3+} are contrast agents for MRI applications due to their unique magnetic properties. Moreover, many lanthanides also exhibit luminescence in the visible or near infrared region enabling their use for *ex vivo* and *in vivo* fluorescence measurements.

Most clinically approved lanthanide-based contrast agents are gadolinium chelates. Some examples (Table 3) include: gadoversetamide (OptiMARK™, Mallinckrodt Imaging), gadopentetate dimeglumine (Magnevist™, Bayer Healthcare), gadobutrol (Gadovist™, Bayer Healthcare), gadobenate dimeglumine (MultiHance™, Bracco Imaging), gadoterate meglumine (Dotarem™, Guerbet), gadoxetate disodium (Eovist™, Bayer Healthcare).

Clinically approved gadolinium-based MRI contrast agents can be used for successful CT imaging of the cardiovascular system, and for pulmonary and aortic angiography.[66] For example, Dy-EOB-DTPA [(4*S*)-4-(4-ethoxybenzyl)-3,6,9-tris(carboxylatomethyl)-3,6,9-triazaundecanedioic acid, dysprosium (Dy) complex, disodium salt] is used as a liver-specific MRI or CT contrast agent.[67] Additionally, a gadolinium analog, gadoxetate disodium salt (Gd-EOB-DTPA disodium salt), is now clinically approved under the brand name Eovist™ (Bayer Healthcare) as a liver-specific contrast agent (Figure 13).[68]

While all Gd compounds can by their very nature serve as dual-modality MRI/CT contrast media, preparing improved multimodal lanthanide based agents is an active field of study. One avenue to pursue is to take advantage of the photophysical properties of certain lanthanide ions such as Eu^{3+} and Tb^{3+} to act as imaging agents and sensors. For example, the development and evaluation of several chelate designs to detect microdamage in bovine tibia bones *ex vivo* by means of fluorescence scanning microscopy is reported.[69] The general design of these lanthanide chelating ligands employs a macrocyclic amine, a covalently attached antenna (e.g., naphthalene, phenyl), and one or more Ca^{2+}-binding aminodiacetate arms. As expected by incorporating a Gd^{3+} ion into the ligand structure, the authors show the applicability of the ligands for preparation of MRI/CT agents as well. The toxicity studies and applications for these multi-modal lanthanide imaging media *in vivo*, however, are not yet reported.

Alongside small-molecule lanthanide agents, several macromolecular and nanoparticle lanthanide based CT imaging media designs are being explored. A DTPA-conjugated dextran polymer is described as a macromolecular lanthanide-complexing imaging agent (Figure 14). Attempts at preparing dextran conjugated CT contrast agents have previously resulted in crosslinking of the dextran polymer and consequent nanoparticle insolubility. However, both Gd and Dy based agents can be prepared as reported, and used as CT contrast media for imaging of vasculature and tumors in animal models (Figure 15).[70] The mean macromolecular diameter of the [Gd]DTPA-dextran agent is 18 nm. The advantage of such contrast media is the longer blood circulation time as compared to common clinically approved lanthanide-based imaging agents. It is worth noting that (through selecting the optimal molecular weight of the dextran polymer: 40,000 Da) the contrast agent does not get rapidly taken-up by the macrophages, an issue often observed for nanoparticulate CT contrast agents, sometimes hindering their use *in vivo* applications.

Many nanoparticle lanthanide CT agents are designed as multimodal imaging media. As an example, multimodal fluorescent/MRI/CT nanoparticles are described.[71] These particles of ~100 nm are prepared using a ruthenium/SiO_2 particle core, which is labeled with Gd contrast agent [Ru(bpy):Gd^{III}/SiO_2], and their imaging performance is assessed *in vitro*. To assess the CT imaging properties, the nanoparticles were directly compared to iohexol at an equivalent concentration. The results show a somewhat lower attenuation for the nanoparticles as compared to the commercial contrast agent. However, further optimization of the nanomaterial is ongoing. Alternatively, hydroxyapatite nanocrystals (nHAp) can be doped with high quantities of Eu^{3+} and Gd^{3+} ions to prepare a multimodal fluorescence/MRI/CT contrast agent, with particles averaging 30 nm in size. The cytotoxicity studies (HUVEC, KB, A549, and L929 cell lines) of the contrast media *in vitro* show good cell viability along with excellent image enhancement for all three modalities.[72] These types of agents are of interest as a single injection of the contrast agent would enable imaging via several different instruments.

Alternatively, nanoparticles containing a rare-earth core (consisting of a mixture of lanthanides such as Gd, Yb, Er, Tm and yttrium), and conjugated with additional X-ray attenuating material such as gold or iodine are being explored as multimodal (CT/MRI/

upconversion-fluorescence) nanoparticulate contrast media.[73] The particles are prepared by coating the rare-earths core (~25–28 nm in size) with amine-functionalized SiO_2 shell, and then grafting the particle with PEG-moieties and additional X-ray CT media (e.g., 5-amino-2,4,6-triiodoisophthalic acid,[73a] or ~2 nm gold nanoparticles[73b]). These silica coatings are an alternative to polymer coatings. Their thickness can be readily controlled and they exhibit good biocompatibility, and are stable to high-energy nanosecond laser irradiation. The hydrodynamic volumes of the particles are shown as 54 nm and 113 nm, for the iodine- and gold-containing media respectively. These contrast media are found to be non-toxic in cell culture (HeLa, or MCF-7 cells). The particles show good upconversion-fluorescence properties *in vivo* in subcutaneous tissue and can even be optically detected after injection in the abdominal cavity of mice. Following an i.v. injection of the contrast media the nanoparticles are shown to accumulate in the liver, signifying uptake by RES cells.

Outlook

Along with high atomic numbers, lanthanide atoms possess higher *k* absorption edge values than iodine (50 keV for Gd, and 54 keV for Dy), allowing for increased CT instrument sensitivity. Lanthanide atoms thus offer higher X-ray attenuation and higher CT sensitivity on a “per mol” basis as compared to the iodine atoms. However, the molar concentration of Gd in commercially available contrast agents for MRI imaging is generally much lower than molar concentration of iodine in clinically approved CT imaging agents, resulting in lower X-ray attenuation properties of Gd agents on a “per dose” basis and the unit dose will need to be significantly increased for CT application. But the lanthanide agents are better CT agents on a “per mole” basis.

Gadolinium ions generally form very thermodynamically stable chelates. Gadolinium chelate agents are normally considered clinically safe for MRI use. However, some recent data shows that in certain at-risk patients gadolinium imaging media can be a cause of nephrotoxicity and a rare disorder, nephrogenic systemic fibrosis (NSF).[74] A closer look at the underlying problem and better understanding of the Gd-chelate chemistry reveals that the toxicity of the Gd-complexes in a physiological setting is directly related not so much to the thermodynamic stability of the chelate complex, but rather to the kinetic stability of the complexes.[65b,75] Moreover, it is known that Gd-chelates with macrocyclic ligands (e.g., gadobutrol and gadoterate), while possessing lower thermodynamic stability, tend to be more kinetically stable than the Gd-chelates utilizing linear ligands (e.g., gadoversetamide and gadopentetate). This kinetic stability of the macrocyclic Gd-complexes ensures virtually no free Gd^{3+} ion is released from the chelate within the time frame of the MRI scan and excretion from the body. It is of note however, that not all macrocyclic Gd-complexes are more inert than the linear Gd-complexes. Future toxicity and pharmacokinetic studies on Gd contrast agents are needed at concentrations relevant to CT imaging, since higher doses might exacerbate already known health concerns (such as NSF).

Overall, Gd-based agents may offer an alternative for CT imaging of patients that are contraindicated for iodine-based imaging agents. Gadolinium based agents are currently about 4 to 5 times as expensive per “mL’ of media as non-ionic iodinated contrast agents. However, it is of interest to the discussion that a recent analysis comparing equal-attenuating doses of iodinated media vs. gadolinium-containing media had concluded that the cost of using gadolinium-based media could be up to 20 fold-higher than when non-ionic iodinated media are used in a CT imaging procedure.[74e]

5.0 Gold nanoparticle contrast agents

Gold nanoparticles (AuNPs) are an ideal radiopaque nanoparticulate contrast media since gold has both a high density and a high atomic number, and thus AuNPs will possess favorable X-ray attenuating properties. Gold provides about 2.7 times greater contrast per unit weight than iodine.[26] AuNPs are and have been investigated for many years in various biological applications. This is partly due to the relative ease of synthesis and good control over their size, ease of surface modification with various biologically or diagnostically important molecules, and good bio-tolerability and non-toxicity.

Some of the simpler contrast media designs are PEGylated AuNPs. Such AuNPs exhibit prolonged blood circulation times and are successfully used in rodents to image the cardiovascular system.[76] These nanoparticles of ~30 nm in diameter also accumulate in phagocytic cells of the liver and spleen, consequently providing a potential imaging agent for identification of hepatocellular carcinoma. No appreciable cytotoxicity by the nanoparticles in an *in vitro* assay (cell types: WI-38, HepG2, RAW 264.7) is reported.

Dendrimer (PAMAM) entrapped AuNPs[77] and entrapped silver nanoparticles (AgNPs)[78] are also described as potential CT contrast agents. Such dendrimer contrast agents provide a high number of modifiable surface groups for conjugation with cell targeting molecules. The particles exhibit high stability in different media and under different pH and temperature conditions. Acetylated, as well as PEGylated, dendritic nanoparticles, 4–15 nm in size, show better “per mol” X-ray attenuation as compared to commercially available iodinated contrast agents (iohexol, or iopamidol) in a mouse model. The use of acetylated generation-5 PAMAM dendrimer entrapped AuNPs with an average diameter of 2.6 nm, to image SPC-A1 (a human lung adenocarcinoma cell line) tumors *in vivo* is also reported.[79] The cytotoxicity studies on these nanomaterials show minimal cytotoxicity. The AuNPs are delivered to the tumor site in mice via an intratumoral, or intraperitoneal injection. The AuNPs are initially taken up by the tumor cells allowing for acquisition of a CT image, and are subsequently accumulated in the spleen and liver. Recently, an approach to dendrimer entrapped AuNPs, that combines both Au and diatrizoic acid (DTA) is reported as an enhanced gold/iodine CT contrast agent.[80] Generation-5 PAMAM dendrimers are used to entrap AuNPs and are then conjugated with DTA, to afford nanoparticles containing an average of 59 DTA molecules per particle and measuring ~5.5 nm in diameter. The synthesized nanoparticles exhibit higher X-ray attenuation values *in vitro* as compared to iohexol at equivalent iodine concentrations, or to non-DTA-conjugated nanoparticles at equivalent concentrations of gold. The complexes also show good stability in aqueous environment. Thus, these finding may serve as a guide for future designs of and studies on dual composition CT contrast agents. An alternative to the dendrimer encapsulation approach described above is presented, where AuNPs are encapsulated in a silica layer and assessed *in vitro* as X-ray contrast agents.[81] Such particles of less than < 25 nm in diameter are found to be stable and biocompatible.

A report on a proprietary AuNP formulation from Nanoprobes Inc. (preparation # 1101 or Aurovist) describes the use of AuNPs as intravenous X-ray imaging agents for visualization of vasculature, kidneys, and tumors in mice.[82] The nanoparticles have an average size of 1.9 nm, and the LD_{50} for the nanomaterial is reported as 3.2 g Au kg^{-1}. Due to their small size, these nanoparticles do not accumulate in the RES rich organs, but are excreted through the kidneys. The AuNPs show significant CT image enhancement as compared to iohexol contrast agent (trade name Omnipaque). Excellent tumor image enhancement is also obtained due to nanoparticle extravasation across tumor capillary pores. Such small NPs show much higher diffusion coefficient than larger NPs. Several additional studies using these same nanoparticles show the potential of using AuNP in X-ray cancer radiotherapy

(RT).[83] A discussion on cancer RT is beyond the scope of this review. However, it is worth noting that AuNPs are excellent candidates as RT treatment media, both due to excellent X-ray absorption properties of gold and the ease of surface modification of AuNPs, allowing for tissue specific targeting. If tumors could be successfully targeted and loaded with large doses of AuNP (as compared to surrounding tissue), the tumor could effectively receive a much higher dose of radiation than normal tissue during a RT treatment. Calculations indicate that this dose enhancement can be significant,[83b] resulting in lower adverse response to RT in patients and better overall treatment outcomes.

An exciting feature of nanoparticles is the opportunity to simultaneously introduce several payloads or functionalities for multipurpose (synergistic) diagnostics or therapy. The surfaces of AuNPs can be easily modified with tissue/receptor targeting moieties and several examples of such targeted contrast agents are next discussed. AuNPs conjugated with heparin polysaccharides (HEPA-AuNPs) afford a highly liver-specific contrast agent in mice.[84] Heparin is a natural polysaccharide that tends to accumulate in Kupffer cells and in endothelial-like cells lining the liver sinusoid. The HEPA-AuNPs show improved localization within mice liver as compared to control AuNPs coated either with PEG, or glycol chitosan. Following an i.v. injection, the HEPA-AuNPs of ~54 nm in diameter enable good 3-D visualization of liver in mice (Figure 16). The HEPA-AuNPs offer improved liver CT imaging *in vivo*, as compared to eXIA160™ (Binitio Biomedical Inc.), a proprietary iodinated contrast agent similar to Fenestra™. However, according to the authors, the high doses of the AuNP required for imaging still remain a cause of concern due to potential toxicity issues. In an analogous targeting study, CD4-antibody conjugated AuNPs show enhanced and selective uptake by lymph nodes.[85] Following an i.v. injection, the labeled nanoparticles (28 nm or 38 nm in diameter) exhibit higher uptake by the lymph nodes than non-labeled AuNPs, and, consequently, afford better CT contrast enhancement of the targeted tissue. Alternatively, AuNPs conjugated with glutamic acid are reported as a Ca^{2+} ion-chelating targeted CT contrast media for imaging of microdamage in bone tissue in *ex vivo* bovine cortical bone specimens.[86] This imaging agent (15 nm or 40 nm in size) shows improved contrast enhancement between the healthy and microdamaged bone tissue.

Patients with a history of heart attacks are at increased risk of suffering a repeat due to development of cardiac and pulmonary fibrosis. Clinically, the overexpression of angiotensin converting enzyme (ACE) is evident prior to the reoccurrence of a heart attack. Hence, methods for monitoring ACE expression represent a crucial step towards prevention of another incident. In order to target contrast media to locations where ACE is over-expressed, AuNPs coated with lisinopril, a tripeptide ACE-inhibitor, are reported. Specifically, lisinopril-coated AuNP (~14 nm)[87] are taken up by lung tissue (highly ACE expressing) *in vitro*, indicating interaction between ACE and the nanoparticles. However, issues regarding stability of the particles in physiological environment need to be addressed prior to attempts at imaging *in vivo*. The lisinopril coating is adsorbed to the surface of AuNPs through primary amines of the peptide, rather than through covalent binding via thiolated linkers. The interaction between the amines and the surface of the AuNP weakens in a buffered solution, resulting in instability of the contrast media.

Imaging methods for early detection and visualization of a tumor will assist in the diagnosis, treatment planning, and outcome monitoring. Thus, the functionalization capabilities of AuNPs are being exploited to selectively target and image tumor tissues. In one such example, the authors take advantage of the higher metabolic rate of tumor cells as compared to normal cells. AuNP coated with 2-deoxy-*D*-glucose (2-DG) are used as tumor-targeting contrast agents in cell culture in human A-549 cancer cells. The 2-DG-labeled AuNPs, 4 nm in diameter, show significant uptake in cancer cells compared to non-labeled AuNPs.[88]

Alternatively, AuNPs conjugated with UM-A9 antibodies can be used to target squamous cell carcinoma *in vitro*.[89] The particles, shaped as gold nanorods of 45 nm in length with a mean diameter of 15 nm, show significant CT contrast enhancement in targeted cancer cells, as opposed to non-targeted cancer cells or normal cells (Figure 17). A follow up study, using 30 nm gold nanospheres coated with EGFR antibodies, targeting squamous cell carcinoma (SCC), in live mice is also described.[90] The authors find that the actively targeted anti-EGFR-AuNPs show significantly higher uptake by the A431 SCC cells *in vitro*, than the "passive" non-specific control AuNPs that were coated with rabbit-IgG antibodies. The A431 cells took up 26.3 ± 2.3 μg of targeted AuNPs (3.9 × 104 AuNPs per A431 cell), while parallel cells in the negative control experiment engulfed only 0.2 ± 0.01 μg of AuNPs (3.4 × 103 AuNPs per cell), as measured by atomic absorption spectroscopy. Similarly, the *in vivo* results show higher accumulation of the actively targeted anti-EGFR-AuNPs vs. passive anti-(rabbit-IgG)-AuNP, at the tumor site (giving 190 HU vs. 78 HU CT attenuation signal, respectively, 6 h after the injection), as shown in Figure 18. No toxicity is observed in the mice 7 days post-injection.

Herceptin is a humanized monoclonal antibody currently used in the clinic to treat breast cancers with upregulated Her2 (human epidermal growth factor receptor 2) expression, which occurs in approximately 30% of breast cancer patients. An *in vitro* study using Her2-antibody labeled 15 nm AuNP shows the potential of specifically targeting human breast cancer BT-474 cells (which express Her2) vs. MCF7 cells (which do not express Her2).[91] In the subsequent murine *in vivo* studies, the AuNPs mostly accumulate in the tumor periphery and the penetration within the tumor mass is poor. However, the tumor periphery (containing high concentrations of anti-Her2-AuNP) shows 22 times higher CT attenuation than the surrounding muscle tissue, making it possible to distinguish and visualize the tumor site.[91] Based on CT attenuation, the anti-Her2-AuNPs show 1.6 times higher accumulation in BT-474 than in MCF7 tumor types, *in vivo*. The control AuNPs exhibit no specific bio-distribution or tumor targeting as compared to anti-Her2-AuNPs.

Gastrin-releasing peptide receptors (GRP) are over-expressed in prostate, breast, and small-cell lung carcinoma cells, representing a potential ligand-receptor for use in targeted CT imaging. A recent study uses AuNPs conjugated with bombesin (BBN) peptides to specifically target pancreatic-acini in normal mice, and tumors in prostate-tumor-bearing severe combined immunodeficiency (SCID) mice.[92] The authors choose an intraperitoneal (i.p.) injection as the preferred delivery mode, as previous studies showed that i.p. delivery results in minimal uptake of AuNPs by Kupffer cells in liver as compared to an i.v. delivery mode, while the subcutaneous delivery mode generally results in slower tissue distribution and kinetics, restricting the AuNP delivery to the target organs. The AuNP-BBN-3 nanoparticles (with diameter of 115–155 nm) show a higher uptake by the pancreas as compared to other organs (liver, kidney, spleen, lung) in normal mice (e.g. uptake levels: 9.3 ppm gold in pancreas, 0.3 ppm gold in liver). GRP-receptor targeting efficiency is confirmed using a radiolabeled ^{198}AuNP-BBN-3 versus a non-specific control AuNP with gum-Arabic protein conjugated AuNP (^{198}AuNP-GA) in SCID mice. The results show that bio-distribution of the AuNP-BBN-3 follows the trend of density of BBN-receptor sites within different tissue/cell types, with greatest uptake by densely-BBN-receptor expressing pancreatic cells. Sufficient uptake is observed by the prostatic-cancer cells to achieve clinically significant CT contrast image with a several-fold increase in HU response. On the other hand, the control AuNPs-GA do not show significant uptake by BBN-receptor expressing cells, and accumulate mostly in the liver, lung, and spleen, with low uptake by the pancreas and prostate-tumor cells.

Folate receptors are upregulated in several cancer types as well as activated macrophages.[93] Consequently, folic acid (FA) has emerged as a key targeting ligand for selective delivery of

diagnostic or therapeutic agents to these cells. AuNPs coated in a silica layer and conjugated with FA are reported as selective, targeted CT imaging agents with potential for photo-thermal therapy (PTT) and radiotherapy (RT) applications.[94] Silica coatings are an alternative to polymer coatings. Their thickness can be readily controlled and they exhibit biocompatibility, as well as stability to high-energy nanosecond laser irradiation. Many nanomaterials, including AuNPs, exhibit localized surface plasmon resonance (LSPR) properties and, thus, these materials are effective photo-thermal therapy agents. Moreover, AuNPs are known to be effective in radio-therapy treatments, either as radiosensitizers or dose enhancers both *in vitro* and *in vivo*. Gold nanorods of ~46 nm by ~18 nm in size (L × W), with a uniform silica layer of ~8 nm, are described with FA conjugated to the surface.[94] These particles are non-toxic to MGC803 gastric cancer cells *in vitro* and exhibit more selective and greater cellular uptake in MGC803 cells as compared to on-targeted nanorod controls. *In vitro* studies using RT and PTT show a gradual decrease in cell viability following RT and an effective and selective PTT effect in cancer cells, compared to control non-targeted cells. *In vivo* tumor targeting is explored in mice, following i.v. injection of the contrast media. The tumor tissue displays strong contrast as compared to healthy tissue, with gradual accumulation of AuNPs over 12 h at the tumor site, demonstrating significant uptake and high targeting specificity of the CT media. The corresponding *in vivo* RT and PTT experiments are not yet reported.

Another example of a multifunctional AuNP is a cell specific combined CT-imaging/drug delivery vehicle (Scheme 3).[95] Specifically, AuNPs conjugated with a prostate-specific membrane antigen-specific RNA aptamer (PSMA-specific RNA aptamer) target prostate adenocarcinoma LNCaP cells. The aptamer is fused with a 21-base CGA extension, which facilitates the binding of a chemotherapeutic drug, doxorubicin. The loaded AuNPs (measuring ~30 nm in diameter, and carrying an average of 615 doxorubicin molecules per AuNP) are successfully used for both imaging and drug delivery *in vitro*. The uptake of AuNP is significantly higher in LNCaP cells than in non-targeted prostate epithelial PC3 cells. The cytotoxicity studies show good cell viability for RNA-conjugated AuNPs (without doxorubicin). Additionally, doxorubicin-loaded AuNPs are more cytotoxic to targeted cells than non-targeted cells, as well as being more target specific than free doxorubicin. Drug release studies *in vitro* show that doxorubicin is released from the AuNPs relatively quickly, with about 35% of the drug being released within the first hour.

Along with targeted and multifunctional AuNPs, many examples of multi-modality AuNP imaging agents exist, encompassing a variety of spectroscopic techniques and synthetic designs. The development of such synergistic diagnostic media is of significant interest to the medical field. Multimodal imaging may allow clinicians to obtain comprehensive morphological and molecular profiling of the imaged tissue. Such information will facilitate more accurate clinical diagnosis. Several CT/MRI multimodal imaging agents are reported in recent papers for use *in vitro* and *in vivo*.[96] These dual-modality reporters are commonly AuNP conjugated to Gd-chelates. The particles are generally prepared by coating the surface of the AuNP with a gadolinium chelating ligand, with subsequent coordination of the Gd^{3+} ions. The cytotoxicity studies (14D chick corneal; NIH-353; or HeLa cells) show that the synthesized nanoparticles exhibit high cell viability. No adverse reactions are observed in mice and rats post contrast media injection. The distribution of the nanoparticles is shown to be size dependent, with the 2.4 nm particles cleared via the renal system within 30 min, and the larger > 14 nm particles accumulating in the spleen and liver. The loading of the Gd^{3+} per nanoparticle varies with the size and shape of AuNPs and the synthetic method (e.g., 157 Gd^{3+}/NP for 2.4 nm size nanospheres, 2.9×10^3 Gd^{3+}/NP for 14 nm nanospheres, and 5.12×10^5 Gd^{3+}/NP for 62 × 22 nm nanorods). The nanomaterials exhibit much higher X-ray attenuation than commercially available iodinated contrast agent iopromide, and afford

higher relaxivity in MRI imaging than the clinically approved contrast agent gadodiamide (trade name Omniscan™, GE Healthcare), used as a comparison.

One example of an application of such multi-modality gadolinium-AuNPs is a study showcasing 2.0–2.5 nm AuNP chelates (carrying ~50 Gd^{3+}/NP) to monitor the delivery and location of microcapsules, containing pancreatic islet of Langerhans cells for treatment of type I diabetes in mice.[96d] In type I diabetes, the body is unable to produce insulin owing to an autoimmune response. Transplantation of pancreatic islet cells has shown promise as a therapy; however, immunosuppressive therapy is needed to prevent islet rejection by the patient. In the reported study,[96d] gadolinium-AuNP and human islet of Langerhans cells are co-encapsulated in alginate microcapsules having a mean diameter of ~542 μm, with each capsule containing ~1 ng Au and ~87.7 pg of Gd. After the transplantation of the microcapsules into the liver of the diabetic mice, the blood glucose levels reduced and became equivalent to those of the healthy mice, starting around 7 days after treatment. The microcapsules are visualized *in vivo* and their location can be monitored by means of X-ray CT, MRI, and ultrasound imaging. The gadolinium-AuNP microencapsulation approach could also be applicable to other forms of cell therapy.

High-density lipoproteins (HDL) are naturally produced by liver and the intestine. HDL-based nanoparticles are found to be biocompatible and biodegradable, and are emerging as an alternative platform for diagnostic and/or therapeutic applications. HDL-based nanoparticles are shown to be macrophage specific and to easily enter atherosclerotic plaques (which are macrophage-rich). As a practical example, gold-core nanoparticles, coated by a lipid-based layer, are conjugated with Gdchelates and fluorescent dyes, and reported as (CT/MRI/FI) multimodality imaging media for visualization of atherosclerotic plaques in mice.[73b,96f,97] In a recent *in vivo* atherosclerosis study, Au-HDL-rhodamine nanoparticles (~7.2 nm) are injected i.v. into apolipoprotein E knockout (apo E-KO) mice. Nanoparticles are taken up by the macrophages in the atherosclerotic plaques. It is also possible to simultaneously distinguish the Au-HDL nanoparticles from other radiopaque materials, such as iodinated contrast agents (Fenestra VC™), or calcium deposits by X-ray CT.

Combining single-photon emission computed tomography (SPECT) tracer media with the X-ray CT modality is currently being explored with dual-modality SPECT/CT tumor targeting contrast agents.[98] The authors describe ^{125}I-radiolabeled AuNPs, coated with cyclic-RGD peptides (Arg-Gly-Asp-Tyr-Cys). The AuNPs have a hydrodynamic diameter of ~31 nm and contain ~300 cyclic-RGD moieties, and ~6 ^{125}I atoms per particle. ^{125}I is a low-energy gamma emitter with a $t_{1/2}$ = 60.14 days, which can be used for long term monitoring purposes *in vivo*. Iodine has high affinity for gold and can form Au−I bonds on the surface of the NP. The cyclic-RGD motif is present on the NP and initiates cell uptake via the integrin $\alpha_v\beta_3$-receptor-mediated endocytosis. The particles are stable to a wide range of pH, salt, and temperature conditions, and show no toxicity in cell viability assays using U87MG and MCF7 cell lines. Cellular targeting studies show significant uptake of the ^{125}I/cyclic-RGD/AuNP by the U87MG (high $\alpha_v\beta_3$-integrin expression) cells as compared to MCF7 ($\alpha_v\beta_3$-integrin negative) cells, and compared to control AuNPs containing no cyclic-RGD. Mouse *in vivo* studies demonstrate that the particles are quickly and preferentially taken up by the tumor sites (within 10 min post i.v. injection) and are used to image both tumor tissue and angiogenesis via both SPECT and X-ray CT. Perhaps somewhat surprisingly with respect to their size, the AuNPs are cleared from the body via renal filtration rather than being deposited in the liver and spleen tissue. However, it has been shown in several recent studies that even particles larger than 5.5 nm can, in certain cases, be made to undergo renal clearance, depending on the particle shape and surface chemistry.[99]

Imaging media combining near-IR (NIR) fluorescence with X-ray CT spectroscopy can provide accurate concentration-dependent localization information about the distribution of the AuNPs *in vivo*.[100] The NIR optical window is preferred for imaging of *in vivo* tissue, as compared to light of shorter wavelengths, due to lower auto-fluorescence and relatively deep penetration of NIR light. NIR fluorescent tags do, however, often suffer from photo-bleaching and spectral overlap with other tags. AuNPs coated in a mesoporous silica layer, with embedded indocyanine green (ICG) NIR tags, are demonstrated as dual-modality contrast media in mice, following an intra-tumoral injection. The free ICG dye has a very short $t_{1/2}$ in the blood (< 4 min) due to adsorption by albumin and HDL. In this case, however, the ICG is shielded from the environment by being encapsulated in the silica layer, allowing for NIR imaging for several hours post-injection of the particles. The AuNP used in the study are rod-shaped (44 nm by 15 nm) with a silica shell of 13 nm in thickness. Mesoporous silica structures are easily functionalized or embedded with a payload, allowing for multi-functionality of such nanoparticles. The particles prepared do not exhibit toxicity in MGC803 cells. The biodistribution of the NPs *in vivo*, and *in vivo* toxicity studies are not yet reported.

An alternative spectroscopic technique being explored in conjugation with CT is surface enhanced Raman spectroscopy (SERS). One example of a SERS/CT dual-modality probe is a AuNP labeled with Raman-reporter dyes and coated with a PEG monolayer.[101] A set of six different AuNP media is showcased in this report, where each NP is tagged with a different reporter-dye (each having a unique Raman spectrum). Following the i.v. injection of the AuNPs, the “color coded” particles of ~65 nm in diameter are used to image the spleen via CT and SERS in mice. The authors hypothesize that such SERS/CT contrast media can be tailored to selectively target cancer cells and may be used in tumor diagnosis. However, further applications of this nano contrast media are not yet reported.

Outlook

AuNPs are of significant interest as X-ray imaging agents.[102] They offer increased chemical stability, long circulation times, and an obvious advantage compared to molecular contrast agents in terms of X-ray attenuation. Gold (Z = 79; absorption edge k = 81) has better X-ray attenuation properties than either iodine or gadolinium.[103] In general, AuNPs are largely non-toxic and biocompatible. However, some recently published studies on the toxicity of AuNPs indicate that AuNPs may exhibit toxicity in certain particle-size ranges *in vivo*.[104]

The size of AuNP is easily controlled and can be optimized for vascular extravasation and renal clearance from the organism,[105] or for accumulation in the RES organs. AuNPs also provide for easy surface modification, allowing for targeted biodistribution and tailoring of the physical/chemical properties of the imaging agent. Moreover, ease of conjugation of the AuNP to imaging probes for many alternative imaging methods make it easy to prepare multi-modal contrast media with significantly broadened reporting capabilities. One potential limitation to the use of AuNPs in everyday clinical CT applications is the high market cost of gold. Hence alternatives to AuNPs among other high-density, high-Z, metallic materials are sought after.

6.0 Other metallic contrast agents

Bismuth based contrast agents are being explored for *in vivo* use as an alternative to AuNPs. Bismuth has a high atomic number (Z = 83) and good X-ray attenuating properties (absorption edge k = 91), and is used in many cosmetic and medical applications. The use of poly(vinylpyrrollidone) (PVP) polymer-coated bismuth sulphide (Bi_2S_3) nanocrystals as CT contrast agents is recently reported (Figure 19).[106] The particles (quasi-rectangular shapes of 10 to 50 nm in width or length and about 4 nm in thickness) exhibit long vascular half-life

and are subsequently taken up by the phagocytic cells in the liver and spleen, in mice. The nanoparticles can also be used to image lymph nodes in mice, following a subcutaneous injection (Figure 20). This study successfully demonstrates the potential of Bi materials as CT contrast media. However, several problems associated with the synthesis (i.e., controlling the size and shape of the particles), difficulties with surface modification, and potential toxicity of such Bi_2S_3 nanoparticles remain. To address these issues, a method for large-scale preparation of Bi_2S_3 nanodots, having a diameter of 2–3 nm, is recently described.[107] The authors report the synthesis of oleic acid coated Bi_2S_3 nanoparticles with narrow size distribution and excellent monodispersity, the surface of which can be easily modified with polymers such as PVP. The cell viability studies (HeLa cells) show fairly high viability of over 80% even at contrast media concentrations of 3 mg Bi/mL. Considering the relatively small size of the particles, *in vivo* imaging in rats shows perhaps a somewhat unexpected uptake of the Bi_2S_3 nanoparticles by the liver and spleen, suggesting macrophage activation, as opposed to renal clearance. The nanoparticles exhibit fairly long blood-circulation times of several hours and are cleared from the rats within 1 month after the i.v. administration with no gross damage to organ tissue.

Novel coordination-polymer based nanoparticles containing Bi^{3+} ions are recently reported as CT contrast medium.[108] Water-soluble, biocompatible $KBi(H_2O)_2[Fe(CN)_6]\cdot H_2O$, PVP-coated nanoparticles are synthesized in a one-step procedure in aqueous conditions. As prepared, the nanoparticles exhibit a relatively wide size distribution from 10 to 30 nm, which is somewhat disadvantageous. Toxicity studies in HeLa cells show cell viability to be over 90% with concentrations of up to 0.83 mg Bi/mL. Additional studies on leaching of the CN^{1-} and Bi^{3+} ions from the complex show the concentration of CN^{1-} to reach ~0.5 ± 0.2 ppm at neutral pH, and ~1.2 ± 0.2 ppm at pH 1; and the concentration of Bi^{3+} to be ~2 ± 1 ppm at pH 7, and ~7 ± 1 ppm at pH 1; after 24 h. The values are considered relatively low and the CN^{1-} levels are comparable to those found in certain plants and fruit seeds. It is expected that the small amount of CN^{1-} can be readily detoxified by the Rhodanese enzyme *in vivo*. However, the actual evaluation of the CT performance and toxicity of the nanoparticles *in vivo* is not yet reported.

Another viable alternative to AuNPs are water-soluble tantalum oxide (Ta_2O_5) nanoparticles, which are described as potential CT contrast agents for use *in vitro* and *in vivo*.[109] Ta_2O_5 particles possess better CT attenuation properties than iodinated agent iopromide on a per-mole basis. The particle size can be easily and uniformly controlled between 5–15 nm, and the surfaces of the nanoparticles can be readily modified using silane derivatives. PEGylated/rhodamine-labeled Ta_2O_3 are used successfully as multimodal contrast media for simultaneous CT and fluorescence imaging of tissues in rats. Following i.v. delivery, the nanoparticles are shown to have prolonged blood-pool residency, and are eventually taken up by RES cells in spleen and liver. They can also be used to image lymph nodes after intradermal injection. Cytotoxicity studies demonstrate good cell viability (RAW264.7 cells), and no appreciable toxicity in rats is observed over a period of 2 weeks post injection.

Iron/platinum alloy (FePt) nanoparticles can be synthesized with controllable size and shape for CT imaging. The surface modification methods of the FePt nanoparticles are similar to those used in AuNP synthesis, commonly via thiol derivatives. FePt nanoparticles of 3, 6, or 12 nm in size, labeled with Her2 antibody are described as tumor targeting MRI/CT dual-modality contrast media.[110] As mentioned earlier, Her2 upregulation occurs in approximately 30% of breast cancer tumor types. Significant contrast enhancement of tumor tissue is observed *in vivo* in mice bearing MBT2 tumors, following an i.v. injection. The particles are subsequently taken up by RES system and cleared form the body within ~1 week. The 12 nm size particles show the best results in tumor imaging applications, as

compared to particles of other sizes; while the 3 nm particles are found to easily permeate blood-brain barrier, allowing for potential future applications in brain imaging. No notable cytotoxicity up to 10 mM Fe (Vero cell line) is observed for any particle size and the particles exhibit good biocompatibility.

Barium based contrast agents such as barium sulfate (Z_{Ba} = 56; absorption edge k_{Ba} = 37) are some of the oldest and most commonly used contrast agents in a clinical and preclinical setting.[111] Barium sulfate is usually taken orally (as a suspension) for imaging of the gastrointestinal tract.[111a,b] It is also reported that barium sulfate can be used as a contrast medium to identify and image microcracks in bovine tibiae *ex vivo*. The researchers took advantage of the fundamental solubility rules using $BaCl_{2(aq)} + Na_2SO_{4(aq)} \rightarrow BaSO_{4(s)} + 2\ NaCl_{(aq)}$ to stain bovine bone samples. The void of the microcracks is penetrated by the soluble Ba^{2+} and SO_4^{2-} ions, where they combine to form an X-ray attenuating precipitate for subsequent imaging of the bone microdamage.[112] A similar technique is employed to use $BaSO_4$ as a CT contrast agent in identification of dentinal cracks in *ex vivo* human and elephant teeth.[113]

ExiTron™ Nano 6000 and 12000 (Miltenyi Biotec Inc.) are proprietary alkaline-earth based NP formulations, designed for CT imaging of vasculature and liver in small-animal models. The NPs are composed of a solid core containing barium, and a proprietary coating. The hydrodynamic volume of the NPs is 110 nm. ExiTron™ Nano formulations have been assessed as preclinical *in vivo* liver imaging agents in mice.[111c,d] The contrast agent formulation is delivered via i.v. and the authors observe a peak contrast enhancement in the liver after 4 to 8 h. The contrast agent is mostly taken up by liver and spleen. However, uptake by lymph nodes is also observed. Good contrast enhancement allows for detection of liver tumor lesions down to app. 300 μm in diameter and delineation of splenic tumors. ExiTron™ Nano gets retained in mice liver for up to 6 months, following a single injection, allowing for multiple CT scans over time, without the need for repeated contrast media administration. No visible toxicity in mice has been noted, following the use of the ExiTron™ Nano formulations.

As another alternative medium for CT bone imaging, lead-uranyltetraacetate ($PbUC_8H_{12}O_{10}$) is applied for detection of microdamage in *ex vivo* human trabecular bone.[114] The contrast agent provides excellent X-ray attenuation properties due to high Z and *k* values of lead (Z = 82; absorption edge *k* = 88) and uranium (Z = 92; absorption edge *k* = 116). However, concerns regarding the toxicity of this contrast medium prevent its use *in vivo*.

Outlook

Alongside the well accepted and widely used barium sulfate formulations in gastrointestinal imaging applications, several novel materials are being explored as CT contrast agents *in vitro* and *in vivo*. These new nanomaterials are intended as alternatives to AuNP imaging media and their use is explored for imaging of the cardiovascular and lymphatic systems, as well as tumor tissues. The nanoparticulate nature of these materials allows for conjugation with a range of surface functionalities, leading to improved tissue-targeting, and multiple-modality contrast media.

Bismuth possesses better X-ray attenuation properties than gold. Recent advances in the field show success in addressing the disadvantages stemming from initial difficulties in controlling the size and shape of the synthesized nanoparticles, as well as the lack of easily modifiable surfaces. However, detailed studies on toxicity of Bi containing nanoparticles *in vivo* in a variety of animal models are necessary in order for Bi-materials to achieve more widespread use.

Ta_2O_5 is a chemically inert, biocompatible material with relatively good radiopacity (Z_{Ta} = 73, absorption edge k_{Ta} = 67.4). It has historically been used as contrast medium in tracheobronchial and gastrointestinal imaging. Novel synthetic approaches allow for preparation of water-soluble, size controlled, bioinert nanoparticles. Much like AuNPs, Ta_2O_5 nanoparticles also possess easily modifiable surfaces. Such materials hold promise in the field of CT contrast agents and may be an inexpensive alternative to AuNPs.

Pt atoms (Z = 78; absorption edge *k* = 79) exhibit significant X-ray attenuation. FePt alloy particles are shown to exhibit excellent biochemical stability and favorable magnetic properties, making this material an option for dual-mode CT/MRI imaging applications. The particle size and shape can be easily controlled and the surface modification chemistry is similar to that of AuNP materials.

7.0 Xenon gas in CT imaging applications

"High Z" noble gasses also represent a class of contrast media used in certain applications of X-ray CT imaging. The most commonly used noble gas for CT imaging is xenon (Z_{Xe} = 54; absorption edge k_{Xe} = 34.6 keV). Xenon is a readily diffusible monoatomic gas with low but not insignificant solubility in blood and fairly good solubility in adipose tissue.[115] Xenon gas can pass across cell membranes, exchange between blood and tissue, and can cross the blood-brain barrier. Drawbacks to xenon gas use are related to its anesthetic properties, and may include respiratory depression, headaches, nausea, and vomiting.[116] Thus the xenon enhanced X-ray CT (xenon-CT) technique is not recommended for patients with severe respiratory disease, ventilated patients with low tidal volume, patients with full stomach, and patients who cannot be adequately sedated.[117] The undesired side-effects can be adequately managed by controlling the xenon gas concentration and the length of time xenon is inhaled for. In several countries the stable xenon gas (non-radioactive ^{131}Xe) is approved for clinical use in X-ray CT imaging. In the U.S., xenon-CT is not FDA approved (as of the writing of this document) and is only available under investigational new drug (IND) status.

Xenon-CT has been used for several decades to evaluate cerebral blood flow and perfusion in patients experiencing cerebrovascular disorders (e.g., following a brain injury, brain surgery, or stroke).[118] It is considered a valuable imaging modality used as an alternative or complement to PET, SPECT, MRI, etc.[117] Current standard for the xenon-CT cerebral blood flow evaluation calls for inhalation of 28 ± 1% medical grade xenon gas with at least 25% oxygen, for the duration of ~4.5 minutes.[119] Following the procedure, xenon is rapidly washed out from cerebral tissues due to its short half-life of < 40 s. In the U.S., xenon-CT is often replaced by perfusion X-ray CT technique (PCT), which commonly employs non-ionic iodinated small molecule contrast agents, frequently in combination with vasodilatory challenge (e.g., acetazolamide) to measure brain hemodynamics.

In addition to being used in evaluation of cerebral blood flow, xenon-CT is frequently applied in determination of regional ventilation and perfusion in the lung, particularly in combination with dual-energy, dual-source, and multidetector CT instrumentation.[115a,120] It has been shown that xenon-CT imaging results correlate strongly with regional pulmonary function (or loss thereof) in patients with diseases such as bronchiolitis obliterans, emphysema, and asthma.

Furthermore, xenon-CT is being explored as an imaging modality in hepatic and pancreatic diagnostics. The technique is used to evaluate and compare hemodynamic changes in the liver during progression of several types of liver diseases such as: hepatocellular carcinoma, hepatitis C, alcoholic and non-alcoholic cirrhosis, and hepatic steatosis in non-alcoholic steatohepatitis.[121] Likewise, xenon-CT has been applied to assess tissue blood flow in

pancreatic tumors.[122] The technique allows for a noninvasive estimation of tumor blood flow, perfusion, and microvascular density. Xenon-CT results can be used to discern between pancreatic adenocarcinoma and pancreatic neuroendocrine tumors. The correlation between xenon-CT results and microvascular density in tumor tissue is useful in predicting the success of chemotherapy in patients and can help the clinicians decide on best treatment regimen on a case per case basis.

Outlook

Xenon gas has X-ray attenuating properties similar to iodine. Xenon is chemically inert, biocompatible, and non-allergenic and can be safely used in patients with renal dysfunction. The undesired side-effects of xenon inhalation, related to its anesthetic properties, can be minimized by controlling the concentration of xenon gas being inhaled and the duration of the procedure. The rapid rate of xenon clearance from the body can be advantageous and conducive to repeat examinations. Xenon-CT has so far gained clinical approval in a number of countries, where the technique is most frequently used for cerebral blood flow assessment. Overall, xenon-CT is a useful clinical alternative to CT imaging using iodinated imaging media, especially when and where the diagnostic equipment is readily available.

8.0 Commercial footprint of CT imaging media

As mentioned at the beginning of the article, the advances in CT imaging instrumentation have lead to a resurgence of research and clinical interest due to the ability to obtain high resolution images and 3D reconstruction of hard and soft tissues, and to collect such data quickly with lower patient X-ray exposure. According to a report titled “North American Contrast Media Markets,” by Frost & Sullivan,[123] a non-profit market-analysis institute, the total North American contrast media market for the current year (2011) is being valued at ~ $2 billion, with a projected compound annual growth rate (2006–2013) of 6.7%. In 2011, the share of X-ray contrast media is predicted at 52.4% of the total market, or ~$998 million. Approximately 87.9% of the revenue from the sales of X-ray contrast media is projected to come from “injectable” iodinated imaging media. Oral iodinated contrast agents are expected to account for ~3.2% of the market share, while oral barium imaging agents are predicted to capture ~8.9% of the total revenue.

There are seven competitive companies in the X-ray contrast media market. Three of those companies (Bracco Diagnostics, GE Healthcare, and Mallinckrodt) are considered as full-product-line companies, offering a variety of products to address multiple needs for imaging agents. These three companies accounted for ~85% of the market share in revenue for the 2006 fiscal year.[123] The X-ray contrast media market growth is projected to be steady over the next three years, with the compound annual growth rate (2006–2013) of 2.7%. Market growth is being driven primarily by the increase in prevalence of cardiovascular disease and the ability to develop diagnosis and treatment using such technologies as CT angiography.

In order to translate the new compositions and technologies described in this review to the clinic, a number of experiments need to be performed and requirements need to be satisfied prior to use in humans. The pathway to the phase I safety clinical trial for an intravenously administered imaging agent is likely to include a series of research and development activities as outlined below in Table 4 and Table 5. These activities are based on the requirements for submission of an Investigational New Drug (IND) consistent with Food and Drug Administration (FDA) Guidance on Medical Imaging Contrast Agents in the US. As with any new medical product, the FDA should be consulted prior to beginning the development activities to ensure that the requested data/information will be obtained from the experiments planned.

9.0 Conclusion

Advances in CT instrumentation combined with improved CT contrast media formulations are accelerating the field of CT imaging in both laboratory and clinical settings. Good contrast enhancement and high resolution CT images, as well as the low cost and the wide-spread availability of clinical CT scanners, are some of the reasons CT is becoming an imaging technique of choice in clinics and hospitals around the world.

Many currently clinically approved iodinated contrast agents have proven to be less than optimal for use in at-risk patients, especially when repeated CT scans are necessary in order to monitor the progress of the disease or the treatment. Similarly, the use of lanthanide chelates for CT imaging, requires markedly higher doses of media as opposed to MRI, and may increase the incidence of adverse health effects in patients. However, the favorable X-ray attenuation properties of lanthanide imaging media suggest that these complexes deserve continued investigation in an effort to maximize performance and minimize toxicity.

Significant progress is being made in understanding the relationship between structure, physical-chemical properties, and performance of different imaging agents, be it a small molecule, macromolecule, or particle contrast agent. In the field of small-molecule non-ionic iodinated contrast agents, the structures of the molecules can be tailored to significantly reduce either (or both) the osmolality or the viscosity of the formulations, and thus mitigate associated adverse health effects. Another example is the use coulombic interactions between the negatively charged GAGs and a cationic CT agent to image cartilage tissue as well as to assess the biochemical health of the tissue. In an effort to better understand the chemistry of lanthanide chelates, the development of new macrocyclic ligands is leading to lanthanide contrast agents with significantly reduce toxicity. These novel designs diminish or avoid many of the problems that are associated with the current generation of small-molecule contrast agents in the clinic as well as provide a means to gather additional biochemical information on a tissue.

In an effort to create contrast agents with improved X-ray attenuation profiles, thus requiring lower administered doses of the media, many researchers are exploring materials containing high atomic number elements, which possess a more optimal absorption edge *k* value, than the traditional iodine-based contrast agents. These imaging media composed of gold, platinum, tantalum, and bismuth offer exciting possibilities; with the tantalum and bismuth agents being of additional value as relatively inexpensive (compared to Au) and functionalizable materials. Advances in nanoparticle design and labeling techniques are improving the *in vivo* performance, biodistribution profiles, reporting capability, and reducing the overall toxicity of nanosize metallic CT imaging agents.

In the larger picture, contrast agents that assess in real-time: the biochemical composition; the biomechanical state of a tissue; organ function or performance; or highlight a damaged site, are highly sought after. Specifically, imaging media that can provide qualitative (and more importantly potentially quantitative) information on concentration levels and localization of important bio-molecules (e.g., sugars, proteins, enzymes, etc.) in a tissue-specific manner, along with morphological and biomechanical assessment will be valuable for basic research and pre-clinical studies. The number of such agents reported is limited, and thus significant opportunities exist to design, synthesize, and evaluate functional CT agents.

From a clinical perspective, improvements in CT and multi-modality media may allow for earlier and better detection of a disease or trauma, as well as for monitoring the outcome of an administered therapy. Continued research and development of new CT contrast agents

will afford new chemical structures, modes of activity or functionality, enhanced image sensitivity, and will increase our knowledge base. These activities will also stimulate new ideas for contrast agent compositions and their uses to address deficiency in patient care – be it diagnosis or monitoring the progression of a disease.

Acknowledgments

The authors thank the Coulter Foundation and the NIH (R01GM098361) for funding and support.

Biographies

Mark W. Grinstaff was born in 1965 and attended Occidental college where he received his undergraduate A.B. degree in Chemistry with Honors. Mark received his Ph.D. from the University of Illinois under the mentorship of Professor Kenneth S. Suslick and was an NIH postdoctoral fellow at the California Institute of Technology with Professor Harry B. Gray. He is currently a Professor of Biomedical Engineering and Chemistry at Boston University, a College of Engineering Distinguished Faculty Fellow, and a Kern Faculty Fellow. Mark's awards include the ACS Nobel Laureate Signature Award, NSF Career Award, Pew Scholar in the Biomedical Sciences, Camille Dreyfus Teacher-Scholar, Alfred P. Sloan Research Fellowship, and the Edward M. Kennedy Award for Health Care Innovation. His current research activities involve the synthesis of new macromolecules and materials for biomedical applications such as wound repair and drug delivery as well as the development of new imaging agents to assess the biochemical and biomechanical health of cartilage.

Hrvoje Lusic began his college education at Wright State University, where he obtained a B.Sc. in Chemistry in 2002, and a M. Sc. in Polymer Chemistry in 2004, under the direction of Eric Fossum. Hrvoje continued his graduate studies at the lab of Alexander Deiters at North Carolina State University, where his research focused on the synthesis and evaluation of unnatural nucleosides and small-molecule probes as a means of control of biological processes. After earning his Ph.D. in the summer of 2009, he began working as a post-doctoral fellow at Boston University under the direction of Mark Grinstaff. His current research focuses on the synthesis and characterization of computed tomography contrast agents.

References

1. (a) Webb, WR.; Brant, W.; Major, N. Fundamentals of body CT. 3rd ed.. Philadelphia, PA: Saunders Elsevier; 2005. (b) Kalender WA. Phys. Med. Biol. 2006; 51:R29. [PubMed: 16790909] (c) Buzug, TM. Computed Tomography: From Photon Statistics to Modern Cone-Beam CT. 1st ed.. Berlin, Germany: Springer; 2010. (d) Badea CT, Drangova M, Holdsworth DW, Johnson GA. Phys. Med. Biol. 2008; 53:R319. [PubMed: 18758005] (e) Hielscher AH. Curr. Opin. Biotechnol. 2005; 16:79. [PubMed: 15722019] (f) Schambach SJ, Bag S, Schilling L, Groden C, Brockmann MA. Methods. 2010; 50:2. [PubMed: 19706326]

2. (a) Smith-Bindman R, Lipson J, Marcus R, Kim K-P, Mahesh M, Gould R, Berrington de Gonzalez A, Miglioretti DL. Arch. Intern. Med. 2009; 169:2078. [PubMed: 20008690] (b) Berrington de Gonzalez A, Mahesh M, Kim K-P, Bhargavan M, Lewis R, Mettler F, Land C. Arch. Intern. Med. 2009; 169:2071. [PubMed: 20008689]

3. Tabulation and Graphical Summary of 2000 Survey of Computed Tomography. Conference of Radiation Control Program Directors Inc.; Frankfort, KY. 2007.

4. Lindsten, J., editor. Nobel Lectures: Physiology or Medicine 1971–1980. Vol. Vol. 1. Singapore: World Scientific Publishing Co.; 1992.

5. (a) Kalender, WA. Computed Tomography: Fundamentals, System Technology, Image Quality, Applications. 3rd ed.. Munich, Germany: Publicis; 2011. (b) Romans, LE. Computed Tomography for Technologists: A Comprehensive Text. 1st ed.. Baltimore, MD: Lippincott Williams & Wilkins; 2010. (c) Seeram, E. Computed Tomography: Physical Principles, Clinical Applications, and Quality Control. 3rd ed.. St. Louis, MO: Saunders Elsevier; 2009. (d) Hsieh, J. Computed Tomography: Principles, Design, Artifacts, and Recent Advances. 2nd ed.. Bellingham, WA: SPIE Publications; 2009. (e) Figueiredo G, Brockmann C, Boll H, Heilmann M, Schambach SJ, Fiebig T, Kramer M, Groden C, Brockmann MA. Clin. Neuroradiol. 2012; 22:21. [PubMed: 22109696] (f) Figueiredo G, Boll H, Kramer M, Groden C, Brockmann MA. Am. J. Neuroradiol. 2012; 33 In Press.

6. (a) Mattrey RF, Aguirre DA. Acad. Radiol. 2003; 10:1450. [PubMed: 14697013] (b) Krause W. Adv. Drug Deliv. Rev. 1999; 37:159. [PubMed: 10837733] (c) Torchilin VP. Adv. Drug Deliv. Rev. 2002; 54:235. [PubMed: 11897148] (d) Hallouard F, Anton N, Choquet P, Constantinesco A, Vandamme T. Biomaterials. 2010; 31:6249. [PubMed: 20510444] (e) Hasebroock KM, Serkova NJ. Expert Opin. Drug Metab. Toxicol. 2009; 5:403. [PubMed: 19368492] (f) Ghaghada, KB.; Annapragada, AV. Handbook of particulate drug delivery. 1st ed.. Kumar, MNVR., editor. Vol. Vol. 2. Stevenson Ranch, CA: American Scientific Publishers; 2008. (g) Yu SB, Watson AD. Chem. Rev. 1999; 99:2353. [PubMed: 11749484] (h) Rongved P, Klaveness J, Strande P. Carbohydr. Res. 1997; 297:325.

7. Aspelin P. Eur. Radiol. Suppl. 2006; 16:D22.

8. (a) Himi K, Takemoto A, Himi S, Hayasaka K, Okuhata Y, Urahashi S, Tanaka Y, Hirayama T, Katayama Y, Hossain MIZ, Negishi N, Sezai Y. Acad. Radiol. 1996; 3:S214. [PubMed: 8796565] (b) Grainger RG. Br. J. Radiol. 1980; 53:739. [PubMed: 7437683] (c) Meijenhorst GCH, Bruin J. Neuroradiology. 1980; 20:29. [PubMed: 6999377]

9. Christiansen C. Toxicology. 2005; 209:185. [PubMed: 15767033]

10. (a) McClennan BL. Am. J. Roentgenol. 1990; 155:225. [PubMed: 2115244] (b) Katayama H, Yamaguchi K, Kozuka T, Takashima T, Seez P, Matsuura K. Radiology. 1990; 175:621. [PubMed: 2343107]

11. (a) Jost G, Lenhard DC, Sieber MA, Lengsfeld P, Huetter J, Pietsch H. Invest. Radiol. 2011; 46:796. [PubMed: 21808199] (b) Jost G, Lengsfeld P, Lenhard DC, Pietsch H, Huetter J, Sieber MA. Eur. J. Radiol. 2011; 80:373. [PubMed: 21376497] (c) Jost G, Pietsch H, Lengsfeld P, Hutter J, Sieber MA. Invest. Radiol. 2010; 45:255. [PubMed: 20375847] (d) Jost G, Pietsch H, Sommer J, Sandner P, Lengsfeld P, Seidensticker P, Lehr S, Hutter J, Sieber MA. Invest. Radiol. 2009; 44:114. [PubMed: 19104440] (e) Mahnken AH, Jost G, Bruners P, Sieber M, Seidensticker PR, Gunther RW, Pietsch H. Eur. Radiol. 2009; 19:290. [PubMed: 18751712]

12. (a) Zwicker C, Langer M, Langer R, Keske U. Invest. Radiol. 1991; 26:S162. [PubMed: 1808117] (b) Thomsen HS, Dorph S. Acta Radiol. 1993; 34:205. [PubMed: 8489830] (c) Morcos SK, Thomsen HS, Webb JAW. Contrast Media Safety Comm, E. Eur. Radiol. 1999; 9:1602. [PubMed: 10525875] (d) Schild HH, Kuhl CK, Hubner-Steiner U, Bohm I, Speck U. Radiology. 2006; 240:56. [PubMed: 16720865]

13. (a) Seitz W, Weber WH, Jiang J-Q, Lloyd BJ, Maier M, Maier D, Schulz W. Chemosphere. 2006; 64:1318. [PubMed: 16464487] (b) Perez S, Barcelo D. Anal. Bioanal. Chem. 2007; 387:1235. [PubMed: 17180339]

14. Anelli, P.; Brocchetta, M.; Fretta, R.; Lattuada, L.; Mortillaro, A. Process for the preparation of triiodinated carboxylic aromatic derivatives. WO 2010105983 (A1). 2010.

15. (a) Pillai KMR, Diamantidis G, Duncan L, Ranganathan RS. J. Org. Chem. 1994; 59:1344.(b) Bohle F, Carretero JM, Gonzalez L, Martin JL. Invest. Radiol. 1994; 29:S264. [PubMed: 7928252]

(c) Ranganathan RS, Arunachalam T, Song B, Mantha S, Ogan M, Wedeking P, Yost F, Jagoda E, Tweedle M. Acad. Radiol. 1998; 5:S23. [PubMed: 9561036] (d) Marinelli ER, Arunachalam T, Diamantidis G, Emswiler J, Fan H, Neubeck R, Pillai KMR, Wagler TR, Chen CK, Natalie K, Soundararajan N, Ranganathan RS. Tetrahedron. 1996; 52:11177.(e) Newington IM, Humphries G, Lasbistes N, Morisson-Iveson V, Nairne J, Passmore J, Thanning M, Wistrand L-G, Wynn D. Tetrahedron Lett. 2011; 52:3065.(f) Wynn DG, Humphries G, Morisson-Iveson V, Nairne J, Newington IM, Passmore J, Wistrand L-G. Tetrahedron Lett. 2011; 52:3068.(g) Namasivayam S, Kalra MK, Torres WE, Small WC. Emerg. Radiol. 2006; 12:210. [PubMed: 16688432] (h) Aspelin P, Aubry P, Fransson S, Strasser R, Willenbrock R, Berg KJ, Investigators NS. New Engl. J. Med. 2003; 348:491. [PubMed: 12571256] (i) Davidson C, Stacul F, McCullough PA, Tumlin J, Adam A, Lameire N, Becker CR, Panel CINCW. Am. J. Cardiol. 2006; 98:42K. [PubMed: 16784918] (j) Missri J, Jeresaty RM. Catheter. Cardio. Diag. 1990; 19:4.(k) Scanlon PJ, Faxon DP, Audet AM, Carabello B, Dehmer GJ, Eagle KA, Legako RD, Leon DF, Murray JA, Nissen SE, Pepine CJ, Watson RM. J. Am. Coll. Cardiol. 1999; 33:1756. [PubMed: 10334456] (l) Arunachalam T, Fan H, Pillai KMR, Ranganathan RS. J. Org. Chem. 1995; 60:4428.

16. (a) Riefke B, Gonzalez L, Carretero J, Gonzalez C, Jimenez I, Alguacil LF, Bohle F, Martin F, Martin JL. Acad. Radiol. 2002; 9:S178. [PubMed: 12019862] (b) Sovak M, Terry R, Abramjuk C, Faberova V, Fiserova M, Laznicek M, Leuschner J, Malinak J, Zahradnik P, Masner O, Seligson A. Invest. Radiol. 2004; 39:171. [PubMed: 15076009] (c) Fernandez Cabezudo MJ, Petroianu G, Al-Ramadi B, Langer RD. Br. J. Radiol. 2007; 80:713. [PubMed: 17768167] (d) Chai CM, Rasmussen H, Eriksen M, Hvoslef AM, Evans P, Newton BB, Videm S. Acta Radiol. 2010; 51:1007. [PubMed: 20799918] (e) Wistrand LG, Rogstad A, Hagelin G, Roed L, Oulie I, Gram A, Evans P, Rasmussen H, Grant D, Iveson P, Newton B, Thaning M. Acta Radiol. 2010; 51:1014. [PubMed: 20849319]
17. (a) Estep KG, Josef KA, Bacon ER, Illig CR, Toner JL, Mishra D, Blazak WF, Miller DM, Johnson DK, Allen JM, Spencer A, Wilson SA. J. Med. Chem. 2000; 43:1940. [PubMed: 10821706] (b) Shalem H, Shatzmiller S, Feit BA. J. Chem. Soc. Perk. T. 1. 2000; 16:2831.
18. (a) Lee TC, Mohsin S, Taylor D, Parkesh R, Gunnlaugsson T, O'Brien FJ, Giehl M, Gowin W. J. Anat. 2003; 203:161. [PubMed: 12924817] (b) Parkesh R, Gowin W, Lee TC, Gunnlaugsson T. Org. Biomol. Chem. 2006; 4:3611. [PubMed: 16990936] (c) Parkesh R, Lee TC, Gunnlaugsson T, Gowin W. J. Biomech. 2006; 39:1552. [PubMed: 15927193]
19. (a) Goldring SR. J. Bone Joint Surg.-Am. Vol. 2009; 91A:4.(b) Winalski C, Rajiah P. Skeletal Radiol. 2011; 40:1197. [PubMed: 21847750] (c) Taylor C, Carballido-Gamio J, Majumdar S, Li XJ. Magn. Reson. Imaging. 2009; 27:779. [PubMed: 19269769] (d) Trattnig S, Domayer S, Welsch GW, Mosher T, Eckstein F. Eur. Radiol. 2009; 19:1582. [PubMed: 19283387] (e) Read SJ, Dray A. Expert Opin. Inv. Drug. 2008; 17:619.
20. (a) Kallioniemi AS, Jurvelin JS, Nieminen MT, Lammi MJ, Toyras J. Phys. Med. Biol. 2007; 52:1209. [PubMed: 17264381] (b) Xie L, Lin ASP, Guldberg RE, Levenston ME. Osteoarthr. Cartilage. 2010; 18:65.(c) Xie L, Lin ASP, Levenston ME, Guldberg RE. Osteoarthr. Cartilage. 2009; 17:313.(d) Palmer AW, Guldberg RE, Levenston ME. Proc. Natl. Acad. Sci. U. S. A. 2006; 103:19255. [PubMed: 17158799] (e) Silvast TS, Jurvelin JS, Lammi MJ, Toyras J. Osteoarthr. Cartilage. 2009; 17:26.(f) Silvast TS, Jurvelin JS, Aula AS, Lammi MJ, Toyras J. Acta Radiol. 2009; 50:78. [PubMed: 19052932]
21. Bansal PN, Joshi NS, Entezari V, Grinstaff MW, Snyder BD. Osteoarthr. Cartilage. 2010; 18:184.
22. (a) Joshi NS, Bansal PN, Stewart RC, Snyder BD, Grinstaff MW. J. Am. Chem. Soc. 2009; 131:13234. [PubMed: 19754183] (b) Hayward LNM, de BCM-J, Lusic H, Gerstenfeld LC, Grinstaff MW, Morgan EF-I. Microsc. Res. Tech. 2011; 75:7. [PubMed: 22038692]
23. Bansal PN, Joshi NS, Entezari V, Malone BC, Stewart RC, Snyder BD, Grinstaff MW. J. Orthop. Res. 2011; 29:704. [PubMed: 21437949]
24. Stewart RC, Bansal PN, Lusic H, Entezari V, Snyder BD, Grinstaff MW. Radiology. 2012 In Press.
25. (a) Riella MC. Kidney Int. 2006; 69:S1.(b) Hizoh I, Haller C. Invest. Radiol. 2002; 37:428. [PubMed: 12138358] (c) Haller C, Kubler W. Deut. Med. Wochenschr. 1999; 124:332.(d) Haller C, Schick CS, Zorn M, Kubler W. Cardiovasc. Res. 1997; 33:655. [PubMed: 9093536] (e) Rudnick MR, Goldfarb S, Wexler L, Ludbrook PA, Murphy MJ, Halpern EF, Hill JA, Winniford M, Cohen MB, Vanfossen DB. Kidney Int. 1995; 47:254. [PubMed: 7731155] (f) Shigenaga A,

Tsuji D, Nishioka N, Tsuda S, Itoh K, Otaka A. ChemBioChem. 2007; 8:1929. [PubMed: 17899557]

26. Pietsch, H. Small Animal Imaging Basics and Practical Guide. Kiessling, F.; Pichler, BJ., editors. New York: Springer-Verlag; 2011.
27. Idé J-M, Lancelot E, Pines E, Corot C. Invest. Radiol. 2004; 39:155. [PubMed: 15076008]
28. (a) Weichert JP, Lee FT, Longino MA, Chosy SG, Counsell RE. Acad. Radiol. 1998; 5:S16. [PubMed: 9561034] (b) Krause W, Gerlach S, Muschick P. Invest. Radiol. 2000; 35:493. [PubMed: 10946977] (c) Lim SJ, Lim JS, Choi J, Choi JY, Hyung WJ, Kim HS, Suh J, Kim KW. Acad. Radiol. 2010; 17:985. [PubMed: 20617548]
29. (a) Szebeni J. Crit. Rev. Ther. Drug. 2001; 18:567.(b) Szebeni J. Toxicology. 2005; 216:106. [PubMed: 16140450] (c) Szebeni J, Muggia F, Gabizon A, Barenholz Y. Adv. Drug Deliv. Rev. 2011; 63:1020. [PubMed: 21787819]
30. (a) Kao CY, Hoffman EA, Beck KC, Bellamkonda RV, Annapragada AV. Acad. Radiol. 2003; 10:475. [PubMed: 12755534] (b) de Vries A, Custers E, Lub J, van den Bosch S, Nicolay K, Grull H. Biomaterials. 2010; 31:6537. [PubMed: 20541800]
31. (a) Seltzer SE, Shulkin PM, Adams DF, Davis MA, Hoey GB, Hopkins RM, Bosworth ME. Am. J. Roentgenol. 1984; 143:575. [PubMed: 6331738] (b) Desser TS, Rubin DL, Muller H, McIntire GL, Bacon ER, Toner JL. Acad. Radiol. 1999; 6:176. [PubMed: 10898037] (c) Erdogan S. J. Biomed. Nanotechnol. 2009; 5:141. [PubMed: 20055092] (d) Leander P, Hoglund P, Borseth A, Kloster Y, Berg A. Eur. Radiol. 2001; 11:698. [PubMed: 11354769]
32. (a) Mukundan S, Ghaghada KB, Badea CT, Kao CY, Hedlund LW, Provenzale JM, Johnson GA, Chen E, Bellamkonda RV, Annapragada A. Am. J. Roentgenol. 2006; 186:300. [PubMed: 16423931] (b) Kamps J, Scherphof GL. Liposomes, Pt D. 2004; 387:257.
33. (a) Sachse A, Leike JU, Schneider T, Wagner SE, Rossling GL, Krause W, Brandl M. Invest. Radiol. 1997; 32:44. [PubMed: 9007647] (b) Awasthi VD, Garcia D, Goins BA, Phillips WT. Int. J. Pharm. 2003; 253:121. [PubMed: 12593943]
34. Burke SJ, Annapragada A, Hoffman EA, Chen E, Ghaghada KB, Sieren J, van Beek EJR. Acad. Radiol. 2007; 14:355. [PubMed: 17307669]
35. Karathanasis E, Chan L, Karumbaiah L, McNeeley K, D'Orsi CJ, Annapragada AV, Sechopoulos I, Bellamkonda RV. PLoS One. 2009; 4:e5843. Article No. [PubMed: 19513111]
36. (a) Samei E, Saunders RS, Badea CT, Ghaghada KB, Hedlund LW, Qi Y, Yuan H, Bentley RC, Mukundan S. Int. J. Nanomed. 2009; 4:277.(b) Badea, CT.; Samei, E.; Ghaghada, K.; Saunders, R.; Yuan, H.; Qi, Y.; Hedlund, LW.; Mukundan, S. Medical Imaging 2008: Physics of Medical Imaging. San Diego, CA: 2008. p. 691303(c) Karathanasis E, Suryanarayanan S, Balusu SR, McNeeley K, Sechopoulos I, Karellas A, Annapragada AV, Bellamkonda RV. Radiology. 2009; 250:398. [PubMed: 19188313] (d) Karathanasis E, Chan L, Balusu SR, D'Orsi CJ, Annapragada AV, Sechopoulos I, Bellamkonda RV. Biomaterials. 2008; 29:4815. [PubMed: 18814908]
37. Danila D, Partha R, Elrod DB, Lackey M, Casscells SW, Conyers JL. Tex. Heart Inst. J. 2009; 36:393. [PubMed: 19876414]
38. Elrod DB, Partha R, Danila D, Casscells SW, Conyers JL. Nanomed.-Nanotechnol. Biol. Med. 2009; 5:42.
39. Kweon S, Lee HJ, Hyung WJ, Suh J, Lim JS, Lim SJ. Pharm. Res. 2010; 27:1408. [PubMed: 20424895]
40. Montet X, Pastor CM, Vallee JP, Becker CD, Geissbuhler A, Morel DR, Meda P. Invest. Radiol. 2007; 42:652. [PubMed: 17700281]
41. (a) Perkins, GJ.; Zheng, J.; Brock, K.; Allen, C.; Jaffray, DA. Medical Imaging 2005: Physiology, Function, and Structure from Medical Images. San Diego, CA: 2005. p. 31(b) Hoisak, JDP.; Zheng, J.; Allen, C.; Jaffray, DA. Medical Imaging 2008: Image Processing. San Diego, CA: 2008. p. 69140Z(c) Zheng, J.; Hoisak, JD.; Allen, C.; Jaffray, DA. Medical Imaging 2007: Physiology, Function, and Structure from Medical Images. San Diego, CA: 2007. p. 65111D(d) Zheng JZ, Liu JB, Dunne M, Jaffray DA, Allen C. Pharm. Res. 2007; 24:1193. [PubMed: 17373581] (e) Zheng JZ, Perkins G, Kirilova A, Allen C, Jaffray DA. Invest. Radiol. 2006; 41:339. [PubMed: 16481918]
42. Rabinow BE. Nat. Rev. Drug Discov. 2004; 3:785. [PubMed: 15340388]

43. Hyafil F, Cornily JC, Feig JE, Gordon R, Vucic E, Amirbekian V, Fisher EA, Fuster V, Feldman LJ, Fayad ZA. Nat. Med. 2007; 13:636. [PubMed: 17417649]
44. (a) Hyafil F, Cornily J-C, Rudd JHF, Machac J, Feldman LJ, Fayad ZA. J. Nucl. Med. 2009; 50:959. [PubMed: 19443582] (b) Van Herck JL, De Meyer GRY, Martinet W, Salgado RA, Shivalkar B, De Mondt R, Van De Ven H, Ludwig A, Van Der Veken P, Van Vaeck L, Bult H, Herman AG, Vrints CJ. Basic Res. Cardiol. 2010; 105:51. [PubMed: 19693628]
45. Aillon KL, El-Gendy N, Dennis C, Norenberg JP, McDonald J, Berkland C. Mol. Pharm. 2010; 7:1274. [PubMed: 20575527]
46. Solans C, Izquierdo P, Nolla J, Azemar N, Garcia-Celma MJ. Curr. Opin. Colloid Interface Sci. 2005; 10:102.
47. (a) Sugarbaker PH, Vermess M, Doppman JL, Miller DL, Simon R. Cancer. 1984; 54:1489. [PubMed: 6089990] (b) Miller DL, Vermess M, Doppman JL, Simon RM, Sugarbaker PH, Oleary TJ, Grimes G, Chatterji DG, Willis M. Am. J. Roentgenol. 1984; 143:235. [PubMed: 6331144]
48. (a) Peene P, Wilms G, Baert AL, Stockx L, Marchal G, Rigauts H, Matthys P, Sttenbergen W, Breysem Y, Isveldt J, Fevery J. Eur. Radiol. 1991; 1:131.(b) Ryder SD, Rizzi PM, Metivier E, Karani J, Williams R. Gut. 1996; 38:125. [PubMed: 8566839]
49. (a) De Ruyck K, Lambert B, Bacher K, Gemmel F, De Vos F, Vral A, de Ridder L, Dierckx RA, Thierens H. J. Nucl. Med. 2004; 45:612. [PubMed: 15073257] (b) Takayasu K, Arii S, Ikai I, Kudo M, Matsuyama Y, Kojiro M, Makuuchi M, Japan tLCSGo. Am. J. Roentgenol. 2010; 194:830. [PubMed: 20173167] (c) Novell JR, Hilson AJW. J. Nucl. Med. 1994; 35:1318. [PubMed: 8046486] (d) Raoul JL, Boucher E, Roland Y, Garin E. Q. J. Nucl. Med. Mol. Imag. 2009; 53:348.
50. (a) Bakan DA, Lee FT, Weichert JP, Longino MA, Counsell RE. Acad. Radiol. 2002; 9:S194. [PubMed: 12019866] (b) Weichert JP, Longino MA, Bakan DA, Spigarelli MG, Chou TS, Schwendner SW, Counsell RE. J. Med. Chem. 1995; 38:636. [PubMed: 7861412]
51. Bakan DA, Weichert JP, Longino MA, Counsell RE. Invest. Radiol. 2000; 35:158. [PubMed: 10719825]
52. Weichert JP, Lee FT, Chosy SG, Longino MA, Kuhlman JE, Heisey DM, Leverson GE. Radiology. 2000; 216:865. [PubMed: 10966724]
53. (a) Willekens I, Lahoutte T, Buls N, Vanhove C, Deklerck R, Bossuyt A, de Mey J. Mol. Imaging. Biol. 2009; 11:128. [PubMed: 19067081] (b) Ford NL, Graham KC, Groom AC, MacDonald IC, Chambers AF, Holdsworth DW. Invest. Radiol. 2006; 41:384. [PubMed: 16523021] (c) Henning T, Weber AW, Bauer JS, Meier R, Carlsen JM, Sutton EJ, Prevrhal S, Ziegler SI, Feussner H, Daldrup-Link HE, Rurnmeny EJ. Acad. Radiol. 2008; 15:342. [PubMed: 18280932] (d) Suckow CE, Stout DB. Mol. Imaging. Biol. 2008; 10:114. [PubMed: 18204990] (e) Weber SM, Peterson KA, Durkee B, Chen Q, Longino M, Warner T, Lee FT, Weichert JP. J. Surg. Res. 2004; 119:41. [PubMed: 15126080] (f) Badea CT, Hedlund LW, De Lin M, Mackel JFB, Johnson GA. Contrast Media Mol. I. 2006; 1:153.
54. (a) Badea C, Fubara B, Hedlund L, Johnson G. Mol. Imaging. 2005; 4:110. [PubMed: 16105509] (b) Kindlmann GL, Weinstein DM, Jones GM, Johnson CR, Capecchi MR, Keller C. Mol. Imaging. 2005; 4:417. [PubMed: 16285903]
55. Wisner ER, Weichert JP, Longino MA, Counsell RE, Weisbrode SE. Acad. Radiol. 2002; 9:S191. [PubMed: 12019865]
56. Kong WH, Lee WJ, Cui ZY, Bae KH, Park TG, Kim JH, Park K, Seo SW. Biomaterials. 2007; 28:5555. [PubMed: 17904632]
57. (a) Aviv H, Bartling S, Kieslling F, Margel S. Biomaterials. 2009; 30:5610. [PubMed: 19592085] (b) Galperin A, Margel D, Baniel J, Dank G, Biton H, Margel S. Biomaterials. 2007; 28:4461. [PubMed: 17644171]
58. (a) Ahn S, Jung SY, Lee JP, Lee SJ. J. Phys. Chem. B. 2011; 115:889. [PubMed: 21222463] (b) Lee SJ, Jung SY, Ahn S. Biosens. Bioelectron. 2010; 25:1571. [PubMed: 20022479]
59. Nishiyama N, Kataoka K. Pharmacol. Ther. 2006; 112:630. [PubMed: 16815554]
60. (a) Torchilin VP, Frank-Kamenetsky MD, Wolf GL. Acad. Radiol. 1999; 6:61. [PubMed: 9891154] (b) Trubetskoy VS, Gazelle GS, Wolf GL, Torchilin VP. J. Drug Target. 1997; 4:381. [PubMed: 9239578]

61. Fu YJ, Nitecki DE, Maltby D, Simon GH, Berejnoi K, Raatschen HJ, Yeh BM, Shames DM, Brasch RC. Bioconjugate Chem. 2006; 17:1043.
62. (a) Raatschen HJ, Fu YJ, Brasch RC, Pietsch H, Shames DM, Yeh BM. Invest. Radiol. 2009; 44:265. [PubMed: 19346961] (b) Simon GH, Fu YJ, Berejnoi K, Fournier LS, Lucidi V, Yeh B, Shames DM, Brasch RC. Invest. Radiol. 2005; 40:614. [PubMed: 16118555]
63. Yordanov AT, Mollov N, Lodder AL, Woller E, Cloninger M, Walbridge S, Milenic D, Brechbiel MW. J. Serb. Chem. Soc. 2005; 70:163.
64. Dekrafft KE, Xie ZG, Cao GH, Tran S, Ma LQ, Zhou OZ, Lin WB. Angew. Chem. Int. Edit. 2009; 48:9901.
65. (a) Sosnovsky G, Maheswara Rao NU. Eur. J. Med. Chem. 1988; 23:517.(b) Schmitt-Willich H. Br. J. Radiol. 2007; 80:581. [PubMed: 17704318] (c) Idee JM, Port M, Robic C, Medina C, Sabatou M, Corot C. J. Magn. Reson. Imaging. 2009; 30:1249. [PubMed: 19938037]
66. (a) Coche EE, Hammer FD, Goffette PP. Eur. Radiol. 2001; 11:2306. [PubMed: 11702176] (b) Smadja L, Remy-Jardin M, Dupuis P, Deken-Delannoy V, Devos P, Duhamel A, Laffitte JJ, Dequiedt P, Remy J. J. Radiol. 2009; 90:287. [PubMed: 19421113] (c) Bloem JL, Wondergem J. Radiology. 1989; 171:578. [PubMed: 2704827] (d) Albrecht T, Dawson P. Br. J. Radiol. 2000; 73:878. [PubMed: 11026864] (e) Remy-Jardin M, Bahepar J, Lafitte JJ, Dequiedt P, Ertzbischoff O, Bruzzi J, Delannoy-Deken V, Duhamel A, Remy J. Radiology. 2006; 238:1022. [PubMed: 16505397]
67. Rupp K, Handreke K, Schuhmann-Giampieri G, Krause W. Invest. Radiol. 2002; 37:241. [PubMed: 11979149]
68. Schmitt-Willich H, Brehm M, Ewers CLJ, Michl G, Muller-Fahrnow A, Petrov O, Platzek J, Raduchel B, Sulzle D. Inorg. Chem. 1999; 38:1134. [PubMed: 11670895]
69. (a) McMahon BK, Mauer P, McCoy CP, Lee TC, Gunnlaugsson T. Aust. J. Chem. 2011; 64:600. (b) Lincheneau C, Stomeo F, Comby S, Gunnlaugsson T. Aust. J. Chem. 2011; 64:1315.(c) McMahon B, Mauer P, McCoy CP, Lee TC, Gunnlaugsson T. J. Am. Chem. Soc. 2009; 131:17542. [PubMed: 19916488]
70. (a) Vera DR, Mattrey RF. Acad. Radiol. 2002; 9:784. [PubMed: 12139092] (b) Sirlin CB, Vera DR, Corbeil JA, Caballero MB, Buxton RB, Mattrey RF. Acad. Radiol. 2004; 11:1361. [PubMed: 15596374]
71. Santra S, Bagwe RP, Dutta D, Stanley JT, Walter GA, Tan W, Moudgil BM, Mericle RA. Adv. Mater. 2005; 17:2165.
72. Ashokan A, Menon D, Nair S, Koyakutty M. Biomaterials. 2010; 31:2606. [PubMed: 20035998]
73. (a) Zhang G, Liu YL, Yuan QH, Zong CH, Liu JH, Lu LH. Nanoscale. 2011; 3:4365. [PubMed: 21904751] (b) Xing HY, Bu WB, Zhang SJ, Zheng XP, Li M, Chen F, He QJ, Zhou LP, Peng WJ, Hua YQ, Shi JL. Biomaterials. 2012; 33:1079. [PubMed: 22061493]
74. (a) Perazella MA. Clin. J. Am. Soc. Nephrol. 2009; 4:461. [PubMed: 19201920] (b) Morcos SK. Eur. Radiol. 2011; 21:496. [PubMed: 20848109] (c) Perazella MA. Curr. Opin. Nephrol. Hypertens. 2009; 18:519. [PubMed: 19623065] (d) Perazella MA. Curr. Drug. Saf. 2008; 3:67. [PubMed: 18690983] (e) Nyman U, Elmstahl B, Leander P, Nilsson M, Golman K, Almen T. Radiology. 2002; 223:311. [PubMed: 11997530]
75. (a) Kuo PH. J. Am. Coll. Radiol. 2008; 5:29. [PubMed: 18180006] (b) Rofsky NM, Sherry AD, Lenkinski RE. Radiology. 2008; 247:608. [PubMed: 18487530] (c) Sherry AD, Caravan P, Lenkinski RE. J. Magn. Reson. Imaging. 2009; 30:1240. [PubMed: 19938036] (d) Carbonaro LA, Pediconi F, Verardi N, Trimboli RM, Calabrese M, Sardanelli F. Am. J. Roentgenol. 2011; 196:942. [PubMed: 21427349] (e) Runge, VM. Contrast Agents: Safety Profile. Temple, TX: Texas A&M University Health Science Center; 2008.
76. (a) Kim D, Park S, Lee JH, Jeong YY, Jon S. J. Am. Chem. Soc. 2007; 129:7661. [PubMed: 17530850] (b) Cai QY, Kim SH, Choi KS, Kim SY, Byun SJ, Kim KW, Park SH, Juhng SK, Yoon KH. Invest. Radiol. 2007; 42:797. [PubMed: 18007151]
77. (a) Guo R, Wang H, Peng C, Shen MW, Pan MJ, Cao XY, Zhang GX, Shi XY. J. Phys. Chem. C. 2010; 114:50.(b) Kojima C, Umeda Y, Ogawa M, Harada A, Magata Y, Kono K. Nanotechnology. 2010; 21(c) Peng C, Zheng LF, Chen Q, Shen MW, Guo R, Wang H, Cao XY, Zhang GX, Shi XY. Biomaterials. 2012; 33:1107. [PubMed: 22061490]

78. Liu H, Wang H, Guo R, Cao XY, Zhao JL, Luo Y, Shen MW, Zhang GX, Shi XY. Polym. Chem. 2010; 1:1677.

79. Wang H, Zheng LF, Peng C, Guo R, Shen MW, Shi XY, Zhang GX. Biomaterials. 2011; 32:2979. [PubMed: 21277019]

80. Guo R, Wang H, Peng C, Shen MW, Zheng LF, Zhang GX, Shi XY. J. Mater. Chem. 2011; 21:5120.

81. (a) Park YS, Kasuya A, Drnytruk A, Yasuto N, Takeda M, Ohuchi N, Sato Y, Tohji K, Uo M, Watari F. J. Nanosci. Nanotechnol. 2007; 7:2690. [PubMed: 17685285] (b) Park YS, Liz-Marzan LM, Kasuya A, Kobayashi Y, Nagao D, Konno M, Mamykin S, Dmytruk A, Takeda M, Ohuchi N. J. Nanosci. Nanotechnol. 2006; 6:3503. [PubMed: 17252799]

82. Hainfeld JF, Slatkin DN, Focella TM, Smilowitz HM. Br. J. Radiol. 2006; 79:248. [PubMed: 16498039]

83. (a) Hainfeld JF, Dilmanian FA, Zhong Z, Slatkin DN, Kalef-Ezra JA, Smilowitz HM. Phys. Med. Biol. 2010; 55:3045. [PubMed: 20463371] (b) Hainfeld JF, Dilmanian FA, Slatkin DN, Smilowitz HM. J. Pharm. Pharmacol. 2008; 60:977. [PubMed: 18644191] (c) Hainfeld JF, Slatkin DN, Smilowitz HM. Phys. Med. Biol. 2004; 49:N309. [PubMed: 15509078]

84. Sun IC, Eun DK, Na JH, Lee S, Kim IJ, Youn IC, Ko CY, Kim HS, Lim D, Choi K, Messersmith PB, Park TG, Kim SY, Kwon IC, Kim K, Ahn CH. Chem.-Eur. J. 2009; 15:13341. [PubMed: 19902441]

85. Eck W, Nicholson AI, Zentgraf H, Semmler W, Bartling S. Nano Lett. 2010; 10:2318. [PubMed: 20496900]

86. Zhang ZY, Ross RD, Roeder RK. Nanoscale. 2010; 2:582. [PubMed: 20644762]

87. Ghann, WE.; Aras, O.; Fleiter, T.; Daniel, MC. Smart Biomedical and Physiological Sensor Technology VIII. Bellingham, FL: 2011. p. 80250H

88. (a) Li J, Chaudhary A, Chmura SJ, Pelizzari C, Rajh T, Wietholt C, Kurtoglu M, Aydogan B. Phys. Med. Biol. 2010; 55:4389. [PubMed: 20647599] (b) Aydogan B, Li J, Rajh T, Chaudhary A, Chmura SJ, Pelizzari C, Wietholt C, Kurtoglu M, Redmond P. Mol. Imaging. Biol. 2010; 12:463. [PubMed: 20237857]

89. Popovtzer R, Agrawal A, Kotov NA, Popovtzer A, Balter J, Carey TE, Kopelman R. Nano Lett. 2008; 8:4593. [PubMed: 19367807]

90. Reuveni T, Motiei M, Romman Z, Popovtzer A, Popovtzer R. Int. J. Nanomed. 2011; 6:2859.

91. Hainfeld JF, O'Connor MJ, Dilmanian FA, Slatkin DN, Adams DJ, Smilowitz HM. Br. J. Radiol. 2011; 84:526. [PubMed: 21081567]

92. Chanda N, Kattumuri V, Shukla R, Zambre A, Katti K, Upendran A, Kulkarni RR, Kan P, Fent GM, Casteel SW, Smith CJ, Boote E, Robertson JD, Cutler C, Lever JR, Katti KV, Kannan R. Proc. Natl. Acad. Sci. U. S. A. 2010; 107:8760. [PubMed: 20410458]

93. Low PS, Henne WA, Doorneweerd DD. Accounts Chem. Res. 2007; 41:120.

94. Huang P, Bao L, Zhang CL, Lin J, Luo T, Yang DP, He M, Li ZM, Gao G, Gao B, Fu S, Cui DX. Biomaterials. 2011; 32:9796. [PubMed: 21917309]

95. Kim D, Jeong YY, Jon S. ACS Nano. 2010; 4:3689. [PubMed: 20550178]

96. (a) Park JA, Kim HK, Kim JH, Jeong SW, Jung JC, Lee GH, Lee J, Chang Y, Kim TJ. Bioorg. Med. Chem. Lett. 2010; 20:2287. [PubMed: 20188545] (b) Sun HM, Yuan QH, Zhang BH, Ai KL, Zhang PG, Lu LH. Nanoscale. 2011; 3:1990. [PubMed: 21384042] (c) Md NS, Kim HK, Park JA, Chang Y, Kim TJ. Bull. Korean Chem. Soc. 2010; 31:1177.(d) Arifin DR, Long CM, Gilad AA, Alric CE, Roux S, Tillement O, Link TW, Arepally A, Bulte JWM. Radiology. 2011; 260:790. [PubMed: 21734156] (e) Alric C, Taleb J, Le Duc G, Mandon C, Billotey C, Le Meur-Herland A, Brochard T, Vocanson F, Janier M, Perriat P, Roux S, Tillement O. J. Am. Chem. Soc. 2008; 130:5908. [PubMed: 18407638] (f) Kim D, Yu MK, Lee TS, Park JJ, Jeong YY, Jon S. Nanotechnology. 2011; 22:155101. [PubMed: 21389582]

97. (a) Cormode DP, Roessl E, Thran A, Skajaa T, Gordon RE, Schlomka JP, Fuster V, Fisher EA, Mulder WJM, Proksa R, Fayad ZA. Radiology. 2010; 256:774. [PubMed: 20668118] (b) Skajaa T, Cormode DP, Falk E, Mulder WJM, Fisher EA, Fayad ZA. Arterioscler. Thromb. Vasc. Biol. 2010; 30:169. [PubMed: 19815819] (c) Cormode DP, Skajaa T, van Schooneveld MM, Koole R, Jarzyna P, Lobatto ME, Calcagno C, Barazza A, Gordon RE, Zanzonico P, Fisher EA, Fayad ZA,

Mulder WJM. Nano Lett. 2008; 8:3715. [PubMed: 18939808] (d) van Schooneveld MM, Cormode DP, Koole R, van Wijngaarden JT, Calcagno C, Skajaa T, Hilhorst J, t Hart DC, Fayad ZA, Mulder WJM, Meijerink A. Contrast Media Mol. I. 2010; 5:231.

98. Kim YH, Jeon J, Hong SH, Rhim WK, Lee YS, Youn H, Chung JK, Lee MC, Lee DS, Kang KW, Nam JM. Small. 2011; 7:2052. [PubMed: 21688390]
99. (a) Cho MJ, Cho WS, Choi M, Kim SJ, Han BS, Kim SH, Kim HO, Sheen YY, Jeong JY. Toxicol. Lett. 2009; 189:177. [PubMed: 19397964] (b) Caliceti P, Veronese FM. Adv. Drug Deliv. Rev. 2003; 55:1261. [PubMed: 14499706] (c) Lacerda L, Herrero MA, Venner K, Bianco A, Prato M, Kostarelos K. Small. 2008; 4:1130. [PubMed: 18666166]
100. Luo T, Huang P, Gao G, Shen GX, Fu S, Cui DX, Zhou CQ, Ren QS. Opt. Express. 2011; 19:17030. [PubMed: 21935063]
101. Xiao M, Nyagilo J, Arora V, Kulkarni P, Xu DS, Sun XK, Dave DP. Nanotechnology. 2010; 21:1.
102. Hahn M, Singh A, Sharma P, Brown S, Moudgil B. Anal. Bioanal. Chem. 2011; 399:3. [PubMed: 20924568]
103. Jackson PA, Rahman WNWA, Wong CJ, Ackerly T, Geso M. Eur. J. Radiol. 2010; 75:104. [PubMed: 19406594]
104. (a) Chen YS, Hung YC, Liau I, Huang GS. Nanoscale Res. Lett. 2009; 4:858. [PubMed: 20596373] (b) Yildirimer L, Thanh NTK, Loizidou M, Seifalian AM. Nano Today. 2011; 6:585. [PubMed: 23293661] (c) Li YF, Chen CY. Small. 2011; 7:2965. [PubMed: 21932238] (d) Soenen SJ, Rivera-Gil P, Montenegro JM, Parak WJ, De Smedt SC, Braeckmans K. Nano Today. 2011; 6:446.(e) Bar-Ilan O, Albrecht RM, Fako VE, Furgeson DY. Small. 2009; 5:1897. [PubMed: 19437466]
105. Zhou C, Long M, Qin Y, Sun X, Zheng J. Angew. Chem. Int. Edit. 2011; 50:3168.
106. Rabin O, Perez JM, Grimm J, Wojtkiewicz G, Weissleder R. Nat. Mater. 2006; 5:118. [PubMed: 16444262]
107. Ai KL, Liu YL, Liu JH, Yuan QH, He YY, Lu LH. Adv. Mater. 2011; 23:4886. [PubMed: 21956662]
108. Perera VS, Hao JH, Gao M, Gough M, Zayalij PY, Flask C, Basilion JP, Huang SD. Inorg. Chem. 2011; 50:7910. [PubMed: 21797245]
109. (a) Bonitatibus PJ, Torres AS, Goddard GD, FitzGerald PF, Kulkarni AM. Chem. Commun. 2010; 46:8956.(b) Oh MH, Lee N, Kim H, Park SP, Piao Y, Lee J, Jun SW, Moon WK, Choi SH, Hyeon T. J. Am. Chem. Soc. 2011; 133:5508. [PubMed: 21428437]
110. Chou SW, Shau YH, Wu PC, Yang YS, Shieh DB, Chen CC. J. Am. Chem. Soc. 2010; 132:13270. [PubMed: 20572667]
111. (a) Garrett PR, Meshkov SL, Perlmutter GS. Radiology. 1984; 153:545. [PubMed: 6484186] (b) Raptopoulos V. Radiol. Clin. N. Am. 1989; 27:631. [PubMed: 2657845] (c) Fiebig T, Boll H, Figueiredo G, Kerl HU, Nittka S, Groden C, Kramer M, Brockmann MA. PLoS One. 2012; 7:e31179. [PubMed: 22363574] (d) Boll H, Nittka S, Doyon F, Neumaier M, Marx A, Kramer M, Groden C, Brockmann MA. PLoS One. 2011; 6:e25692. [PubMed: 21984939]
112. (a) Leng HJ, Wang X, Ross RD, Niebur GL, Roeder RK. J. Mech. Behav. Biomed. Mater. 2008; 1:68. [PubMed: 18443659] (b) Wang X, Masse DB, Leng H, Hess KP, Ross RD, Roeder RK, Niebur GL. J. Biomech. 2007; 40:3397. [PubMed: 17588588]
113. Landrigan MD, Flatley JC, Turnbull TL, Kruzic JJ, Ferracane JL, Hilton TJ, Roeder RK. J. Mech. Behav. Biomed. Mater. 2010; 3:223. [PubMed: 20129422]
114. Tang SY, Vashishth D. Bone. 2007; 40:1259. [PubMed: 17329178]
115. (a) Kreck TC, Krueger MA, Altemeier WA, Sinclair SE, Robertson HT, Shade ED, Hildebrandt J, Lamm WJE, Frazer DA, Polissar NL, Hlastala MP. J. Appl. Physiol. 2001; 91:1741. [PubMed: 11568158] (b) Chen RY, Fan FC, Kim S, Jan KM, Usami S, Chien S. J. Appl. Physiol. 1980; 49:178. [PubMed: 7400000] (c) Isbister WH, Schofield PF, Torrance HB. Phys. Med. Biol. 1965; 10:243. [PubMed: 14332804]
116. (a) Carlson AP, Brown AM, Zager E, Uchino K, Marks MP, Robertson C, Sinson GP, Marmarou A, Yonas H. AJNR. Am. J. Neuroradiol. 2011; 32:1315. [PubMed: 21700787] (b) Latchaw RE, Yonas H, Pentheny SL, Gur D. Radiology. 1987; 163:251. [PubMed: 3823444]

117. Wintermark M, Sesay M, Barbier E, Borbély K, Dillon WP, Eastwood JD, Glenn TC, Grandin CB, Pedraza S, Soustiel J-F, Nariai T, Zaharchuk G, Caillé J-M, Dousset V, Yonas H. Stroke. 2005; 36:2032.

118. (a) Mette D, Strunk R, Zuccarello M. Transl. Stroke Res. 2011; 2:152. [PubMed: 24323620] (b) Coles JP. Br. J. Anaesth. 2007; 99:49. [PubMed: 17573394] (c) Coles JP. Curr. Opin. Anesthesio. 2006; 19:473.

119. Kosty JA, Kofke WA, Maloney-Wilensky E, Frangos SG, Levine JM, LeRoux PD, Zager EL. Transl. Stroke Res. 2012; 3:375. [PubMed: 24323813]

120. (a) Honda N, Osada H, Watanabe W, Nakayama M, Nishimura K, Krauss B, Otani K. Radiology. 2012; 262:262. [PubMed: 22025733] (b) Goo HW, Yang DH, Hong SJ, Yu J, Kim BJ, Seo JB, Chae EJ, Lee J, Krauss B. Pediatr. Radiol. 2010; 40:1490. [PubMed: 20411254] (c) Chae EJ, Seo JB, Lee J, Kim N, Goo HW, Lee HJ, Lee CW, Ra SW, Oh YM, Cho YS. Invest. Radiol. 2010; 45:354. [PubMed: 20404734] (d) Kang MJ, Park CM, Lee CH, Goo JM, Lee HJ. Radiographics. 2010; 30:685. [PubMed: 20462988] (e) Chae EJ, Seo JB, Goo HW, Kim N, Song KS, Lee SD, Hong SJ, Krauss B. Radiology. 2008; 248:615. [PubMed: 18641254] (f) Park EA, Goo JM, Park SJ, Lee HJ, Lee CH, Park CM, Yoo CG, Kim JH. Radiology. 2010; 256:985. [PubMed: 20651060]

121. (a) Kobayashi M, Suzuki M, Ikeda H, Takahashi H, Matsumoto N, Maeyama S, Sase S, Iino S, Itoh F. Hepatol. Res. 2009; 39:31. [PubMed: 18761681] (b) Ikeda H, Suzuki M, Kobayashi M, Takahashi H, Matsumoto N, Maeyama S, Iino S, Sase S, Itoh F. Hepatol. Res. 2007; 37:104. [PubMed: 17300705] (c) Shigefuku R, Takahashi H, Kobayashi M, Ikeda H, Matsunaga K, Okuse C, Matsumoto N, Maeyama S, Sase S, Suzuki M, Itoh F. J. Gastroenterol. 2012 In press. (d) Takahashi H, Suzuki M, Ikeda H, Kobayashi M, Sase S, Yotsuyanagi H, Maeyama S, Iino S, Itoh F. Alcohol. Clin. Exp. Res. 2010; 34(Suppl 1):S7. [PubMed: 18986379] (e) Hashimoto K, Murakami T, Dono K, Hori M, Kim T, Kudo M, Marubashi S, Miyamoto A, Takeda Y, Nagano H, Umeshita K, Nakamura H, Monden M. Dig. Dis. Sci. 2007; 52:943. [PubMed: 17318388] (f) Murakami T, Hori M, Kim T, Hashimoto K, Dono K, Hayashi S, Sugihara E, Nagano H, Sase S, Sakon M, Monden M, Nakamura H. Invest. Radiol. 2004; 39:210. [PubMed: 15021324] (g) Shimizu J, Oka H, Dono K, Sakon M, Takamura M, Murakami T, Hayashi S, Nagano H, Nakamori S, Umeshita K, Sase S, Gotoh M, Wakasa K, Nakamura H, Monden M. Dig. Dis. Sci. 2003; 48:1510. [PubMed: 12924645]

122. (a) Kubota M, Murakami T, Nagano H, Eguchi H, Marubashi S, Kobayashi S, Wada H, Tanemura M, Dono K, Nakamori S, Sakon M, Monden M, Mori M, Doki Y. Dig. Dis. Sci. 2012; 57:801. [PubMed: 21953140] (b) Abe H, Murakami T, Kubota M, Kim T, Hori M, Kudo M, Hashimoto K, Nakamori S, Dono K, Tomoda K, Monden M, Nakamura H. Radiat. Med. 2005; 23:364. [PubMed: 16342909]

123. Market Analysis Report, Frost & Sullivan. Palo Alto, CA: 2007. North American Contrast Media Markets.

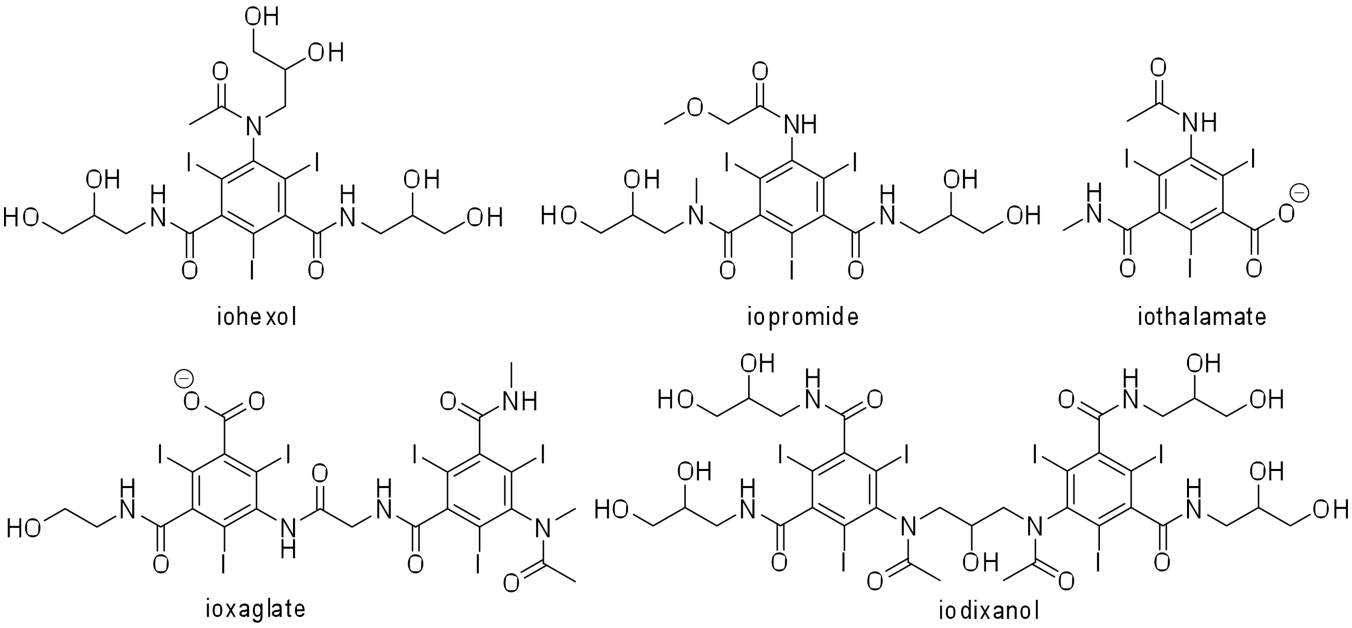

Figure 1.
Structures of some commercially available clinically approved CT contrast agents.

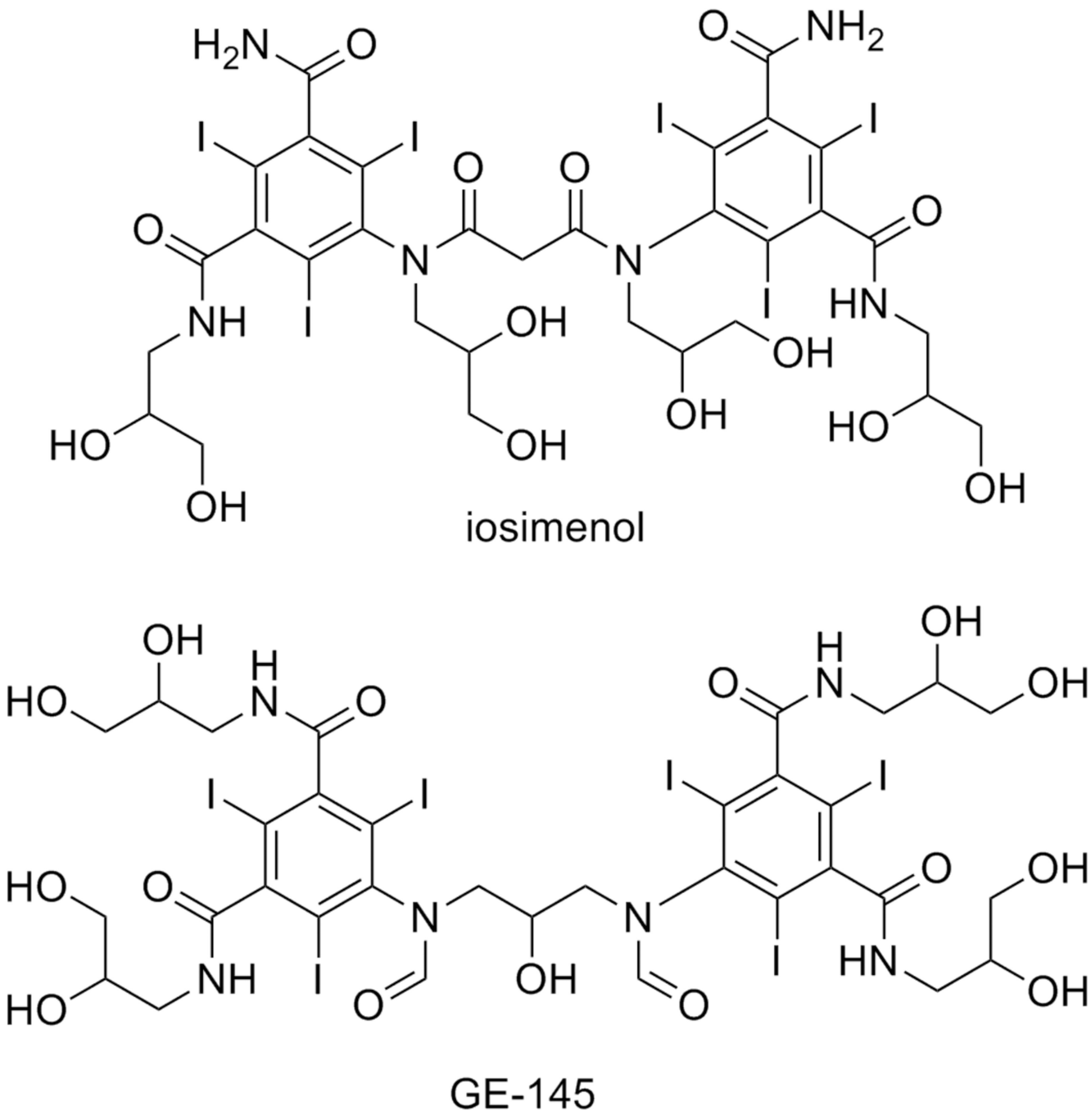

Figure 2.
Two of the novel low-osmolality, non-ionic contrast agents.

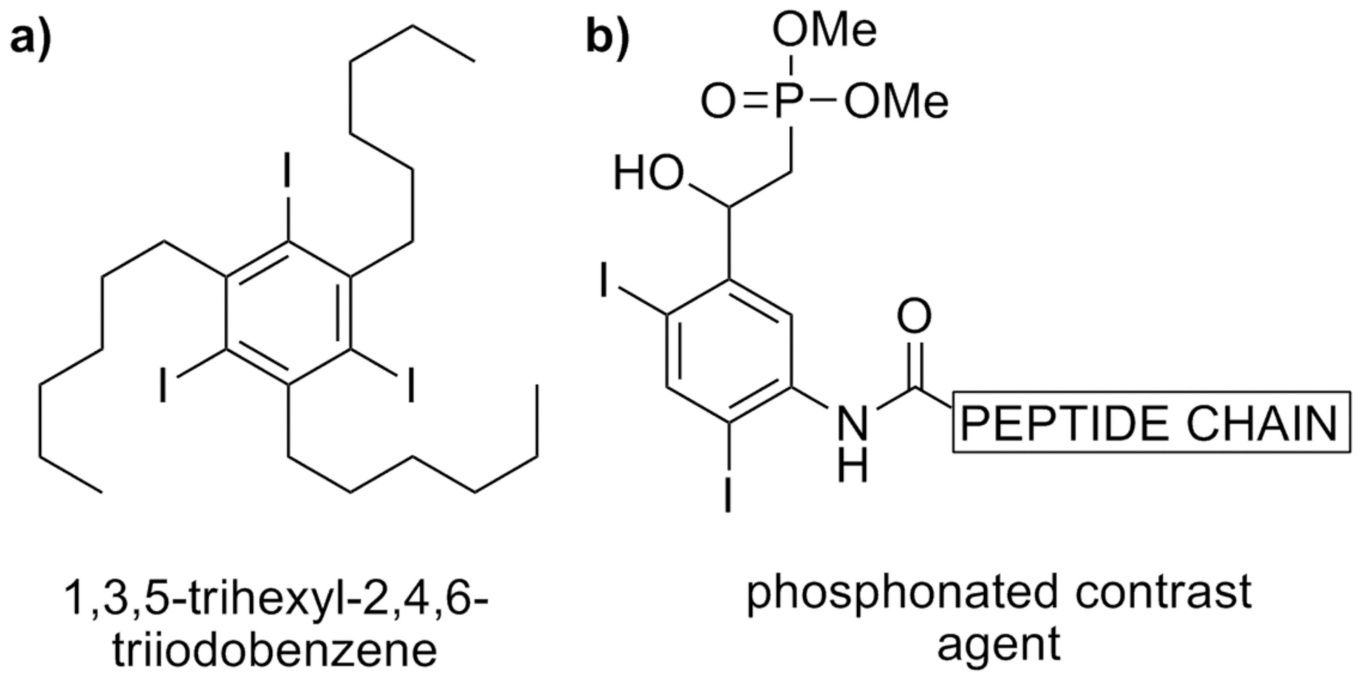

Figure 3.
Two of the several proposed contrast agents: a) for gastrointestinal imaging; b) as potential targeted contrast agents.

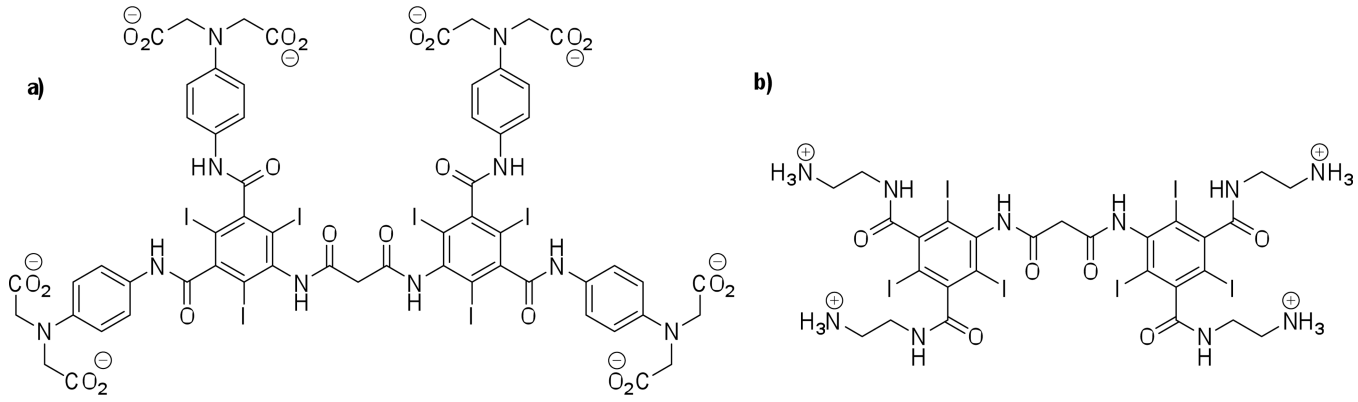

Figure 4.
Structures of two novel tissue-specific small-molecule iodinated CT contrast agents; a) an anionic Ca^{2+} chelating contrast agent for bone microdamage imaging; b) a cationic contrast agent "CA4+" for cartilage tissue imaging.

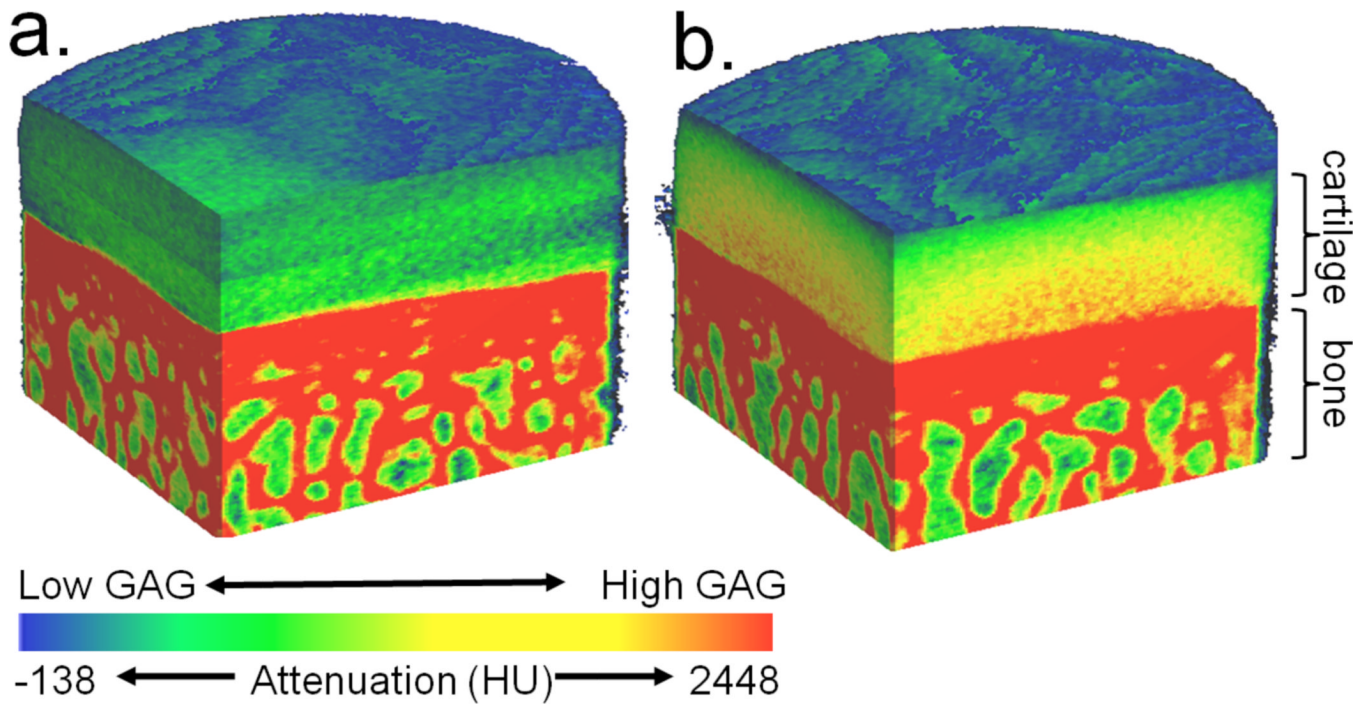

Figure 5.

3D contrast enhanced CT attenuation color-map images *ex vivo* bovine femur cartilage after immersion in a.) ioxaglate or b.) CA4+ contrast agent. Visible correlation between the GAG content and cationic (CA4+) contrast agent can be observed in the imaging of cartilage (b.). No such correlation is observed for anionic contrast agent ioxaglate (a.). Ioxaglate solution concentration 16 mg I/mL; CA4+ solution concentration 8 mg I/mL. The approximate cartilage and bone sections are labeled. (Images from author, unpublished data.)

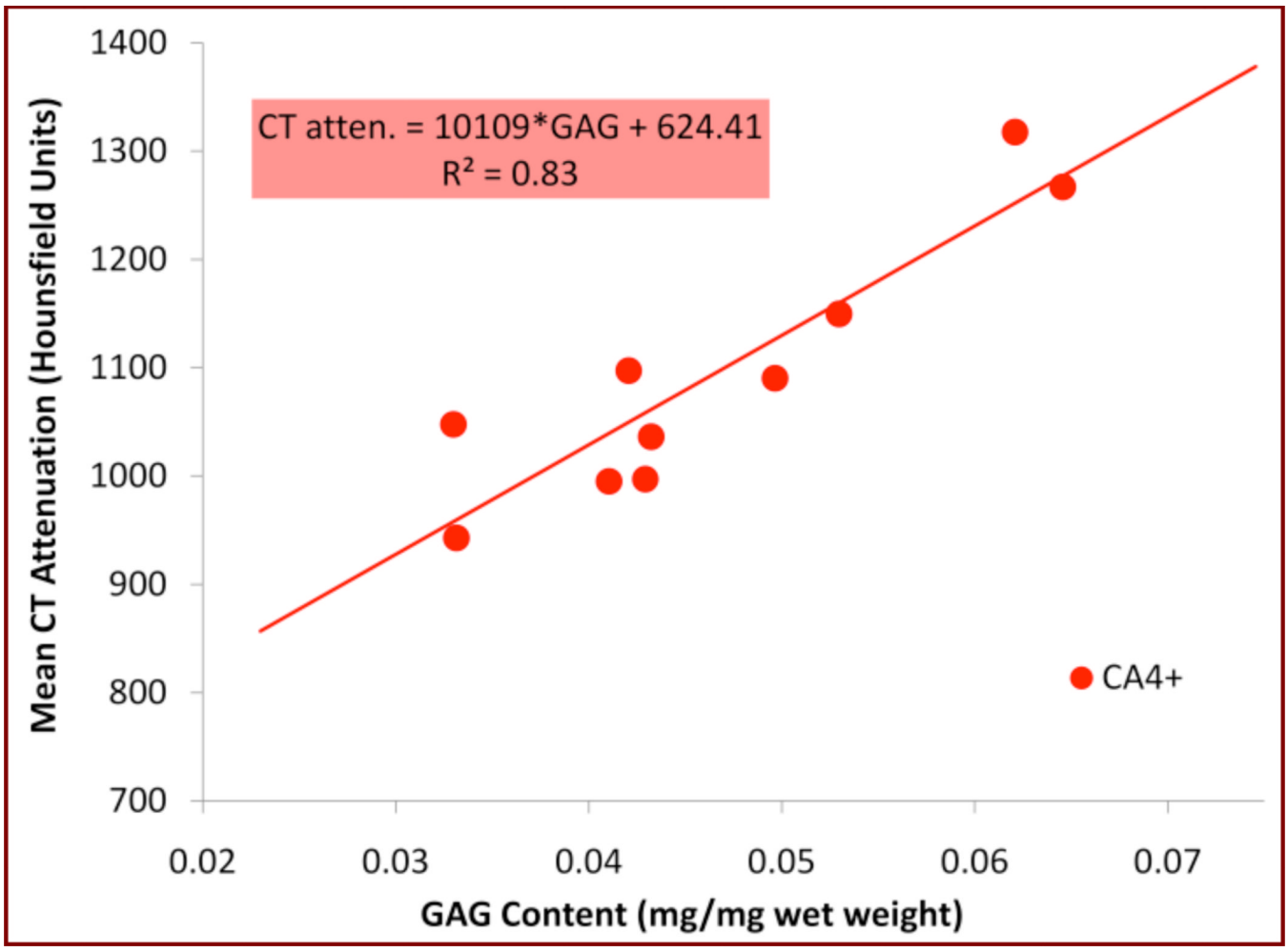

Figure 6.
Linear regression analysis of average CT attenuation (in HU) vs. GAG content of cartilage (reported as [mg of GAG]/[mg of hydrated cartilage]) using the CA4+ contrast agent. The study was performed on healthy bovine femoral cartilage plugs. Samples were prepared for biochemical analysis using the 1,9-dimethylmethylene blue (DMMB) colorimetric assay. (Image from author, unpublished data).

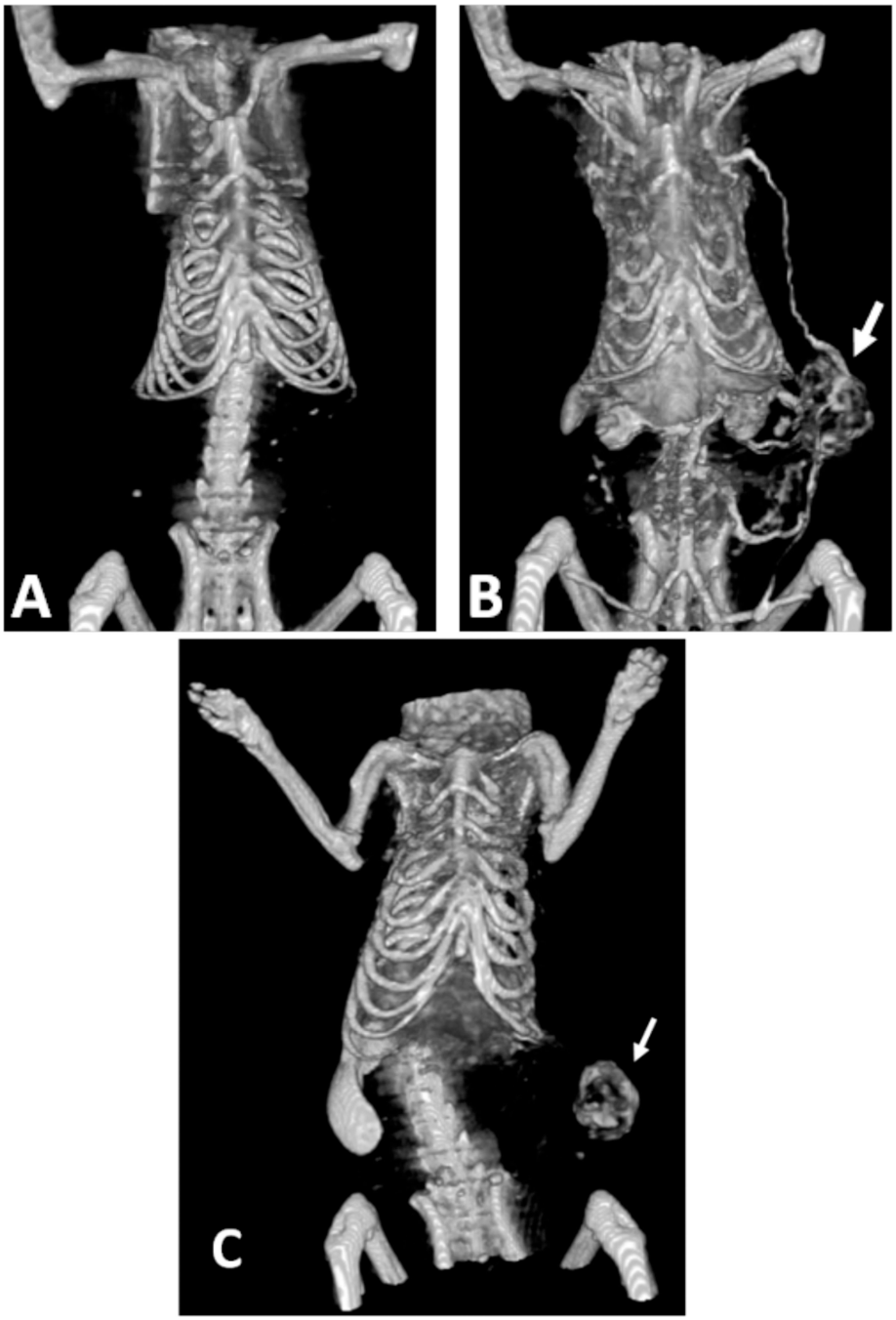

Figure 7.
Whole body CT images of rat with MatBIII breast tumor (arrow) in left flank A) before, and B) 5 minutes after i.v. administration of liposomal contrast agent (2 g of iodine per kg), demonstrating ability to visualize tumor vasculature. C) Accumulation of the contrast agent within tumor allowing for non-invasive visualization of tumor blood vessel permeability. Probe accumulation is visible within tumor (arrow) as well as the liver and spleen, which are responsible for nanocarrier clearance. Image was obtained 3 days after i.v. administration of contrast (455 mg of iodine per kg) using a clinical cone beam CT scanner (Koning Corporation). (Images courtesy of Dr Kathleen McNeeley; Georgia Institute of Technology, Atlanta, GA.)

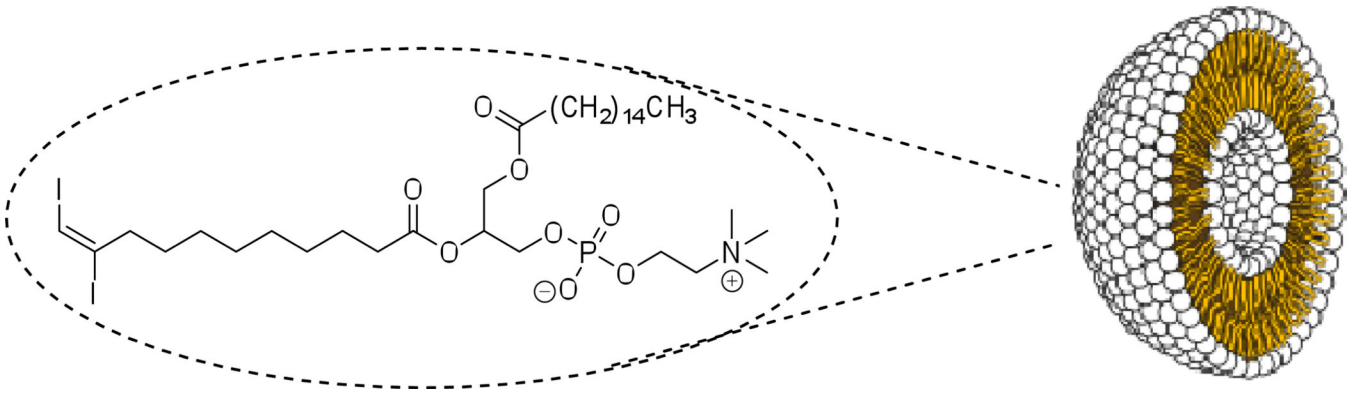

Figure 8.
Liposomal CT contrast agent prepared from a diiodophosphatidylcholine, with iodine covalently incorporated into the bilayer shell, providing an empty cavity with potential drug-delivery applications.

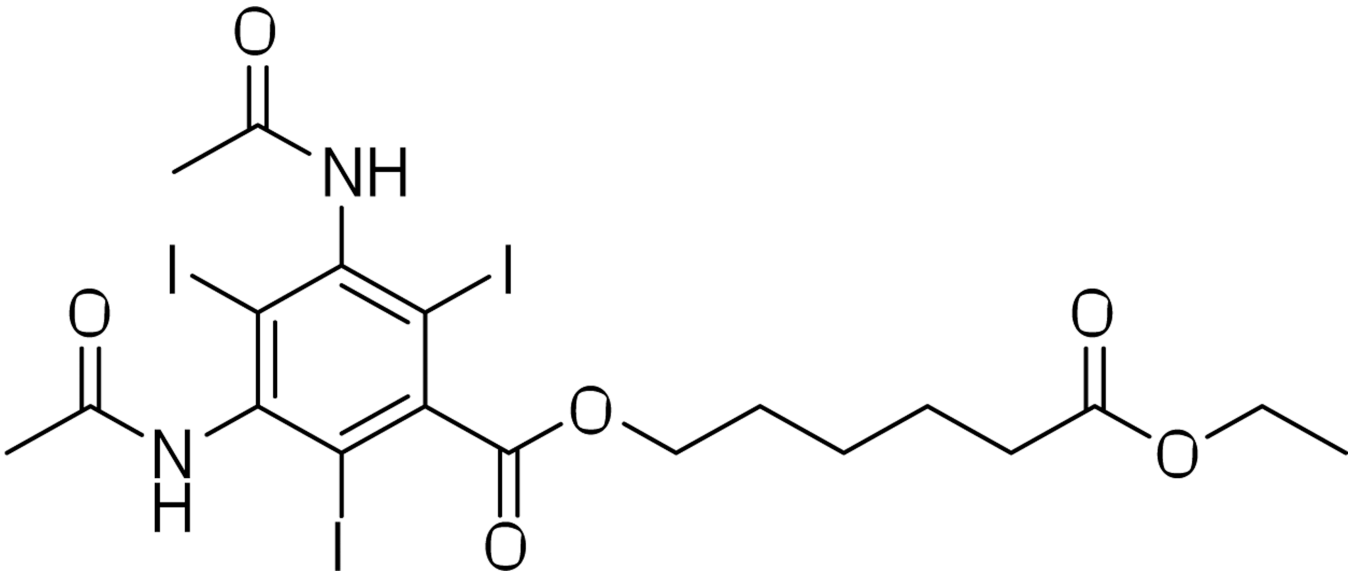

Figure 9.
Molecular structure of the nanoparticulate contrast agent 6-ethoxy-6-oxohexyl 3,5-diacetamido-2,4,6-triiodobenzoate (N1177).

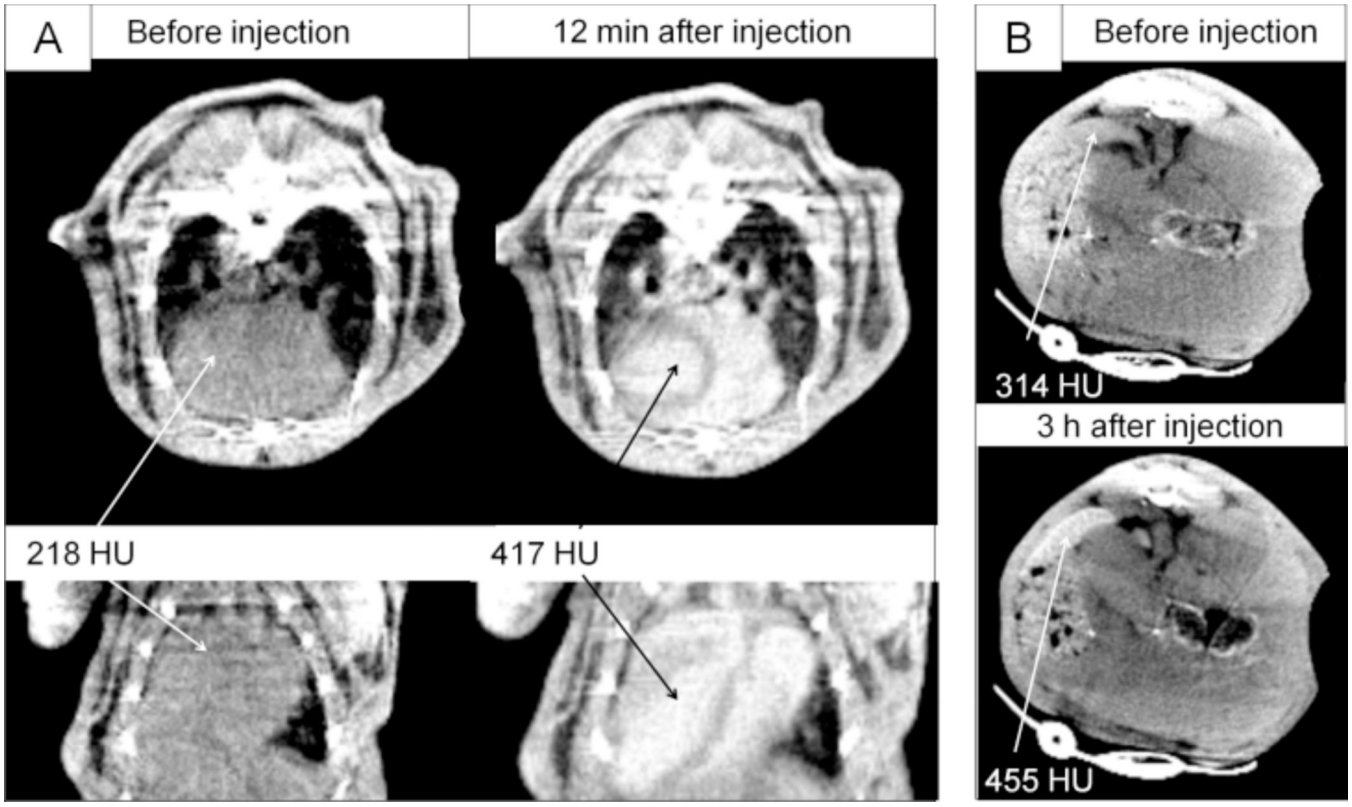

Figure 10.
In vivo CT images and opacification (in HU) after i.v. injection of PBD-PEO nanoemulsion contrast agent in mice; A) the heart before, and 12 min post-injection, transversal (top row) and coronal (bottom row); B) the spleen before, and 3 h post-injection. (Reprinted with permission from ref. 30b. Copyright 2010 Elsevier Ltd.)

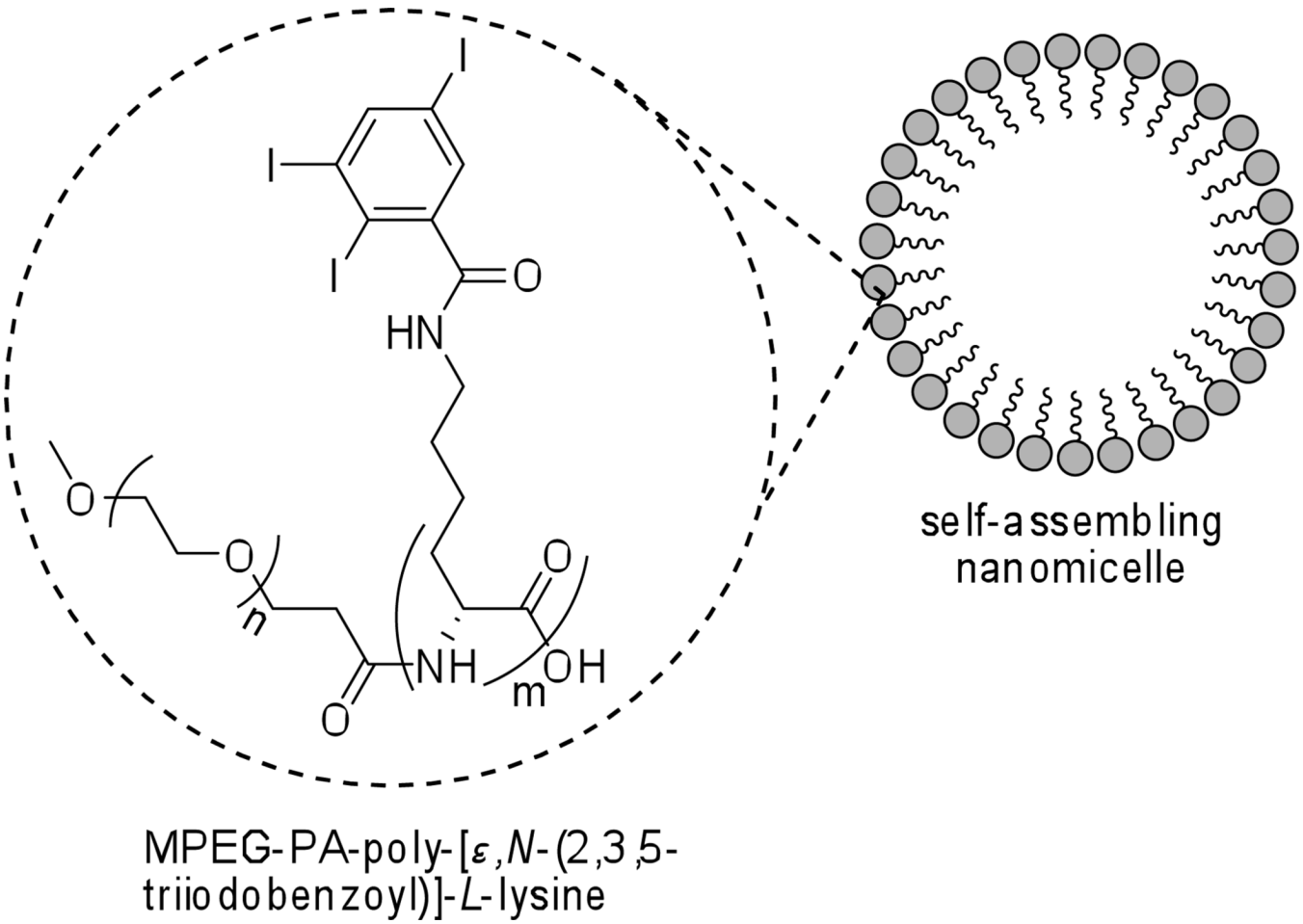

Figure 11.
Self-assembling nanomicellar CT contrast agent.

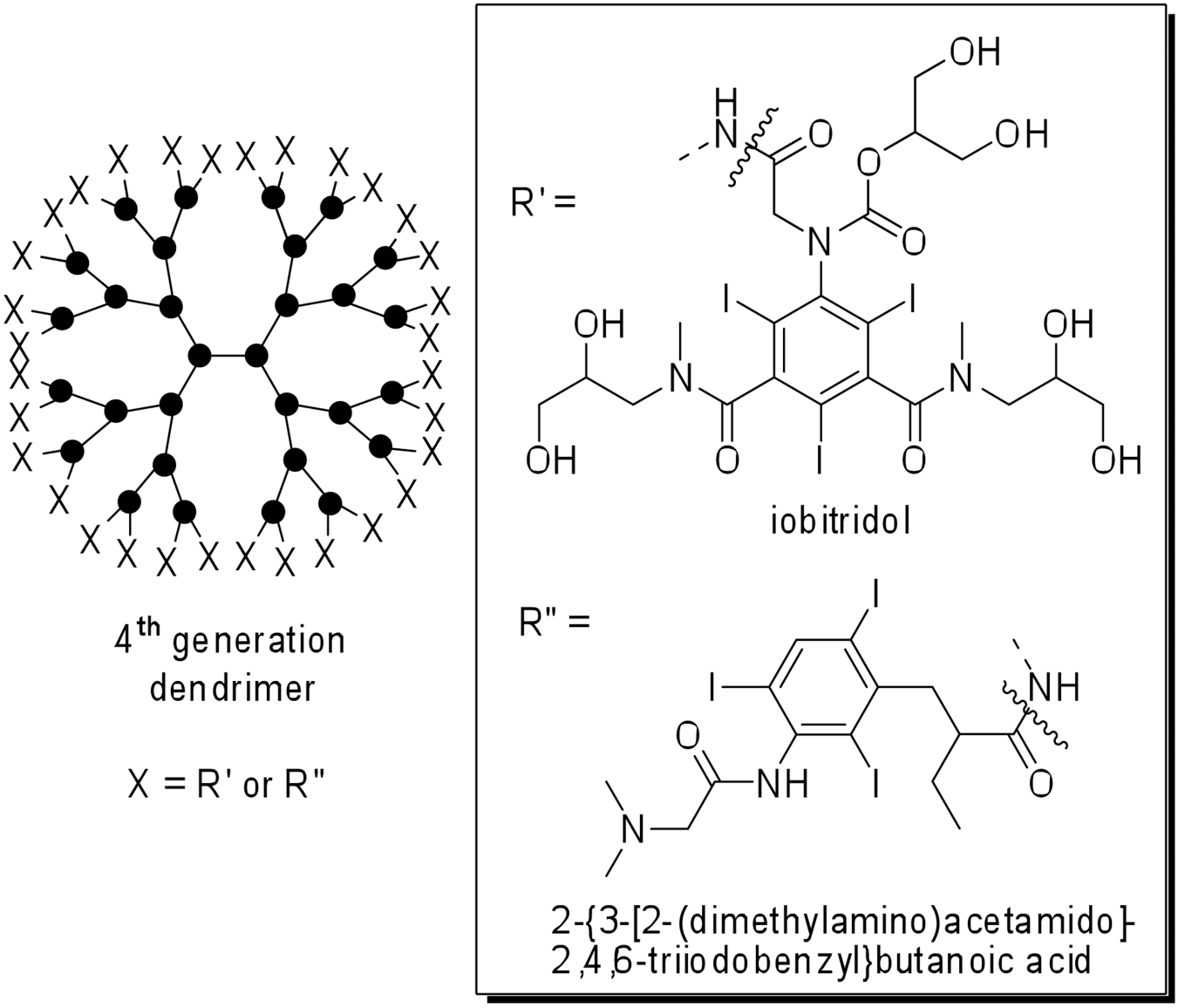

Figure 12.
Schematic representation of 4th generation dendrimer contrast agents. X = iobitridol (R') for poly-L-lysine/MPEG bowtie dendrimer; X = 2-{3-[2-(dimethylamino)acetamido]-2,4,6-triiodobenzyl}butanoic acid (R") for the PAMAM dendrimer imaging agent.

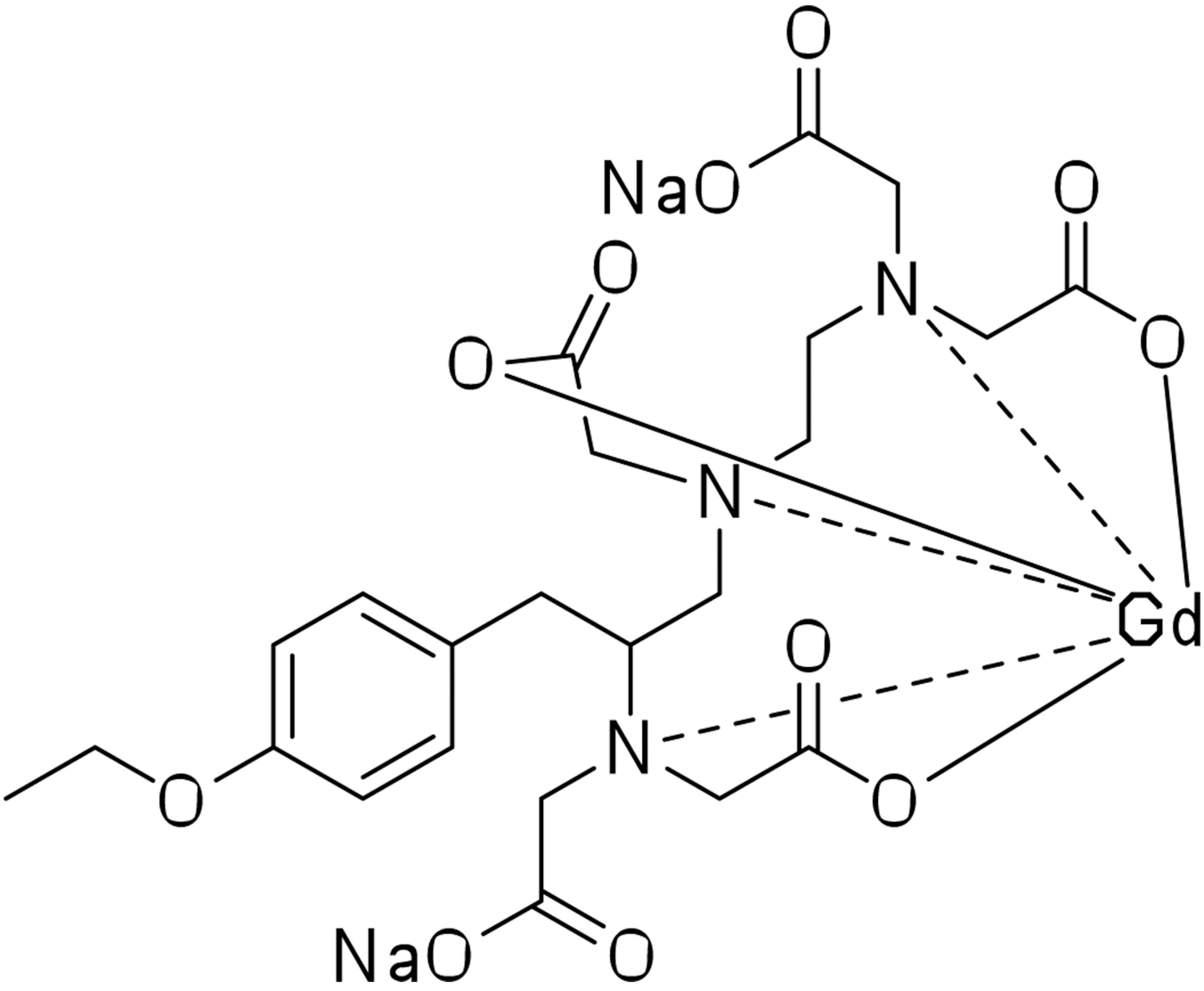

Figure 13.
Gadoxetate disodium salt, a clinically approved MRI liver-specific contrast agent.

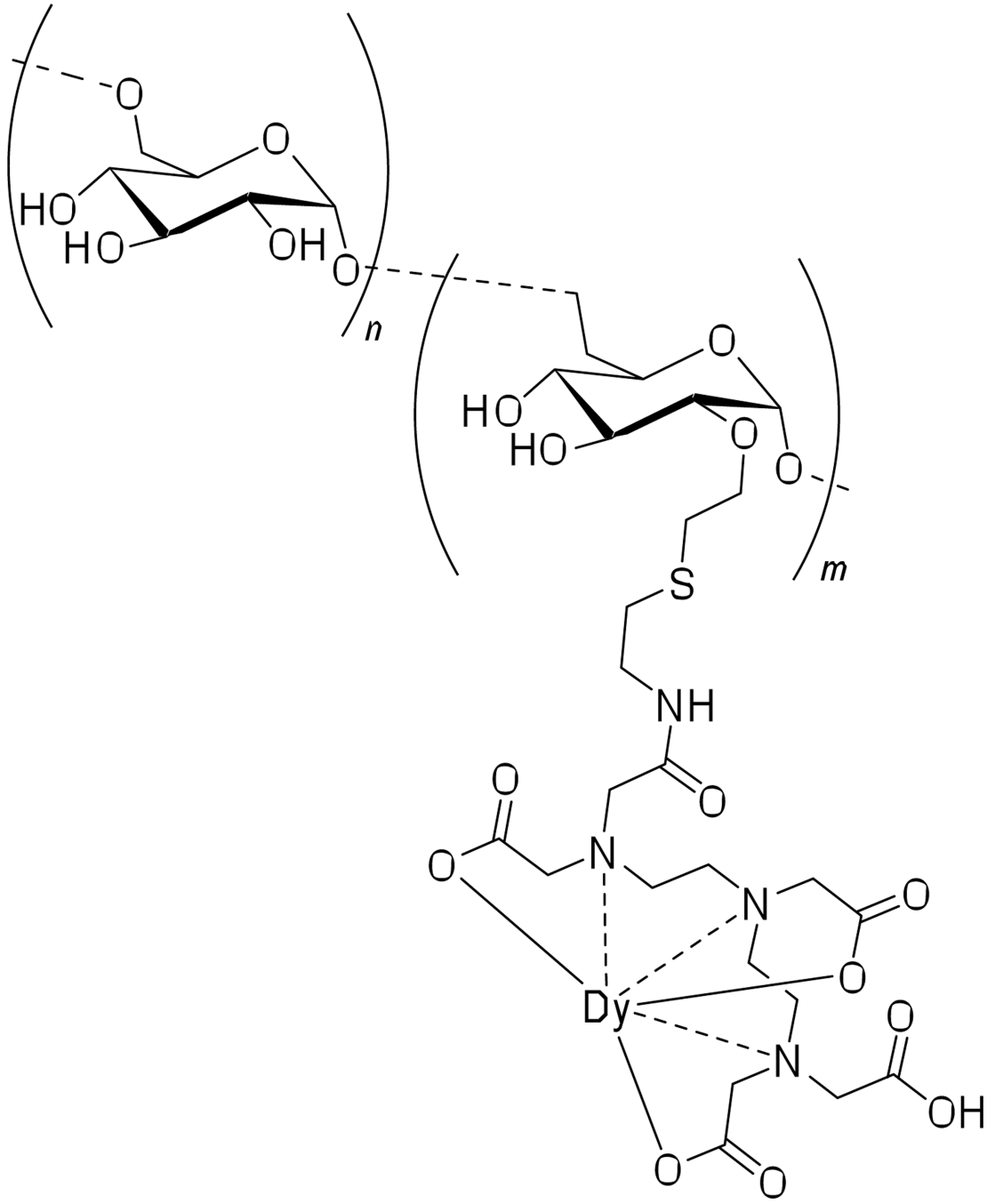

Figure 14.
DTPA-conjugated dysprosium chelating dextran polymer for MRI/CT imaging applications.

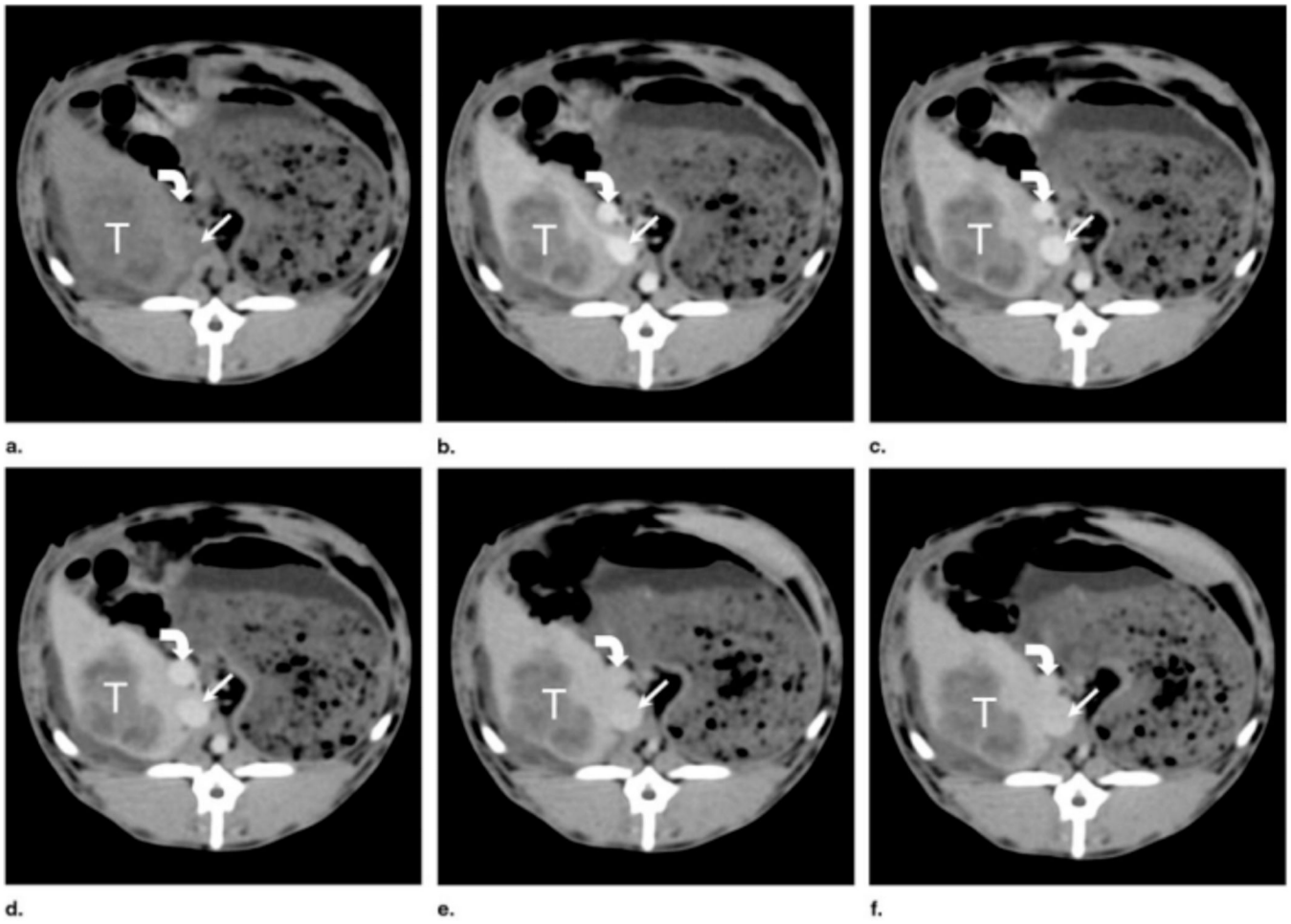

Figure 15.
Rabbit with a VX2 tumor (a) before [Dy]DTPA-dextran injection (1.15 mmol of dysprosium per kilogram) and (b) 2, (c) 5, (d) 8, (e) 37, and (f) 45 minutes after injection. The IVC (straight arrow) and portal vein (curved arrow), which were darker than liver before contrast medium enhancement, became and remained brighter than liver after enhancement. Although tumor (T) enhanced slightly as areas of necrosis became more conspicuous, it became much darker than liver after administration of contrast medium, with better-defined margins. (Reprinted with permission from ref. 70a. Copyright 2002 Elsevier Ltd.)

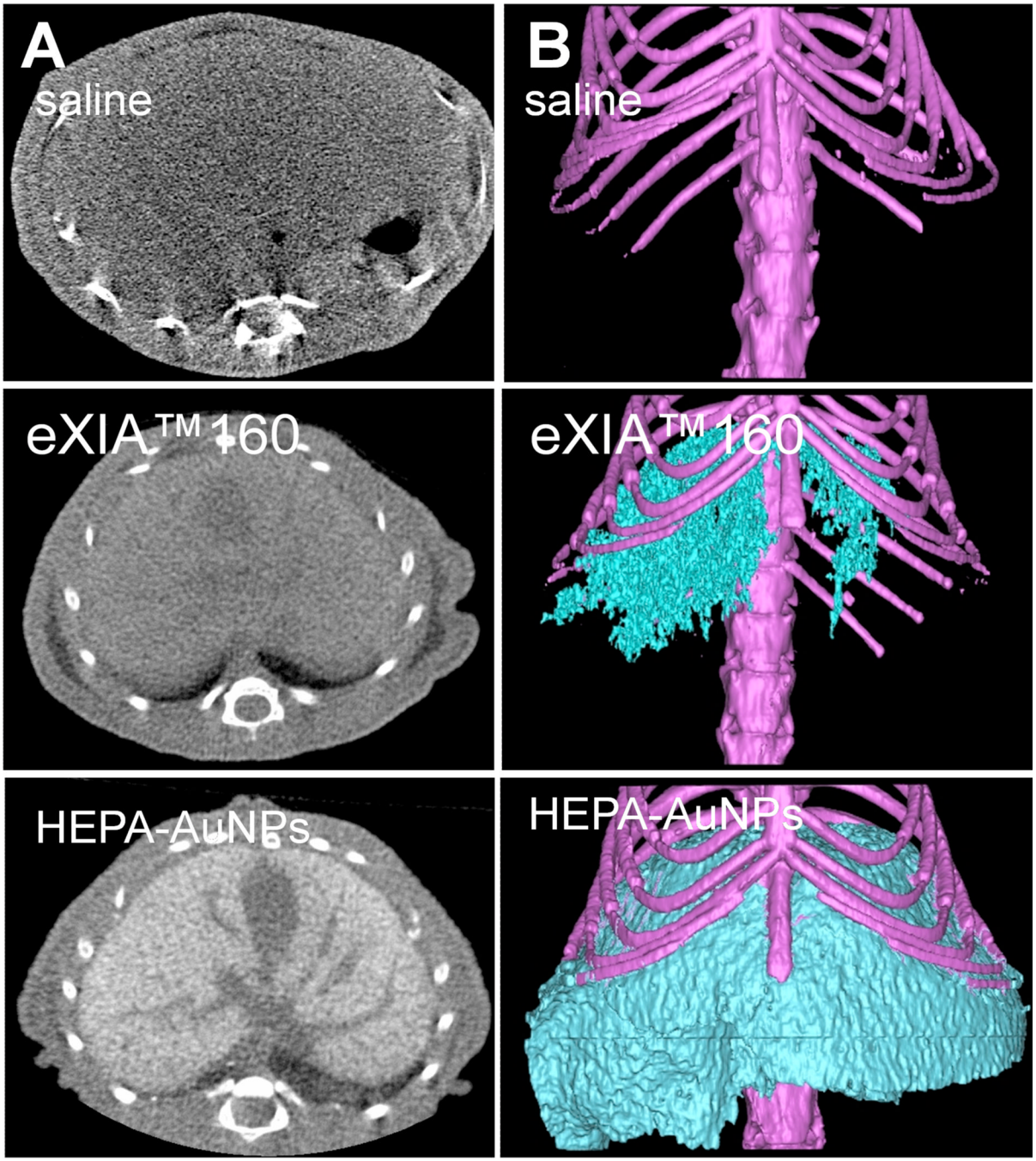

Figure 16.
A) Cross-sectional microCT images in livers 2 h post injection of saline, eXIA 160 (800 mg I kg^{-1}), and HEPA-AuNPs (250 mg Au kg^{-1}). B) Three-dimensional microCT images of livers obtained after 2 h post injection of saline, eXIA 160, and HEPA-AuNPs. (Reprinted with permission from ref. 84. Copyright 2009 John Wiley and Sons.)

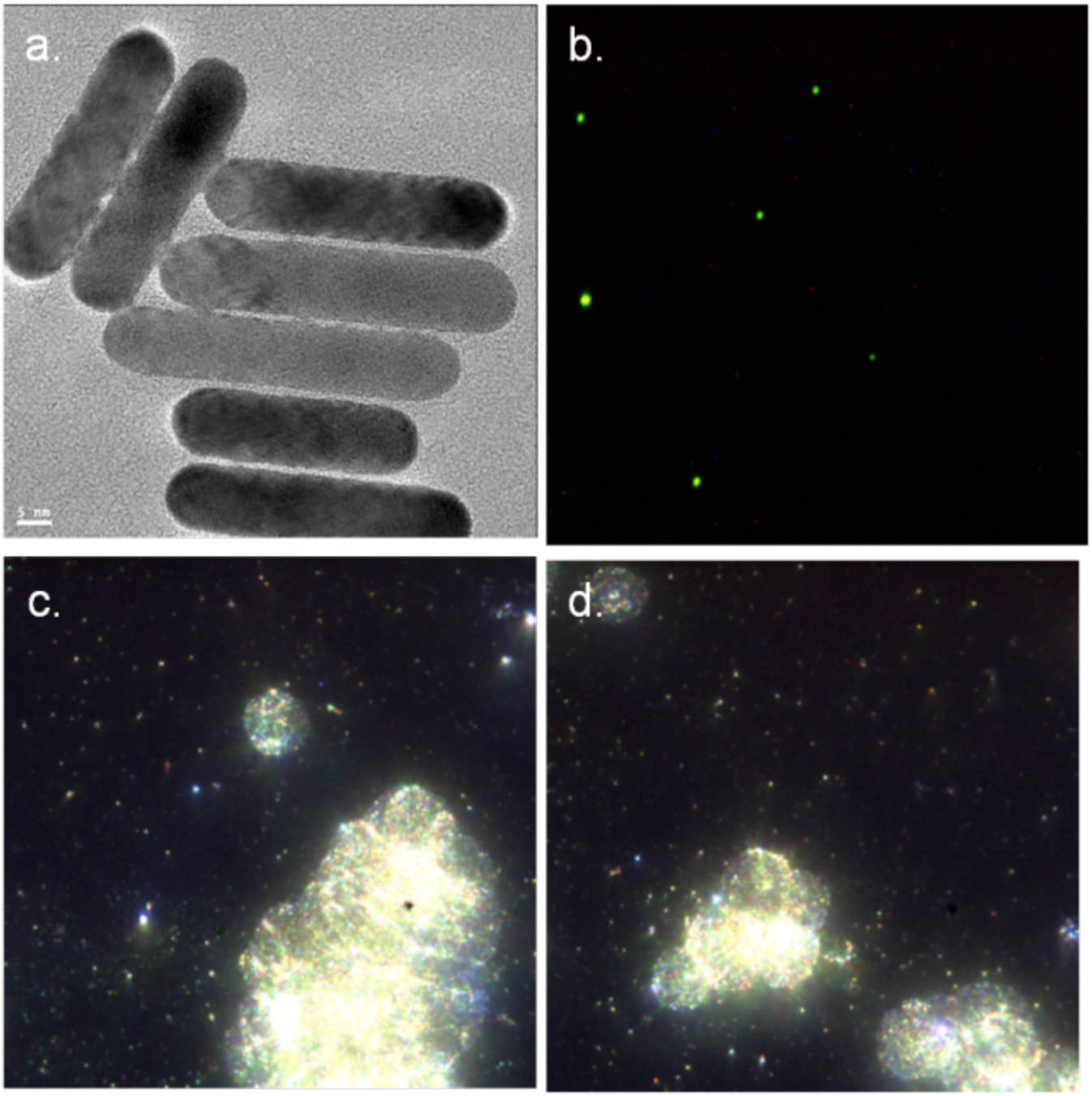

Figure 17.
UM-A9 antibody-conjugated AuNP. a) HRTEM image of gold nanorods (scale bar = 5 nm); b) dark-field microscope of gold nanorods; c) and d) in-vitro dark field images of cancer cells targeted with gold nanorods. (Images courtesy of Dr. Rachela Popovtzer, Bar-Ilan University, Israel).

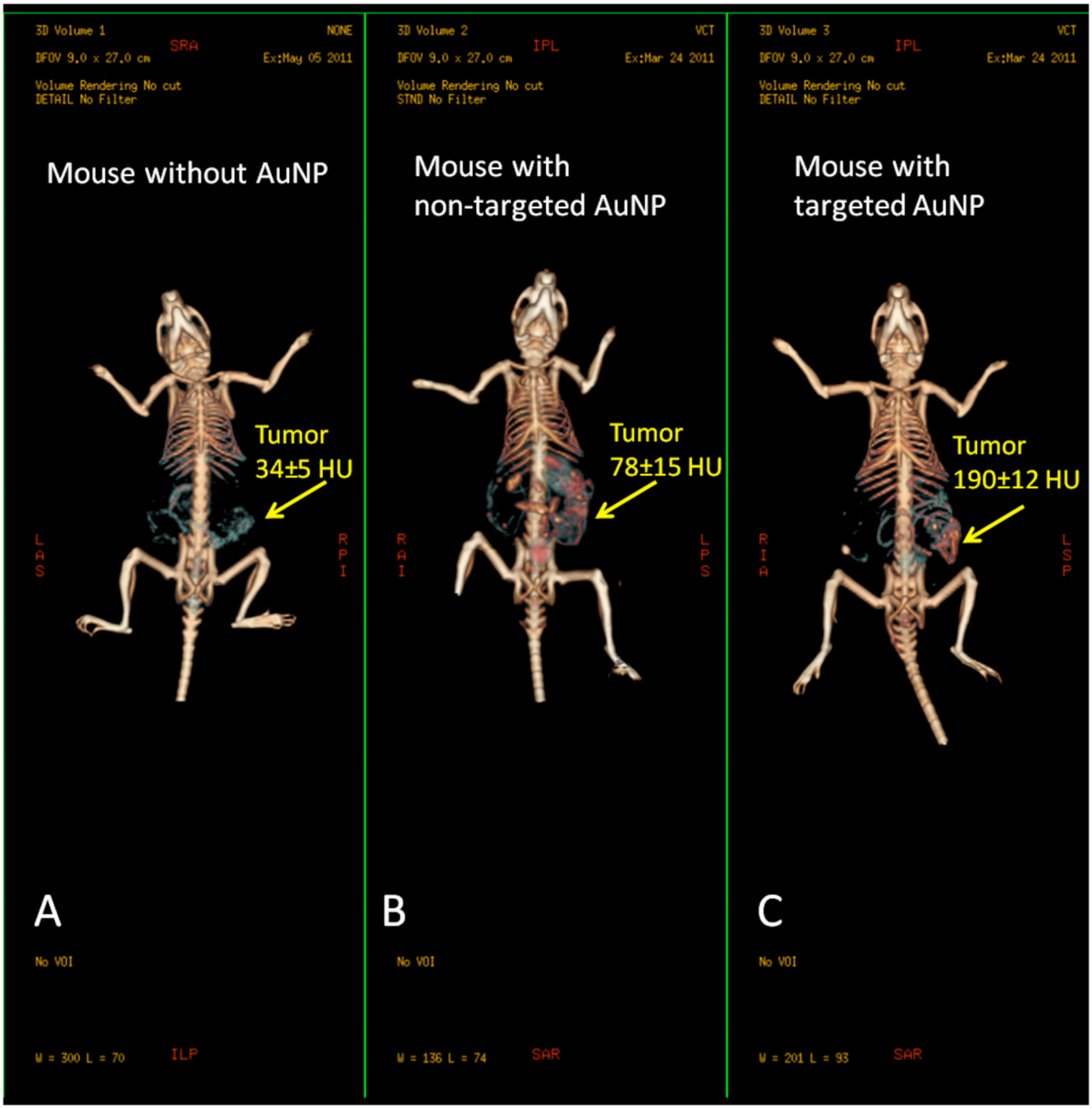

Figure 18.

In vivo X-ray computed tomography (CT) volume-rendered images of (A) mouse before injection of gold nanoparticles (AuNPs), (B) mouse 6 hours post-injection of nonspecific immunoglobulin-G AuNPs as a passive targeting experiment, and (C) mouse 6 hours post-injection of anti-epidermal growth factor receptor (EGFR)-coated AuNPs that specifically targeted the squamous cell carcinoma head and neck tumor. The anti-EGFR-targeted AuNPs show clear contrast enhancement of the tumor (C, yellow arrow), which was undetectable without the AuNPs contrast agents (A, yellow arrow). CT numbers represent the average Hounsfield units (HU) of the whole tumor area. All scans were performed using a clinical

CT at 80 kVp, 500 mAs, collimation 0.625 × 64 mm and 0.521 pitch size (64 detector CT scanner, LightSpeed VCT; GE Healthcare, Little Chalfont, UK). (Images courtesy of Dr. Rachela Popovtzer, Bar-Ilan University, Israel).

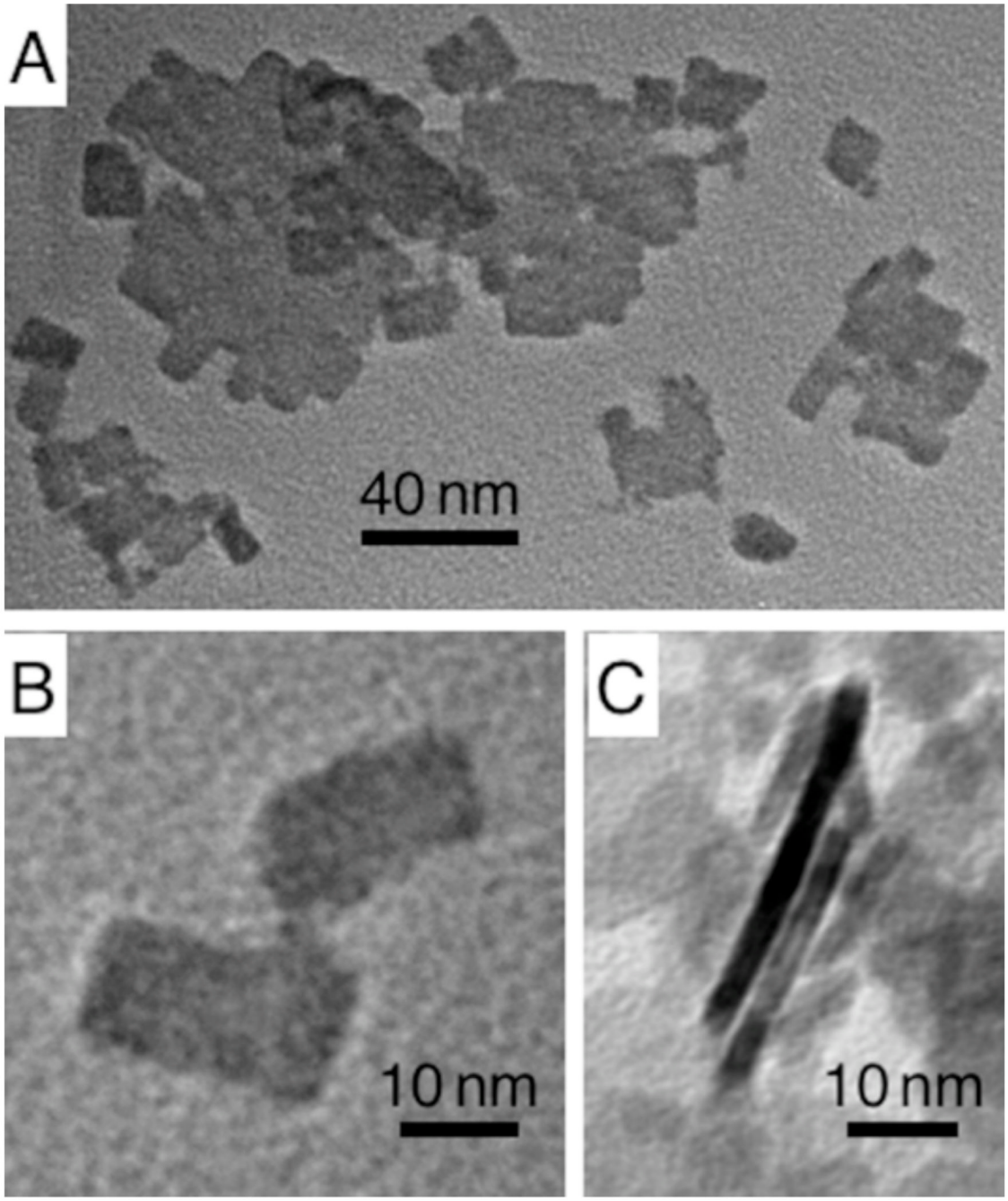

Figure 19.
Transmission electron microscopy (TEM) characterization of the Bi_2S_3 nanoparticles revealed that the nanocrystals had a quasi-rectangular platelet shape, ranging in size from 10 nm to about 50 nm per side, although some larger nanocrystals also had more complex shapes. The thickness of the crystals was 3–4 nm. (Reprinted with permission from ref. 106. Copyright 2006 Nature Publishing Group.)

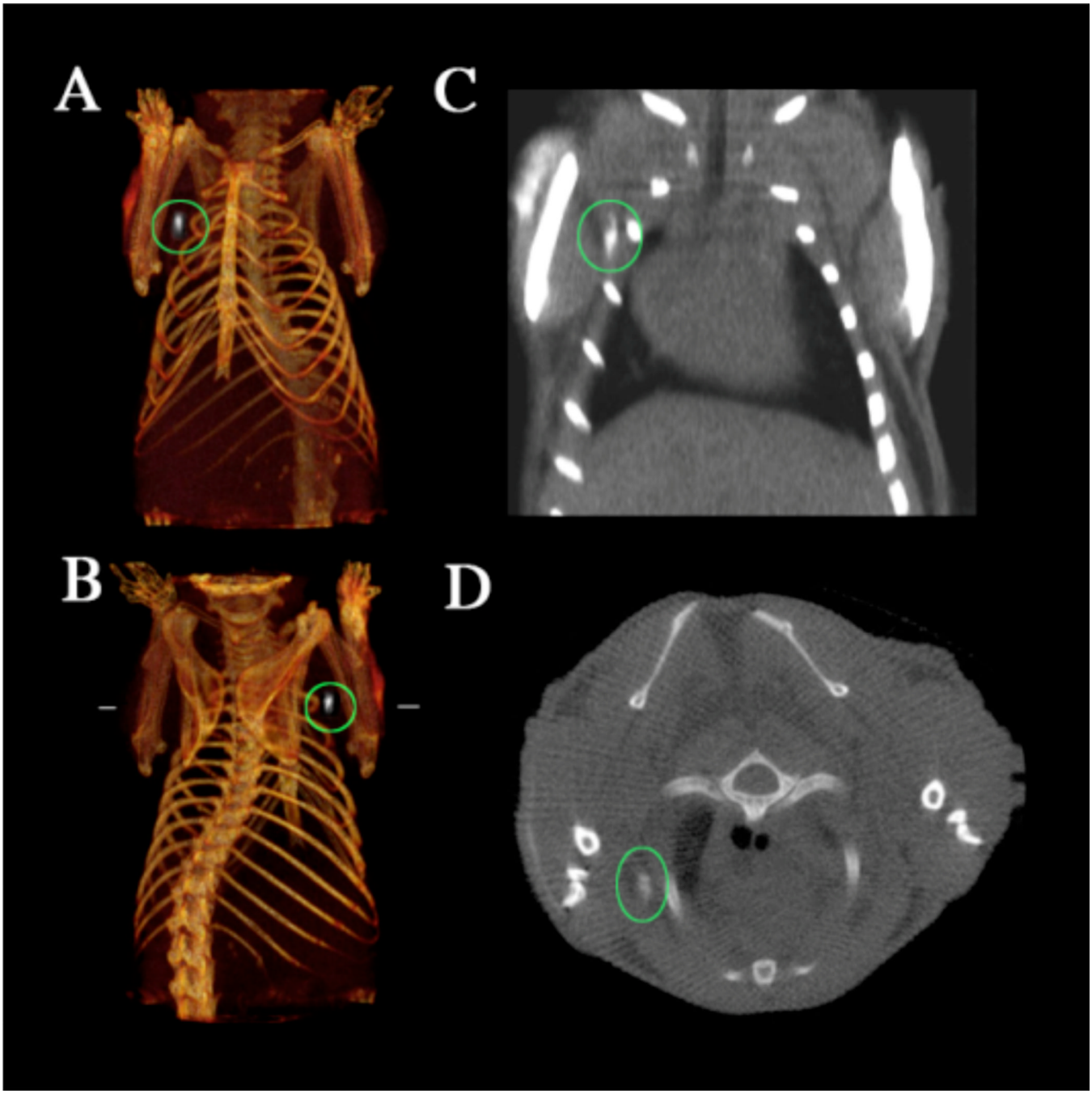

Figure 20.
CT imaging of a lymph node of a mouse with the Bi_2S_3 imaging agent. A) and B) Three-dimensional volume renderings of the CT data set, the length of the reconstruction is 3.8 cm. C) Coronal slice (length of the slice 2.3 cm). D) Transverse slice at the height indicated by the horizontal lines in "B)." The maximal diameter of the mouse 1.8 cm. The position of the lymph node under the right shoulder is indicated by the ovals, and the injection site is shown by the arrows. Note the lack of contrast in the corresponding contra-lateral (left shoulder) lymph node. (Reprinted with permission from ref. 106. Copyright 2006 Nature Publishing Group.)

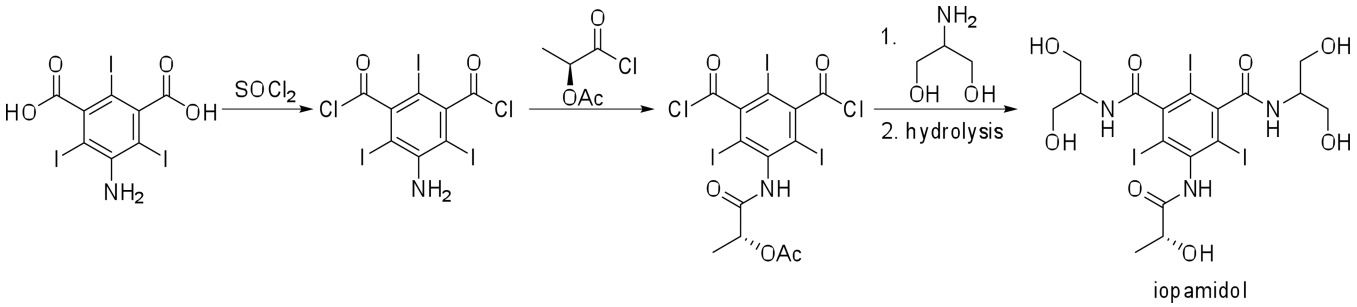

Scheme 1.
Synthesis of iopamidol from commercially available starting materials on an industrial scale.[14]

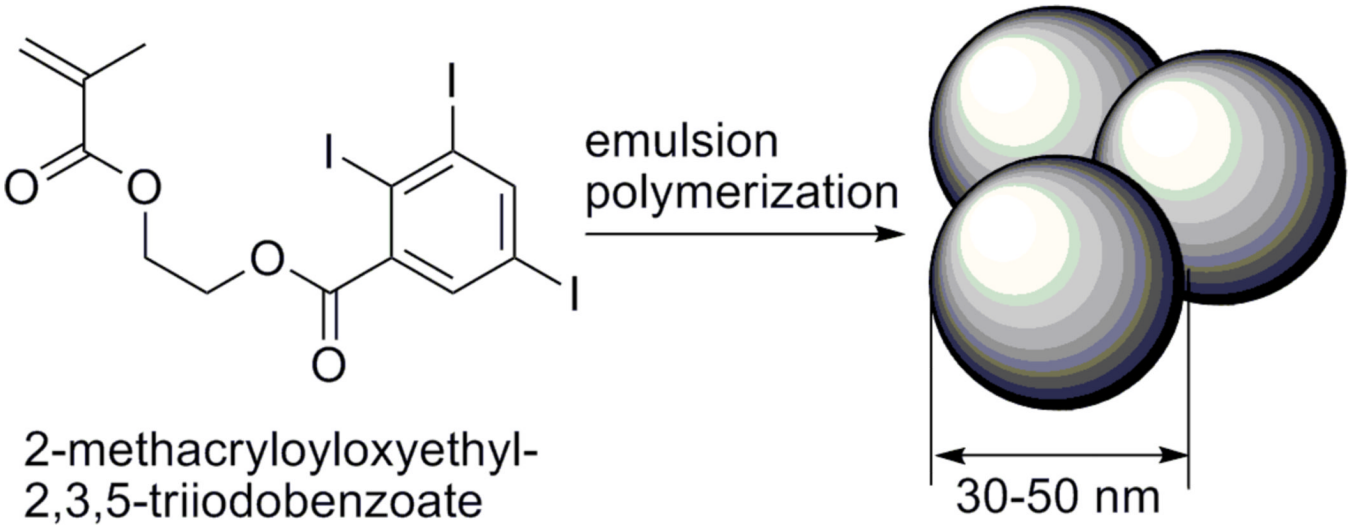

Scheme 2.
Monomer structure and preparation of MAOETIB nanoparticulate contrast agent.

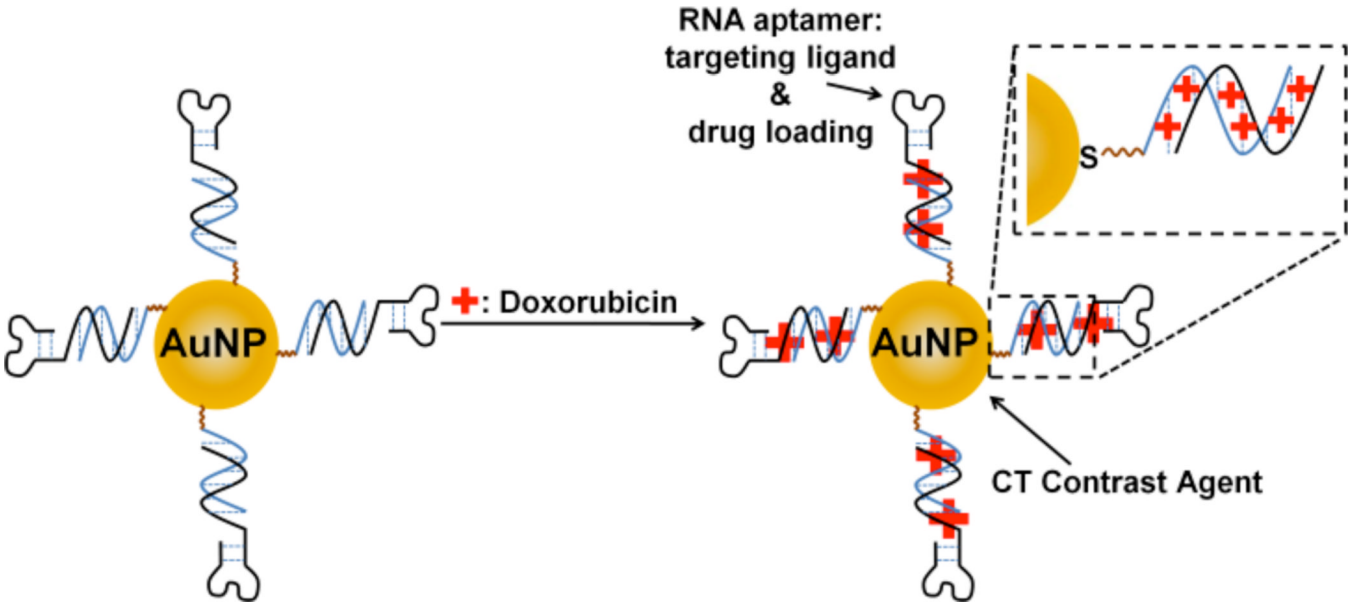

Scheme 3.

Loading of the trifunctional AuNP with chemotherapeutic drug doxorubicin. The gold center serves as the CT imaging agent, while the RNA aptamer modifications turn the nanoparticle into a targeted drug-delivery vehicle. (Image adapted with permission from ref. 95. Copyright 2010 American Chemical Society.)

Table 1

Some common commercially available small-molecule iodinated contrast agents and their indicated clinical uses.

Common name	Commercial name	Manufacturer	Indicated Clinically Approved Use*
iohexol	Omnipaque	GE Healthcare	Indicated for intrathecal administration in adults including myelography (lumbar, thoracic, cervical, total columnar) and in contrast enhancement for computerized tomography (myelography, cisternography, ventriculography).
iopromide	Ultravist	Bayer Healthcare	Intra-arterial: intra-arterial digital subtraction angiography (IA-DSA), cerebral arteriography and peripheral arteriography, coronary arteriography and left ventriculography, visceral angiography, and aortography; intravenous: peripheral venography, excretory urography, for contrast Computed Tomography (CT) of the head and body (intrathoracic, intra-abdominal and retroperitoneal regions) for the evaluation of neoplastic and non-neoplastic lesions.
iodixanol	Visipaque	GE Healthcare	Intra-arterial: intra-arterial digital subtraction angiography, angiocardiography (left ventriculography and selective coronary arteriography), peripheral arteriography, visceral arteriography, and cerebral arteriography; intravenous: CECT imaging of the head and body, excretory urography, and peripheral venography.
ioxaglate	Hexabrix	Mallinckrodt Imaging	Pediatric angiocardiography, selective coronary arteriography with or without left ventriculography, peripheral arteriography, aortography, selective visceral arteriography, cerebral angiography, intraarterial digital subtraction angiography, intravenous digital subtraction angiography, peripheral venography (phlebography), excretory urography, contrast enhancement of computed tomographic head imaging and body imaging, arthrography and hysterosalpingography.
iothalamate	Cysto-Conray II	Mallinckrodt Imaging	Retrograde cystography and cystourethrography
iopamidol	Isovue	Bracco Imaging	Angiography throughout the cardiovascular system, including cerebral and peripheral arteriography, coronary arteriography and ventriculography, pediatric angiocardiography, selective visceral arteriography and aortography, peripheral venography (phlebography), and adult and pediatric intravenous excretory urography and intravenous adult and pediatric contrast enhancement of computed tomographic (CECT) head and body imaging.

* Information obtained from http://www.drugs.com and http://www.fda.gov.

Table 2

Physical data of iosimenol, GE-145, iodixanol, and iotrolan. Viscosity and osmolality data was obtained at 37 °C for a contrast media concentration of 320 milligrams iodine per mL of solution (mg I/mL).

	Iosimenol	GE-145	Iodixanol	Iotrolan
MW (g/mol)	1478.09	1522.13	1550.00	1626.24
Iodine wt %	51.5	50.0	49.1	46.8
Viscosity (mPa · s)	7.7	10.2	11.5	11.6
Osmolality (mOsm/kg H_2O)	166	136	210	320

Table 3

Some common commercially available lanthanide-chelates contrast agents and their indicated use.

Common name	Commercial name	Manufacturer	Indicated Clinically Approved Use*
gadoversetamide	OptiMark	Mallinckrodt Imaging	MRI in patients with abnormal blood-brain barrier or abnormal vascularity of the brain, spine and associated tissues. Providing MRI contrast enhancement and facilitate visualization of lesions with abnormal vascularity in the liver in patients who are highly suspect for liver structural abnormalities on computed tomography.
gadopentetate dimeglumine	Magnevist	Bayer Healthcare	MRI in adults, and pediatric patients (2 years of age and older) to visualize lesions with abnormal vascularity in the brain (intracranial lesions), spine and associated tissues. Magnevist Injection has been shown to facilitate visualization of intracranial lesions including but not limited to tumors. Visualization of lesions with abnormal vascularity in the head and neck, and in the body (excluding the heart).
gadobutrol	Gadovist	Bayer Healthcare	Contrast enhancement in cranial and spinal MRI. First pass MRI studies of cerebral perfusion.
gadobenate dimeglumine	MultiHance	Bracco Imaging	MRI of the central nervous system (CNS) in adults and children over 2 years of age to visualize lesions with abnormal blood brain barrier or abnormal vascularity of the brain, spine, and associated tissues.
gadoterate meglumine	Dotarem	Guerbet	MRI of cerebral, spinal, and vertebral column, and other whole-body pathologies (including angiography).
gadoxetate disodium	Eovist	Bayer Healthcare	T1-weighted MRI of the liver to detect and characterize lesions in adults with known or suspected focal liver disease.

*Information obtained from http://www.drugs.com and http://www.fda.gov.

Table 4

Proposed research phase plan for the clinical application of CT contrast media.

	Research phase
☐	synthesis of a series of contrast agent derivatives
☐	*in vitro* or *ex vivo* imaging of target cells/tissue
☐	identification of a lead contrast agent
☐	formulation development
☐	*in vivo* imaging in a small animal (e.g. mice or rat)
☐	development of large scale synthesis (> 200 g)
☐	analytical method development for assay and characterization of impurities
☐	*ex vivo* imaging of human tissue in a clinical scanner
☐	safety studies in a small animal (e.g., rat) including genotoxicity and local irritation
☐	single-dose increasing concentration toxicity study in a small animal (e.g., rat)
☐	pharmacokinetic studies to determine the blood clearance routes, rates of excretion, and tissue distribution of radio-labeled contrast agent in a small animal (e.g., rat)

Table 5

Proposed development phase plan for the clinical application of CT contrast media.

	Development phase
☐	good manufacturing practice (GMP) for preparation of ~1 kg of contrast agent for safety and stability studies, and potentially for the phase I human safety clinical trial
☐	long term stability studies
☐	qualification of analytical methods for release of the clinical formulation
☐	single-dose-increasing toxicity studies in a large animal (e.g., dog) with cardiovascular, respiratory, and CNS safety pharmacology studies
☐	pharmacokinetic studies to determine the blood clearance routes, rates of excretion, and tissue distribution of radio-labeled contrast agent in a large animal (e.g., dog)